FACULTY OF ENGINEERING AND THE BUILT ENVIRONMENT

DEPARTMENT OF CIVIL ENGINEERING

INVESTIGATING THE OPERATIONAL BEHAVIOUR OF A DOUBLE CURVATURE ARCH DAM

By

Zac James Prins

Submitted in partial fulfillment of the requirements for the degree

M.Eng.

Civil Infrastructure Management and Maintenance

Supervisor: **Professor Pilate Moyo**

PLAGIARISM DECLARATION

I know the meaning of plagiarism and declare that all the work in the document, save for that which is properly acknowledged, is my own. This thesis/dissertation has been submitted to the Turnitin module (or equivalent similarity and originality checking software) and I confirm that my supervisor has seen my report and any concerns revealed by such have been resolved with my supervisor.

Signed by candidate

Signature Removed

Signature: _____

Date: 12 May 2017

DEDICATION

To my loving family for their unwavering support.

ABSTRACT

The safety of dams is crucial in ensuring the continual availability of water, safety of the surrounding communities and infrastructure. Surveillance systems are implemented to monitor the structural integrity of certain dams which have a safety risk. The components and extent of the surveillance systems adopted depends on many factors, which include the type of dam wall structure used to impound the reservoir, geotechnical and environmental conditions.

The case study used for this thesis is Kouga Dam located in the Eastern Cape Province of South Africa. It is a double curvature, concrete arch dam which supplies water for domestic, irrigation, and industrial use to the Gamtoos River Valley and Nelson Mandela Metropolitan. During construction the stability of the right flank was questioned and subsequently remedial measures were taken in order to increase the shear resistance of this flank. Previous dam safety evaluations also noted the possibility of Alkali Silica Reaction (ASR) occurring within the structure which resulted in concrete swelling and loss of strength. Due to these factors and the large hazard potential rating associated with this dam, an intensive surveillance system has been used to monitor the dam's behaviour during operation.

In this thesis the results of the surveillance system is analysed. A strong linear relationship exists between the temperature loading and displacement response of the dam wall. Changes in temperature initiate the response of the structure almost instantaneously. A more complex relationship exists between hydrostatic loading and the displacement response of the structure. A phase lag of approximately one to three months is evident between these two variables. Since construction the displacement and strain rates in the upstream (y) and upward (z) directions are 0.3mm/annum and 8.6με/annum respectively. However, since 1989 there has been a reduction in the average displacement and strain rates in all directions by approximately 70%. This may suggest that the ASR has stabilized. The vertical construction joints, especially the central and upper joints, are relatively open during low water levels. The structure is found to transfer the imposed loading mainly to the central foundation via dominant cantilever action. As a result the reaction forces on the upper foundation have been found to be relatively low, lowering the risk of potential shear failure of the right foundation. Small foundation movements of less than 0.3mm have been observed within the foundation downstream of the dam wall on the right flank. These movements are between 10 and 40m within the foundations.

ACKNOWLEDGEMENT

Firstly I would like to thank Professor Pilate Moyo for his supervision and guidance throughout this thesis. Dr. Chris Oosthuizen for urging me to pursue postgraduate studies and stoking my interest in dam engineering. As well as Patrick Bukenya for his help in the field and during the write-up of the document.

I would also like to acknowledge the Department of Water and Sanitation, for providing the means for further studies, allowing me to utilize invaluable information and also my fellow colleagues who assisted with the research.

Lastly, I would like to thank my family for their continuous support.

TABLE OF CONTENTS

LIST OF TABLES

LIST OF FIGURES

LIST OF ABBREVIATIONS

APP	Approved Professional Person
ASCE	American Society of Civil Engineers
ASR	Alkali Silica Reaction
AVM	Ambient Vibration Measurements
dB	Decibels
DSO	Dam Safety Office
DWA	Department of Water Affairs
DWAF	Department of Water Affairs and Forestry
DWS	Department of Water and Sanitation
EFDD	Enhanced Frequency Domain Decomposition
FEA	Finite Element Analysis
FERC	Federal Energy Regulatory Commission
GNSS	Global Navigation Satellite System
GPS	Global Positioning System
GRGWS	Gamtoos River Government Water Scheme
Ha	Hectares
Hz	Hertz
MDOF	Multiple Degrees of Freedom
NWA	National Water Act
OMA	Operational Modal Analysis
RL	Reduced Level
SDOF	Single Degree of Freedom
TMG	Table Mountain Group
USA	United States of America
USACE	United States Army Corps of Engineers
USBR	United States Bureau of Reclamation

NOMENCLATURE

Latin Upper Case

°C	Degrees Celcius
K	Canyon Shape Factor
P_n	Westergaard hydro-dynamic pressure

Latin Lower Case

c	Damping
f_0	Amplitude of excitation force
g	Acceleration due to gravity
k	Stiffness
k_e	Equivalent stiffness
m	Mass or meters
mm	Millimeters
m^3	Cubic meters
m_e	Equivalent Mass
t	Time
$\ddot{u}^t_n$	Total normal acceleration
x	Displacement
$\dot{x}$	Velocity
$\ddot{x}$	Acceleration

Greek Lower Case

α	Westergaard pressure coefficent
ζ	Damping Ratio
φ	Mode shapes
ρ_w	Density of water
με	Micro-strain
μm	Micron/Micrometer
ω	Excitation Frequency
ω_n	Natural Frequency

CHAPTER 1

1 INTRODUCTION

1.1 Background

South Africa is deemed a water scarce country. In 2014 it averaged less than 500mm of rainfall annually compared to the global average of approximately 1160mm (The World Bank, 2016). The country is significantly reliant on water, not only for domestic purposes, but in order to support major contributing sectors to the country's economy. These include the mining and agricultural sectors. In addition to these water demands, domestic consumption has increased over the years due to population growth and urbanization.

In light of the water demands, the South African government has taken steps to protect this resource[1]. Water impounding infrastructure within the country is subject to legislation which ensures their safety. The National Water Act (NWA) mandates dam safety regulations (NWA, No. 36 of 1998, 1998: s123) which include routine inspections to evaluate the safety of the dams. Monitoring systems are one of the tools used by engineers during these evaluations. These tools assist in understanding the structural behaviour of the dam during operation and when under extreme loading.

The monitoring system records loading and response data. An analysis of this data identifies trends which give insights into the operational behaviour of the structure and assist in highlighting potential modes of failure. These insights allow engineers to make informed decisions regarding dam safety.

Kouga Dam, which is the thesis case study, is categorised as a double curvature, concrete arch dam. These dam types are generally chosen in canyon sites which have high strength abutments. This is because the dam is curved in section and in plan views, resisting the loading not only by self-weight, but also by arch action. Therefore the dam wall is thinner in cross-section compared to gravity dams, which resist the loading through sheer mass.

The relatively smaller cross-sectional area of double curvature arch dams is not large enough to resist the imposed loading by mass alone. Consequently, significant loss in the arch action, or foundation instability in the direction of arch thrusts may lead to potentially catastrophic failure of the structure.

[1] For further reading, see: (National Water Act [NWA], No. 36 of 1998, 1998: chap12); (NWA, No. 36 of 1998. Regulation, 2012); (South African National Congress on Large Dams [SANCOLD], 1991)

1.2 Problem Statement

Double curvature arch dams transfer the imposed loading on the structure via a combination of arch and cantilever action. This unique way in which arch dams transfer forces depend on many factors, which include the environmental conditions, site topography, design assumptions, and construction techniques.

In evaluating the safety of arch dams the operational behaviour of the structure needs to be understood. Especially in light of factors such as; variable material properties of foundations, material deterioration, aging, changes in environmental conditions and loading, which may change the way the structure behaves over time. Thorough data analysis of the monitoring systems installed at dams assist in providing greater insight into the structural response. These insights include general behaviour trends and highlighting potential failure modes. This allows informed decisions to be made with regards to ensuring the safety of the structure.

1.3 Objective

The purpose of this research is to analyse the instrumentation data recorded at Kouga, a double curvature arch dam located in the Eastern Cape Province of South Africa. The objective of this analysis is to gain insight into the operational behaviour of the dam, namely the effects that different measured parameters have on the structure's response, to track deterioration over time, and to identify potential modes of failure.

1.4 Limitations and Scope of Research

The scope of the thesis is limited to Kouga Dam. The parameters considered, as recorded by the monitoring system, include the following;

- Water levels
- Temperature
- Displacements
- Natural frequencies

1.5 Thesis Structure

Chapter 1 - Introduction

This chapter considers the need for dams and the associated governmental dam safety regulations. The objective of the thesis is presented, followed by the scope of the study.

Chapter 2 - Design, Construction, and Management of Arch Dams: A Review

This chapter presents literature relating to arch dams. These works focus on design and analysis, general construction practices, and the management of arch dams.

Chapter 3 - Methodology

This chapter provides background information on the thesis case study and its monitoring system which records the loading, response, and integrity of the structure over time.

Chapter 4 - Results and Discussion

This chapter presents the recorded data of the instrumentation and the identified behavioural trends are discussed. In addition a comparative study is done with a dam of similar size, comparing the determined structural characteristics.

Chapter 5 - Conclusion and Recommendations

This chapter presents conclusions based on the identified behavioural trends and provides recommendations for future studies related to the topic of this thesis.

Appendices

This section consists of the Trivec displacement data recorded at Kouga Dam.

CHAPTER 2

2 DESIGN, CONSTRUCTION, AND MANAGEMENT OF ARCH DAMS: A REVIEW

2.1 Design of arch dams

2.1.1 Brief historical review

The design of arch dams has developed significantly over the past century and is documented in manuals and guidelines[2]. The Trial Load Method (United States Bureau of Reclamation [USBR], 1977a: chap4b) was adopted in the United States of America (USA) before the advent of computers. This method estimates the stresses by assuming a dual structural system consisting of horizontal arch and vertical cantilever units. The method's contribution to analysis of arch dams is further elaborated in Section 2.1.4. In Europe the membrane method was used in defining the arch shape (da Silva & Júlio, 1995: 534). This method involved water being loaded on a rubber membrane which is fixed to a frame. The boundary of the frame would be the shape of the valley in which the dam is situated. The rubber membrane deforms into a funicular shape off which the arch is based. Shaw (2015: 321) notes that in South Africa a similar method was developed by Myburgh (1960), known as the mesh model. In this model perpendicular wires were opted for instead of the rubber membrane, and on the intersections of the wires, weights were applied to simulate the hydraulic loading on the dam wall.

All of these methods proved effective in defining the arch shape during the early period of arch design. However, following the introduction and rapid development of computers, finite element analyses (FEA) has become the primary tool in arch dam design and analysis. This has allowed for the design and construction of efficient structures which require less material and are more economical. In all of the above mentioned methods one of the critical factors in the design of arch dams is the site topography. This is discussed in the section below.

2.1.2 Site considerations

Arch dams function by transferring imposed loads on the structure to the supporting abutments and foundation. The chosen characteristics of the arch structure and how it transfers the forces to the supports is largely dependent on the specific site and foundation conditions.

The site topography may broadly be categorized into four types, namely narrow-V, wide-V, narrow-U, or wide-U (See Figure 1). Canyon shape factors (K) are often used to describe the topography and is defined as the total developed length of

[2] For further reading, see: (United States Bureau of Reclamation [USBR], 1977a); (USBR, 1977b); (United States Army Corps of Engineers [USACE], 1994).

foundation surface divided by the maximum dam height (Shaw, 2015: 323). Arch dams are most effective in narrow valleys and particularly V-shaped with low K values. These topographies allow the dam wall to be relatively thin in section, whilst transferring the majority of the imposed loads to the abutments via arch action. The thin, flexible cantilevers allow the forces to transfer horizontally, which results in a much more distributed load throughout the foundation. Conversely, the wider the canyon and higher the K value, the thicker the arch and the more the dam relies on cantilever action to resist the loading. This in turn requires the structure to increase in wall thickness the closer to the riverbed in order to accommodate for the reliance on cantilever action.

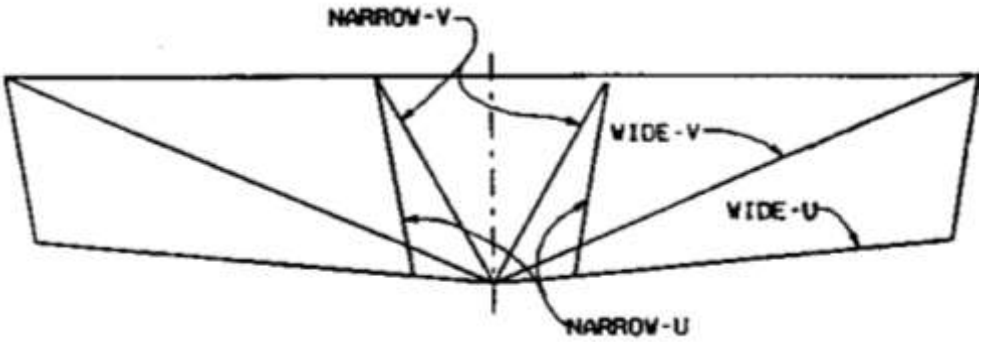

Figure 1: Schematic topography of various dam sites (USACE, 1994:1-3)

2.1.3 Loading

Dams are subjected to loading which are categorised as either static or dynamic. Static loads can be further divided into sustained and cyclic loads. The sustained loading does not change with time and includes loads such as the dead load of the dam wall and appurtenant structures. The magnitude of cyclic loads change with time, ranging from hourly to seasonally. These loads include changing temperature and water level. The response of arch dams to static loading is predominantly governed by the stiffness of the structure.

Dynamic loading implies a load which results in inertial forces. The frequency of this loading is much higher compared to that of cyclic loads. Examples of dynamic loading include micro-seismic vibrations caused by wind loading and oceanic wave motion, as well as macro-seismic activity such as earthquakes. Depending on the ratio of excitation to natural frequency, the structural response to the dynamic excitation is governed by inertia (mass), damping, and stiffness. The dynamic response of structures will be expanded in more detail in Section 2.3.2. Typical loads on dams are summarized in Table 1.

Table 1: Typical static and dynamic loads on dams

<table>
<tr><td>Static: Sustained</td><td colspan="2">• Gravity loads (Own weight)
• Silt loads
• Ice loads
• Concentrated loads (Appurtenant structures)</td></tr>
<tr><td>Static: Cyclic</td><td colspan="2">• Hydrostatic loads
i. Water level
ii. Pore pressure
iii. Uplift

• Thermal loads (Temperature)</td></tr>
<tr><td rowspan="3">Dynamic</td><td>Micro-seismicity (Ambient loads)</td><td>• Waves
• Wind
• Atmospheric phenomena
• Human activities
i. Traffic
ii. Machinery</td></tr>
<tr><td>Macro-seismicity</td><td>Earthquakes</td></tr>
<tr><td>Other</td><td>• Impact loads
i. Explosions ("Acts of war")
ii. Lightning
iii. Collisions
• Landslides
i. Direct contact with dam wall
ii. Resultant wave action</td></tr>
</table>

2.1.4 Analysis

Trial Load Method

One of the earliest analysis procedures adopted for the design of arch dams is known as the Trial Load Method. The method estimates the stresses developed within the structure in a simplistic and acceptably accurate (for the purposes of early design) manner. The underlying assumption is that arch dams resist imposed loads by two systems of structural members, namely horizontal arch and vertical cantilever units (USBR, 1977a: chap4b). Arch units are bound by horizontal planes and transfer the forces as hoop stresses throughout the arch. Cantilever units are bound by vertical planes and transfer the forces as cantilever stresses. This is often referred to as arch and cantilever action respectively. It is assumed that the corresponding arch and cantilever deflections at any point throughout the dam are equal (Shown significantly exaggerated in Figure 2). After grouting the structure is assumed to act as a monolith, resisting imposed loads by a combination of arch and cantilever action.

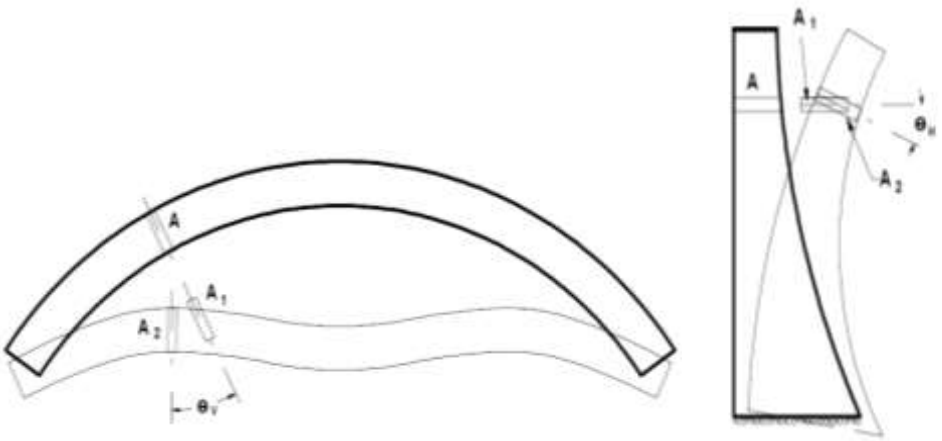

Figure 2: Deflected arch (left) and cantilever (right) units (USACE, 1993:2-4)

Finite Element Analysis

In recent times, FEA has been used in order to calculate stresses at a much greater accuracy compared to previous techniques. This method divides a structure into inter-connected finite elements, and solves for the resultant displacements with the use of equilibrium equations, incorporating the stiffness matrices and load vectors of the system. The stresses for each element can then be determined from the stress-displacement relationship (Bathe, 1996: chap1).

Dynamic Analysis: Generalised Westergaard Method

Westergaard (1933) first developed the notion of using an added mass to represent the interaction between the dam wall and reservoir during the dynamic analysis. Initially the method assumed a concrete gravity dam with vertical upstream face, however this was later extended to a more general form to accommodate other dam types. The generalised Westergaard method (Kuo, 1982) can be applied to arch dams as it accounts, to some extent, for the upstream curvature and three dimensional transfer of forces. For this case the same added mass profile is used, however the hydro-dynamic forces act normal to the curved dam wall surface. See Figure 3 for the graphical representation of this method.

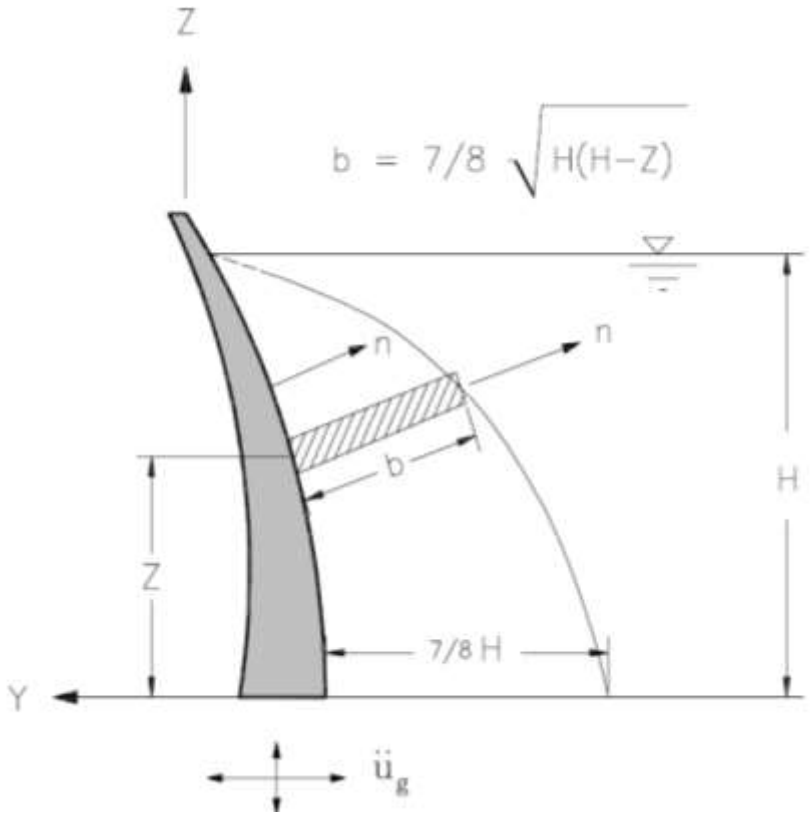

Figure 3: Generalised Westergaard added mass (Federal Energy Regulatory Commission [FERC], 1999: 11-122)

The hydro-dynamic forces exerted on the upstream face are given by the following equation;

$$\boldsymbol{P_n = \alpha \ddot{u}^t{}_n} \tag{2.1}$$

with,

P_n: Hydro-dynamic pressure

α: Westergaard pressure coefficent

$\ddot{u}^t_n$: Total normal acceleration

The pressure coefficient is described by;

$$\boldsymbol{\alpha = \rho_w b} \tag{2.2}$$

$$\boldsymbol{= \rho_w \frac{7}{8}\sqrt{H(H-Z)}}$$

with,

ρ_w: Density of water

H: Height of water level

Z: Distance to point of interest

2.2 Construction of arch dams

The USACE (1994: chap13), notes the following construction considerations for arch dams.

i. Diversion
ii. Foundation excavation
iii. Consolidation and curtain grouting
iv. Concrete operations
v. Monolith joints
vi. Galleries and adits
vii. Drains
viii. Appurtenant structures

Careful consideration and quality assurance of each of these aspects are required in order for the design assumptions to be realised.

Arch dams require competent abutments for the arch to thrust against, therefore the selection and preparation of the foundations are crucial. Weaker regions of the foundations are identified and removed prior to consolidation grouting (Ibid.: 13-5). Inadequate grouting or concrete placement may result in high pore pressures and possibly significant uplift forces in saturated voids within the foundation. Curtain grouting is done in order to control seepage underneath the dam wall.

Arch dams are constructed as independent cantilevers with leader and follower sections as shown in Figure 4. The interfaces between the blocks are vertical contraction joints. The design may incorporate shear keys at these joints in order to increase the shear resistance between adjacent blocks. After all the concrete lifts have been constructed the joints are grouted in order to allow the structure to act as a monolithic system.

Figure 4: Flaming Gorge dam construction in 1962 (USBR, 2016)

2.3 Management of arch dams

2.3.1 Purpose (Statutory requirements)

Chapter 12 of the National Water Act (1998) relates to the safety of dams and aims at "... improving the safety of new and existing dams with a safety risk so as to reduce the potential for harm to the public, damage to property or to resource quality.". Dams with a safety risk are defined as structures "... which can contain, store or dam more than 50 000 cubic metres of water..., and which has a wall of a vertical height of more than five metres...". It is then further classified into categories based on size and hazard potential (NWA, No. 36 of 1998. Reg. 139, 2012). See Tables 2 to 4.

Table 2: Size classification

Size class	Maximum wall height in metres (m)
Small	Less than 12 m
Medium	Equal to or more than 12 m but less than 30 m
Large	Equal to or more than 30 m

Table 3: Hazard potential classification

Hazard potential rating	Potential loss of life	Potential economic loss	Potential adverse impact on resource quality
Low	None	Minimal	Low
Significant	Not more than ten	Significant	Significant
High	More than 10	Great	Severe

Table 4: Category classification of dams with a safety risk

Size class	Hazard potential rating		
	Low	Significant	High
Small	Category I	Category II	Category II
Medium	Category II	Category II	Category III
Large	Category III	Category III	Category III

The NWA further mandates that an approved professional person (APP) should conduct dam safety evaluations at dams with a safety risk. An APP is registered in terms of the Engineering Profession Act (No. 46 of 2000, 2000) and is approved by the Minister of the Department of Water and Sanitation (DWS).

The Regulations Regarding the Safety of Dams (NWA, No. 36 of 1998. Reg. 139, 2012) requires that Category I dams be evaluated on their safety at intervals of

between five and ten years, while Category II and III dams should be evaluated every five years with a possible extension to a maximum of ten years.

2.3.2 Structural response

Structural functioning of arch dams

In order to effectively manage arch dams, the operational behaviour and response to the imposed loading needs to be understood. The idealistic force transfer throughout an arch dam is shown visually in Figure 5. As shown in the image compressive stresses are located at the upstream face, close to the crest of the dam, and subsequently the forces are then transferred towards the downstream abutment contact. The more flexible the cantilevers units of the arch dam wall, the greater the arch action. The degree of double curvature (curved in plan and section views) also increases the horizontal force transfer to the abutments, whilst pushing the dominant compressive forces lower on the upstream face, away from the crest (in elevation). For a well designed arch which exhibits dominant arch action to distribute the loading, the maximum toe stress may be found as high as a third of the dam height during operational loading, as opposed to the maximum toe stress being located at the riverbed. In the case where the cantilevers are stiffer, the horizontal arching zone becomes much shallower, while the forces tend to transfer more to the central foundation via cantilever action (Shaw, 2015: 325).

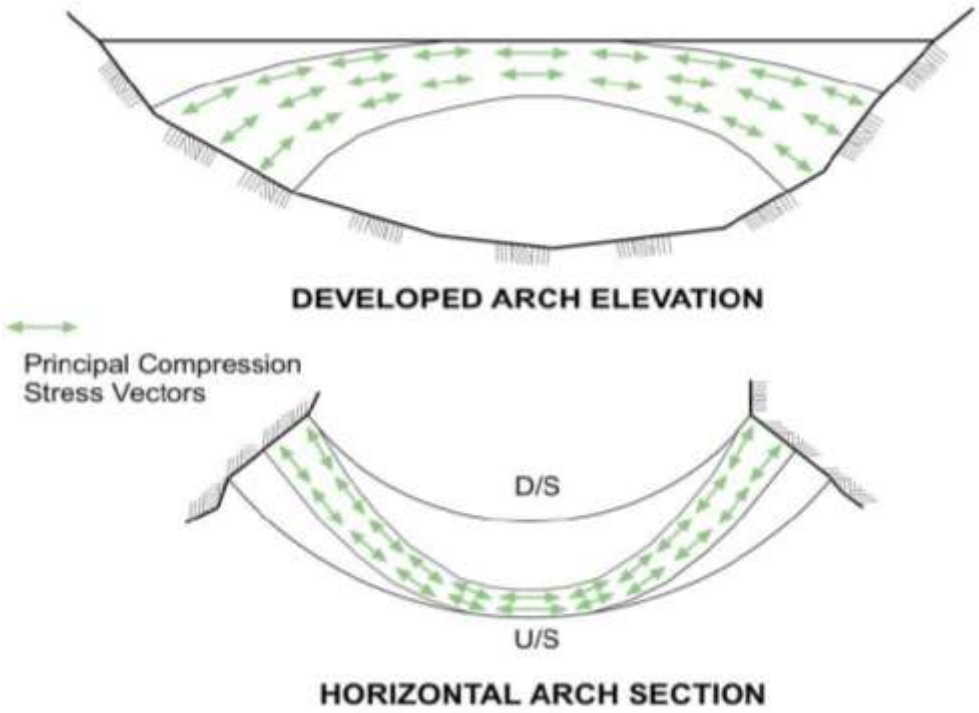

Figure 5: Schematic of force transfer within an arch dam (Shaw, 2015: 324)

The examples in Figure 6 show the minimum principal stress (compression) vectors for a thin double curvature arch which exhibits effective arching (left), and an arch/gravity dam (right) which utilizes larger cantilever forces to resist the loading.

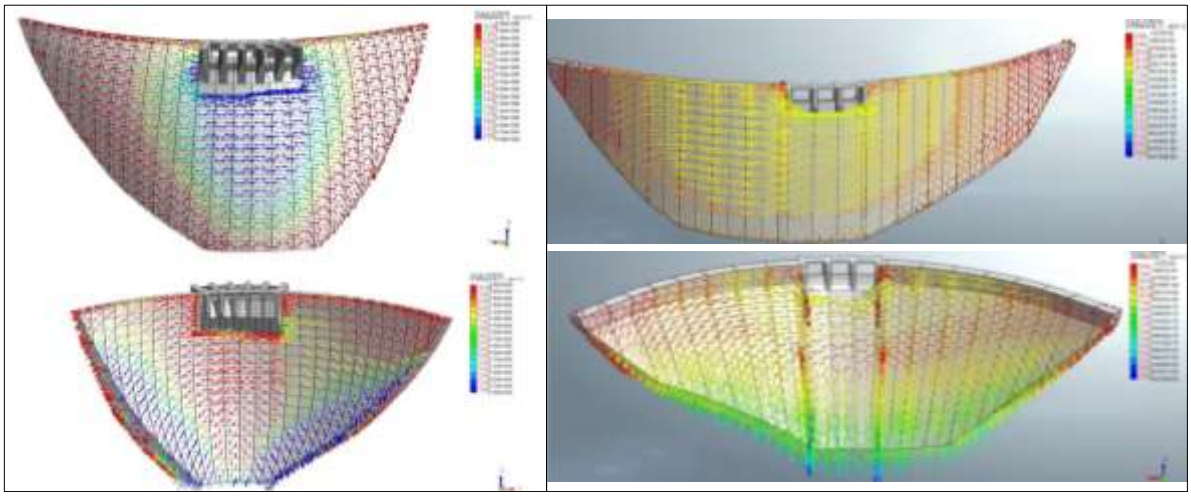

Figure 6: Typical stress distributions for thin arch and arch/gravity dams (Shaw, 2015: 325, 327)

The thin arch displays significant arch action throughout its full height along the upstream face, which peaks at approximately two thirds of the height of the dam. The thrust then transfers toward the downstream face, resulting in maximum compression forces at approximately one third of the dam height along the abutment.

The arching on the upstream face for the arch/gravity dam is considerably less compared to the thin arch. Little to no arching occurs close to the heel of the dam, with these forces predominantly resisted via cantilever action. The maximum compression forces on the downstream are located within the riverbed, as opposed to higher up along the abutment flanks.

Dynamic response

Dynamic systems are defined as structures which are acted on by time varying forces. The structures response to this dynamic loading is oscillating displacements or vibrations. Once a system becomes dynamic certain parameters start having more significant effects on the system's response. These parameters include mass (m), stiffness (k), and damping (c) (Moyo, 2013: 9). Figure 7 describes the dynamic system configuration. The mass, stiffness, damping, and natural frequency (ω_n) collectively constitute the modal parameters of a system. These parameters control the system's behaviour. For a given input or excitation imposed on the system a corresponding response or output will result.

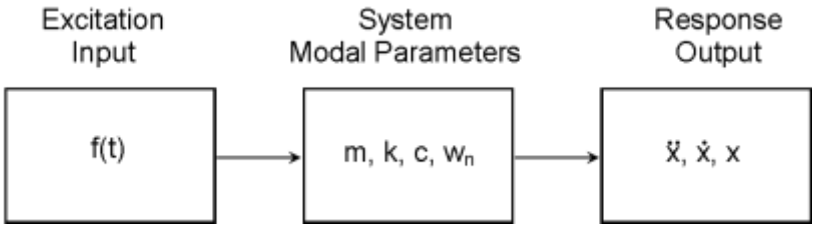

Figure 7: Dynamic system configuration

Damping corresponds to the energy dissipation within a given structure or system and is summarized for concrete arch dams in Table 5.

Table 5: Damping in concrete arch dams (USACE, 1994: 7-11)

Location of Damping	Type of Damping	Description
Concrete Arch	Friction	Internal friction within: • Concrete material • Construction joints
Foundation Rock	Radiation	Propagation of elastic waves away from the dam wall
	Hysteretic	Sliding along cracks/fissures
Reservoir	Refraction	Absorption of the energy by: • Reservoir bottom • Upstream water body

Dynamic systems can be simplified as single or multiple degree of freedom (SDOF/MDOF) systems depending on the complexity of the system. A degree of freedom (DOF) represents the number of independent coordinates in space required to describe the motion of the system (rotations and displacements in particular directions) (Moyo, 2013: 7).

The equation below represents the basic equation of motion of a damped, SDOF system subject to an external dynamic force.

$$m_e\ddot{x}(t) + c\dot{x}(t) + k_e x(t) = f(t) = f_0\cos(\omega t) \quad (2.3)$$

$m_{e:}$ Equivalent mass
c: Damping
k_e: Equivalent stiffness
f_0: Amplitude of excitation force
ω: Excitation frequency
t: Time

As the excitation frequency approaches the natural frequency, the system approaches resonance and the dynamic response is controlled primarily by the damping. At resonance the displacements of the structure in response to the dynamic loading becomes significantly amplified. Therefore it is the excitation

frequency and not the amplitude of the excitation force which is the significant factor when concerned with the magnitude of the response of a dynamic system (Moyo, 2013: 56).

Dams in Southern Africa are rarely exposed to large dynamic excitation, often caused as a result of earthquakes, compared to world standards (Brandt, 2011: 6), but are continually subject to micro-seismic loading during operation. Therefore the structural system can be simplified as a damped, free vibration response system with the input or excitation force being the ambient vibrations recorded on the structure during operational conditions (Moyo, 2014: 2). During large dynamic excitation the excitation frequency may approach the natural frequency of the structure and cause resonance. Coupled with large excitation forces the response of the structure may become exaggerated. In this case it would be more appropriate to represent the system as a damped, forced vibration response system (Moyo, 2013: 53).

Structural Health Monitoring

Comprehensive structural health monitoring (SHM) systems have been intensified in recent years especially within the dam industry. This is due to the aging infrastructure, loss of institutional knowledge, and significant economic and social implications associated with failure, especially for large dams with high hazard potential. The objective of SHM systems is to track the structure's integrity over time, and to assess any damage (Chang, et al., 2003: 257) or change in structural parameters as a result of remedial works. The process involves response data acquisition through relevant instrumentation, analysis, interpretation of this data, and storing the results for future reference and comparison.

Ambient vibration monitoring (AVM) is a form of SHM which aims to determine the dynamic properties of a structure. The ambient vibrations recorded on a dam structure have been shown to exhibit similar response signatures when compared to the larger, macro excitations caused by earthquakes and forced vibration tests (Okuma et. al., 2008: 8). The significance of this type of testing is that it gives insight into the dynamic system of the actual structure in operation. Therefore, AVM is often referred to as Operational Modal Analysis (OMA) (Moyo, 2014: 2). This method is opposed to forced vibration testing which stimulates the structure artificially. For large, stiff civil structures such as dams, it is difficult and expensive to artificially stimulate the structure. Therefore, the benefits associated with AVM are that it is economical, convenient, and records data which is representative of the as-built structure during operation (Ibid.: 32).

The dynamic system consists of dynamic modal parameters and structural parameters. The dynamic parameters include natural frequency, mode shapes (φ), and damping ratio (ζ), which are extracted from the data through data processing techniques. The natural frequency is related to the structural parameters of stiffness and mass as defined in the equation below (Moyo, 2013: 21).

$$\omega_n = \sqrt{\frac{k}{m}} \quad (2.4)$$

Once the system has been defined for a period of time the structural performance can be assessed, tracked over time, and used to develop calibrated finite element models. Shifts in the natural frequencies and in the mode shapes may be indicative of changes to the structural parameters, namely the stiffness of the structure. However, modal parameter shifts are also sensitive to changes in temperature, moisture, and other environmental factors (Chang et al., 2003, 258). Therefore, the interpretation of the recorded data requires significant analysis by experienced engineers who have a good understanding of the structure. This will enable the tracking of trends in the behaviour which may potentially be linked to deterioration and impending failure.

Theoretically the ambient vibrations result in broadband excitation causing all modes of vibration to be excited. However in reality the input has a certain spectral distribution due to differences in weighting of specific modes (Moyo, 2014: 6). All of the structure's modes may not be excited at any given moment and this emphasizes the importance of accumulating AVM records over many periods throughout the operational life of the structure.

2.3.3 Failure modes

Dam safety is defined as a dam's "adequacy against an uncontrolled release of reservoir water" (FERC, 1999:11-2). The result of uncontrolled release of impounded water is downstream flooding which can have catastrophic effects on life, property, and infrastructure.

Operational failure modes occur during normal operation of the dam. The causes range from human error to mechanical malfunction. These failure modes are summarised in Table 6.

Dams may also fail due to the integrity of the structure or the founding conditions not being able to resist the imposed loads acting on the structure. The major structural failure modes associated with concrete arch dams are discussed in the following sections.

Table 6: Operational Failure Modes of Dams

Cause		Mode of failure
Human Error	Negligence in terms of outflow release and water level within dam	Over-topping and/or large out-flow
Maintenance	Lack of lubrication of moving mechanical parts	Faulty operation of gates and outlet works leading to overtopping and/or large out-flow
	Fatigue fracture and loose bolts in gates	
Mechanical Malfunction	Gates fail to open	Overtopping
	Gates open inadvertently	Large outflow
	Outlet works such as valves fail to operate	Overtopping
Technological Malfunction	Communication breakdown	No warning downstream in case of large outflow
		No warning of large inflow from upstream leading to overtopping
Reduced storage capacity	Siltation	Overtopping and/or large out-flow
Reduced release capacity	Debris plugs spillway (log boom failure)	Overtopping
	Ice attack on outlet works	
	Loss of access to operate gates	
Other	Over pumping of upper reservoir in pumped storage project	Overtopping and/or large out-flow
	Loss of power supply resulting in inoperable gates	

Concrete Over-Stressing

Concrete will fail in either compression (crushing) or tension (cracking) when the loading causes stresses which exceed the capacity of the concrete. As the load on the structure is increased to capacity, internal micro-cracks develop into stable larger cracks and the stress strain behaviour varies from linear to non-linear. This results in permanent deformation and strain of the concrete. When the concrete is stressed beyond its capacity the cracks become unstable, fracture, and ultimately leads to material failure (Gillian et. al., 2011: 175).

Vertical construction joints exhibit little to no tensile strength and in the event of significant seismic excitation these joints become vulnerable. Earthquakes impose seismic tensile arch stresses at high frequencies on the dam wall. This rapidly opens and closes the construction joints when the limited tensile capacity of the joints is exceeded. These stresses also tend to increase the tensile cantilever stresses throughout the dam wall. When the tensile capacity is exceeded by this tensile cantilever stress a horizontal joint forms and is most likely to occur at the relatively weaker construction lift joints (cold joints). The heel of the dam wall is an area that is vulnerable to cracking failure due to the maximum tensile stresses which exist during the operational hydraulic loading. The combination of the open vertical joints and

newly formed horizontal joints may lead to the formation of unstable blocks (See Figure 8). In the case where a block fails, the stabilizing compression (arch) stress within the dam can no longer be effectively transferred to the foundations and the remaining structure is compromised and at risk to failure. Slip planes or plastic displacement of the foundations are similar to the abovementioned case. In these cases instead of the seismic tensile arch stresses, the displacement may potentially cause the vertical construction joints to open (Ghanaat, 2004: 4).

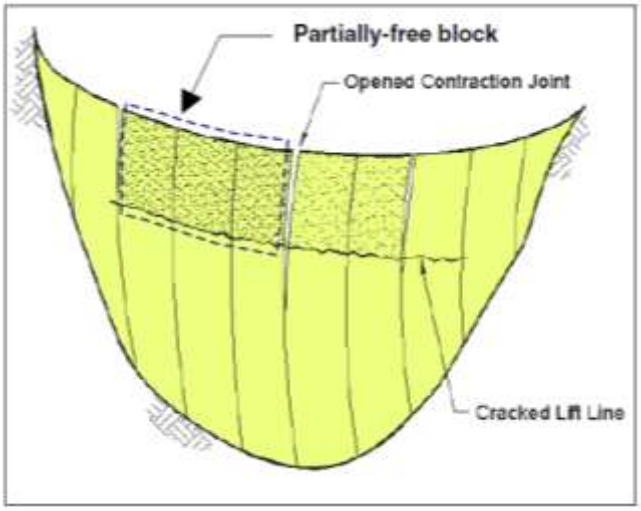

Figure 8: Unstable blocks during seismic loading (Ibid.)

Alkali Silica Reaction (ASR) causes swelling of the dam wall predominantly on the upstream face (See Section 2.3.4). Depending on the severity of the deterioration there is a reduction in stiffness, strength, and modulus of elasticity at the affected area (Oberholster, 2009: 211). In effect this reduces the cross sectional area of the dam. This could have significant structural implications especially if the structure is a thin arch. The swelling also results in a re-orientation of the forces within the arch. Instead of acting perpendicular to the wall-foundation interface on the downstream face, the principal stresses re-orientate into a more parallel orientation (Oosthuizen, 2004). As a result the dam resists loading in a manner it was not designed for and causes the arch to transfer the forces in a way which may initiate sliding in areas where the foundation or dam wall is more vulnerable. Once the resistance of the compromised structure is overcome by the loading, cracks and hinges will develop and could lead to failure (Ibid.).

Sliding Instability

The material characteristics of the concrete dam wall and foundation are notably different. This interface acts as a discontinuity with a potential for sliding failure. Arch dams transfer a significant portion of the imposed loads to the abutments as hoop stresses, therefore the structure is essentially 'wedged' into the foundations (Ibid.). This lowers the likelihood of central foundation failure especially in narrow-V topographies. However certain aspects do make arch dams more susceptible to this mode of failure.

Arch dams built within wider topographies tend to develop dominant cantilever action in resisting the imposed loads (Shaw, 2015: 324). As a result the central foundation becomes much more stressed as the maximum compression forces develop at the toe of the dam wall. In the case where the dam wall-foundation bond is inadequate to resist the developed stress, sliding failure may occur.

The degree of slenderness of a dam influences the structures susceptibility to cracking at the dam-foundation interface. Lombardi and Fanelli (1992) propose that the slenderness and height of a dam relates to the total shear resistance of the dam-foundation interface. The greater the slenderness ratio (as defined by Lombardi) and height of the arch dam, the lower the shear capacity of the structure.

Pore pressure and uplift forces are as a result of the interaction between the dam wall, impounded water, tail water, and foundation. As concrete is a permeable material, water permeates through the voids following the phreatic profile. The water then pressurizes within these voids resulting in a tensile stress gradient within the concrete. Uplift forces develop when this pressure acts normal to a discontinuity (Oosthuizen, 2014). High pore pressures are often caused as a result of inadequate drainage. The discontinuities may be in the form of;

i. Sub-vertical cracks at the heel of the dam
ii. Lift joints within the dam wall
iii. De-bonded dam wall-foundation interfaces
iv. Joints within the rock foundation

Uplift forces reduce the effective normal stress at the dam foundation interface and results in reduced frictional resistance. This lowers the stability of the structure and makes it more susceptible to sliding failure (Ibid.).

Foundation instability may lead to sliding failure in the case where the movement of certain supporting material would jeopardise the integrity of the structure. Un-fractured rock exhibits high intact strength. This inherent strength is significantly compromised by the presence of fractures and discontinuities especially when it is located in an area where significant forces are present. These discontinuities may be in the form of joints, faults, bedding planes, or any other geological change within the foundation (Gillian et. al., 2011: 179). Discontinuities, which may be viewed as potential failure planes, lower the shear capacity of material and increases the risk of shear failure. In the event of one potential failure plane, the failure is described as plane sliding (FERC, 1999: 11-2). When two or more of these planes intersect they may form wedges and could trigger wedge sliding (Ibid.). High pore pressures and uplift forces within the foundation will reduce the shear capacity of discontinuities increasing the likelihood of foundation failure (Ibid.: 11-10).

Certain conditions are required for foundation failure to occur. Firstly, the resultant shear stress imposed on the joint should be greater than the shear capacity of the

joint. The failure plane should be orientated in such a way that the foundation is capable of moving in a direction which could cause failure (Gillian et. al., 2011: 179). Therefore the direction of sliding must intersect a free surface in the downstream direction. Due to the high strength of intact rock, failure becomes more probable the lower the amount of intact rock required to be sheared in order to induce sliding failure. Two or more potential failure planes may result in wedges of various sizes depending on the individual joint orientations and their connectivity with each other. Once again a free surface is required for abutment instability to be a potential failure mode. The Malpasset dam failure of 1959 (FERC, 2014: 35) was as a result of abutment instability (See Figure 9).

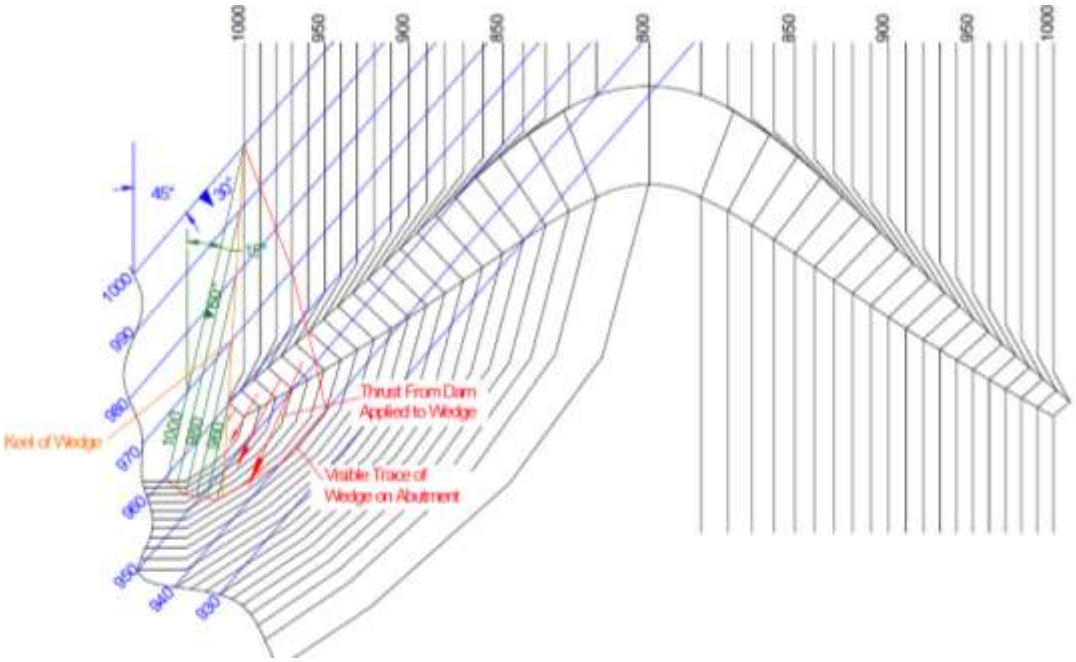

Figure 9: Abutment instability causing Malpasset dam failure (Ibid.: 42)

As previously stated the orientation of a discontinuity is important in assessing the potential of sliding failure as faults naturally have a reduced shear resistance compared to the intact rock foundation. The permeability of the discontinuity is important because it could provide a passage for seepage through the dam wall, or result in abnormally high uplift forces at certain locations in the foundation and this will decrease the shear stability (Oosthuizen, 2014).

Downstream plunge pools are natural dissipating structures for arch dams. In some cases where no concrete apron is provided the erosion of the foundation accompanying the dissipation of energy could impact on the sliding stability of the structure (Gillian et. al., 2011: 181).

2.3.4 Alkali Silica Reaction

Overview of reaction

ASR is a chemical reaction occurring within the pores of the concrete matrix between alkali and reactive silica minerals to form an expansive alkali-silica gel within and on the surface of the aggregate. As the silica component originates from certain aggregates within the concrete the reaction is also referred to as alkali-aggregate reaction. The gel product absorbs water and swells within the concrete matrix and cracking will occur once the expansive pressure exceeds the tensile capacity of the concrete (Oberholster, 2009: 189).

Factors influencing the reaction

In order for the reaction to take place, all of the following factors should be present. Sufficient alkalinity within the pore solution, sufficient reactive minerals within the aggregate, and conducive environmental conditions (Ibid.: 190).

Usually the main source of alkalinity contributing to the pore solution originates from the cement within the concrete. The highly soluble neutral sulphates dissociate in the solution and increase the concentrations of Na^+, K^+ and pH levels (Ibid.). Alkalinity may also be increased due to the products of the hydration process. See Equations 2.5 and 2.6 (Addis, 1998: 73). In the equations below H represents water.

$$C_3S + 6H \rightarrow C_3S_2H_3 + 3Ca(OH)_2 \quad (2.5)$$

$$C_2S + 4H \rightarrow C_3S_2H_3 + Ca(OH)_2 \quad (2.6)$$

Alkali's are produced from the reaction of calcium hydroxides (Portlandite) with alkali minerals within the aggregate, which then dissociate in the pore solution. The calcium hydroxide (and consequent increase in pH levels) also stimulates the development of a "passivating" layer which protects reinforcement from rusting within the concrete matrix (Ballim et. al., 2009: 215). In the case of ASR, these alkali's have a much more detrimental effect as it increases the risk of the swelling reaction. Alkali's may also be introduced into the system externally by sea water, vapour, and salt containing ad-mixtures (Oberholster, 2009: 190).

The fine and course aggregate should be dense and contain sufficient amount of alkali-reactive minerals. The rate of the reaction depends on the amount of reactive minerals, the reactivity, and the surface area of exposed reactive mineral. Aggregate which has been identified as potentially alkali reactive within the Eastern Cape of South Africa are the following;

i. Cape Super Group – Ortho-quartzite of the Table Mountain Group
ii. Enon Formation – Quartzite pebbles
iii. Quaternary Period – Quartzite pebbles (Ibid.: 192)

The rate of swelling approximately doubles for every 10°C increase in mean annual ambient temperature (Ibid.). The reaction also requires the concrete to be moist and exhibit an internal relative humidity of 75-85% or higher (Ibid.). Daily and seasonal fluctuations in temperature and moisture increase the number and width of cracks associated with ASR.

Indicative features of ASR

The swelling effect associated with ASR causes internal stress which results in cracking if the tensile capacity of the concrete is exceeded. The cracks are relatively large (compared to shrinkage cracks), with the pattern for unrestrained concrete being random. This is often referred to as "map" cracking (Ibid.: 205) and is shown in Figure 10.

Figure 10: Classic ASR induced map cracking (Poraver, 2016)

Restrained or load bearing concrete structural elements significantly influence the crack pattern. The macro-cracking tends to be parallel to the direction of constraint. For example, columns are unrestrained laterally therefore the concrete swells in this direction and causes vertical cracks or increases existing structural cracks (Oberholster, 2009: 205). In concrete arch dams the concrete expansion caused by ASR also results in the closure of joints, warping of concrete and misalignment of certain effected elements (Ibid.).

The ASR product or gel may be visible on the surface cracks of the concrete and often form white stains on the perimeter of the aggregate (See Figure 11). Even though the cracks are caused by the reaction, the voids are sealed due to the leaching of the gel product. This limits the ingress of other substances through the cracks.

Figure 11: Cored sample of ASR deteriorated concrete (Concrete Microscope Library, 2016)

Another indicative feature of ASR on the concrete surface can be dark discolouration, which may be due to dampness, with lighter shades immediately surrounding the cracks (Oberholster, 2009: 206), as shown in Figure 12.

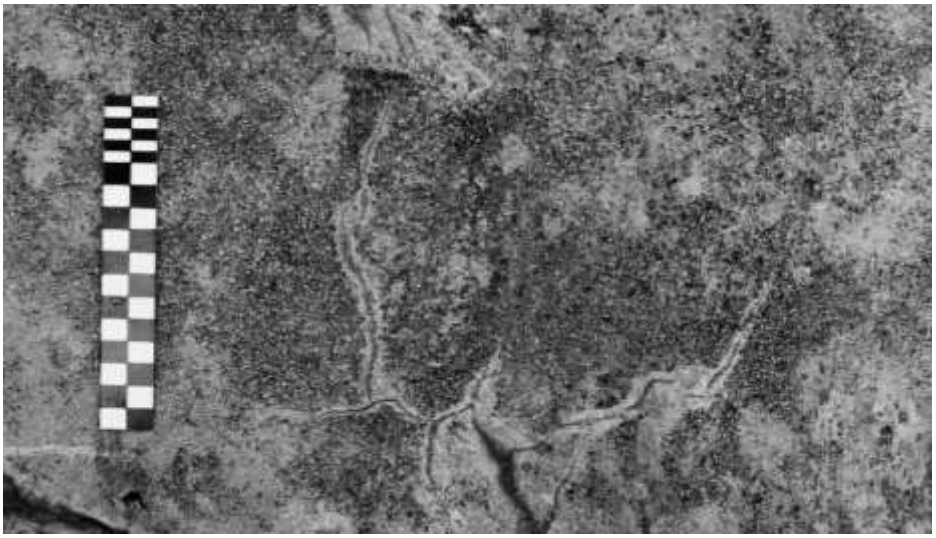

Figure 12: Discolouration arround ASR related cracks (Ibid.: 207)

Structural effects

ASR may in some cases increase the severity of existing structural cracks and as a result degrade the structural integrity even further. The extent, rate, and location of ASR affected areas vary throughout the concrete. For this reason the structural effects on a given element or structure is case specific.

Table 7 shows the effects of ASR on the mechanical properties of concrete. In practice these properties should be larger than the figures in the table due to restraint from adjacent material and bi/tri-axial stress states (Ibid.: 211). It is clear that the properties do decrease the more the concrete is affected by ASR. The

findings also show that tensile strength and stiffness are most significantly reduced due to the deterioration.

Table 7: Affect of ASR on concrete at 28 days (Oberholster, 2009: 211)

Property	Percentage strength as compared with unaffected concrete for free expansion (microstrain) as indicated				
	500	1 000	2 500	5 000	10 000
Compressive strength*	100	85	80	75	70
Uniaxial compressive strength**	95	80	60	60	-
Tensile strength	85	75	55	50	-
Elastic modulus	100	70	50	35	30
* Cube ** Core, length:diameter ratio = 2,5 or greater					

2.3.5 Instrumentation

Surveillance is defined as close observation of a structure to prevent or detect problems and it encompasses monitoring and instrumentation (Oosthuizen, 2014). Monitoring uses equipment or instrumentation to gather information such as loading and response of the structure, to assess performance, and to continue assurance of the safety of the dam throughout its service life. Therefore surveillance is a process of systematic review. Instrumentation monitoring programs for dams compliments dam safety inspections and surveillance programs.

The objective of instrumentation monitoring programs is to diagnose the state of the structure, predict its behaviour, and identify potential failure modes. The instrumentation implemented should answer specific questions that take into account the dam structure type, site specific geotechnical conditions, and environment conditions (Ibid.). The diagnostic aspect is to verify design parameters and to identify the causes of adverse events. Observations from monitoring systems can shed light on unknown variables and assumptions made in the design phase. Therefore it allows for refinement of the analysis of the existing structure and improves future designs. Instrumentation also allows the cause of adverse events to be identified through the recorded data and remedial work effectiveness can also be tracked with this data (Moyo, 2014: 2).

Parameters which may need to be monitored in concrete dams include:

i. Displacements
ii. Cracks
iii. Settlement
iv. Seepage
v. Stress and strains
vi. Uplift pressures within foundation
vii. Integrity shifts (Natural frequencies)

2.4 Chapter Summary

This chapter reviews arch dams from the design stage to construction, and the management of the structure over time. Each section gives insight into aspects integral in understanding how the structure was designed to resist the imposed loading, and the reasons for deviations from this behaviour.

The design of arch dams is largely dependent on the specific site conditions. Competent flank foundations are required as the structure resists the loading to some extent via arch action. Therefore the strength of the concrete is important as the loading is resisted structurally and to a lesser extent by mass. FEA have been used in recent times in the design of new arch dams as well as in the analyses of existing structures. By mathematically modelling the structure and loading conditions accurately enough, a realistic response of the structure can be simulated (Shaw, 2015: 321). It is also a particularly useful tool for assessing remedial alternatives during rehabilitation of existing dams.

The correct construction practice is important in order to materialise the design. The main construction considerations are highlighted such as foundation preparation and grouting. It is essential that the arch is grouted adequately to ensure that the structure acts as a monolith as opposed to individual cantilevers.

Responsible management of large dams is a statutory requirement and calls for a deep understanding of the structural system. Dam safety engineers need to identify potential failure modes, understand the structural response, and consider the effects of deterioration such as ASR. Monitoring systems are crucial tools which give insight into the safety evaluation of dams.

By exploring the various stages associated with arch dams a better understanding of the structure and its response to changing loading over time can be achieved.

CHAPTER 3

3 METHODOLOGY

3.1 Introduction

This chapter focuses on Kouga Dam as the case study of the thesis. The chapter begins with a brief background of the structure followed by a review of previous dam safety evaluations where the important findings and foundation conditions are noted. Lastly the chapter describes in detail the monitoring system installed at the dam.

3.2 Kouga Dam

3.2.1 Locality

The locality of Kouga Dam is shown in Figure 13.

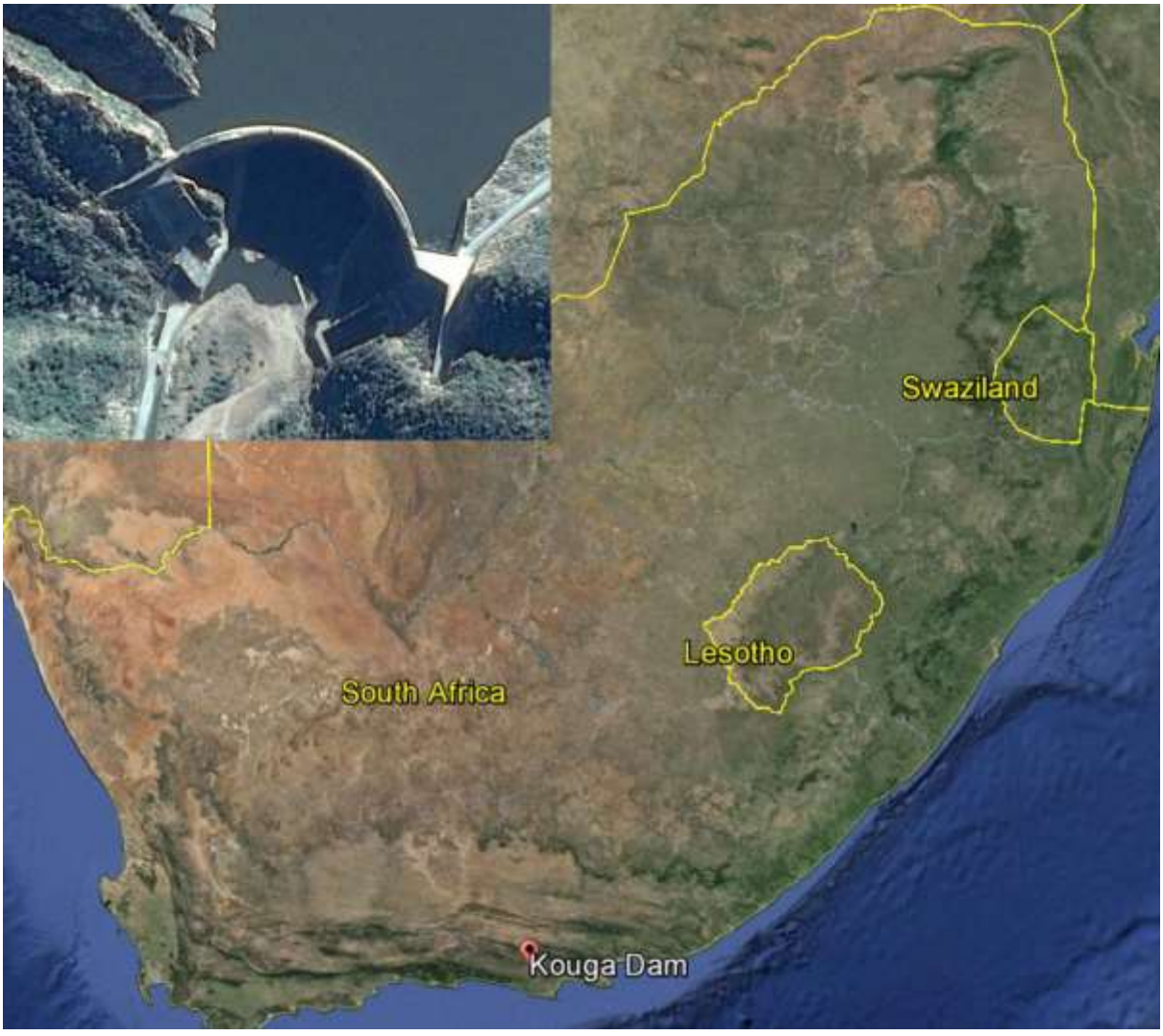

Figure 13: Locality of Kouga Dam (Google Earth, 2013)

3.2.2 Dam Characteristics

Name of dam	Kouga Dam[3]
Locality number:	L820-01
River:	Kouga River
Nearest town:	Patensie
Distance to nearest town:	27km West
Province:	Eastern Cape
Latitude:	33°44'30"
Longitude:	24°35'15"
Wall type:	Double curvature concrete arch
Crest length:	317m
Wall height (LFL to NOC):	69m
Wall thickness (FSL):	6.93m
Wall thickness (NOC):	6.43m
Level of UNOC:	RL169.164m
Level of NOC:	RL156.972m
Level of FSL:	RL149.352m
Level of gauge plate zero:	RL 54.950m
Storage capacity:	128.490×10^6 m^3
FSL area:	554.5 ha
Purpose:	Irrigation, domestic, and industrial use
Owner:	DWS
Designer:	DWS
Contractor:	DWS
Completed:	1969

(Dam Safety Office [DSO], 2011)

[3] Formerly known as Tweerivieren Dam and Paul Sauer Dam

3.2.3 Background

General

Kouga Dam is located approximately 27km West of Patensie, on the Kouga River in the Eastern Cape. The dam forms part of the Gamtoos River Government Water Scheme (GRGWS). It was designed, constructed, and owned by the then Department of Water Affairs (DWA), now known as the Department of Water and Sanitation. Construction on the dam was completed in 1969 (DSO, 2011).

The dam is a double curvature, concrete arch dam (See Figure 14) and was the first of its kind to be built in South Africa. It supplies water primarily for irrigation purposes to the Gamtoos River Valley and also supplements the water supply to the Nelson Mandela Metropolitan. The initial design made provision for the possibility of future raising in order to increase the capacity and provide additional water supply to Port Elizabeth. The dam has an approximate height of 69m and crest length of 317m. The spillway system comprises of a centrally located, uncontrolled ogee spillway and a chute spillway on the left flank which is controlled by two radial gates. The outlet works releases into a concrete channel which is situated on the right flank and closer to the left flank a scour outlet can be found on the concrete lined apron. A post-tensioned concrete stress pad has been provided on the right flank and provides additional stiffness and restraint against sliding failure. The dam was constructed on a pulvino pad which is a thicker layer of concrete which assists in distributing the forces from the dam wall to the foundations. Kouga Dam is classified as a Category III dam due to its high hazard potential rating and size class.

Figure 14: Kouga Dam

Alkali Silica Reaction

Dam safety evaluations and laboratory tests have identified the presence of ASR at Kouga Dam. The dam structure and the surroundings exhibit the three main factors which contribute to the ASR. These factors include high levels of alkalinity within the cement used, reactive minerals associated with the aggregate, and conducive environmental conditions.

The cement used during construction (1960's and 1970's) originated from Port Elizabeth and exhibited a Na_2O equivalent of greater than 0.8% (Elges et. al., 1995: 2). Oberholster (2009: 191) states that a Na_2O equivalent of greater than 0.6% is regarded as a high alkali cement which can contribute to the presence of ASR. In addition the entire catchment of the dam also consists of quartzitic sandstone which are identified as potentially alkali reactive (See Section 2.3.4). The alluvial deposits, which consist of the same quartzitic sandstone, in the Kouga River were processed and used as course and fine aggregate for the concrete during construction. The orientation and conditions on the structure are also conducive to ASR. The ASR is likely to occur on the upstream face of the dam wall because this is the interface which has constant exposure to moisture. The orientation of the upstream face is north facing and as a result is exposed to direct sunlight for most of the day. This translates into high temperatures that fluctuate daily and which increase the rate of the reaction.

After 1981 tests were conducted in order to verify ASR on the structure. The tests were conducted on concrete cores drilled from the structure and included petrographic examinations, X-ray diffraction analysis, scanning electron-micrograph and standardless Energy Dispersive X-ray (EDX) analysis, drying shrinkage, and wetting expansion tests (Elges et. al., 1995: 4). ASR was confirmed from the tested samples and to date no further examinations were done to determine if the reaction has stabilized.

3.2.4 Geology

The rock which the dam is founded on is characterized by stratified and jointed quartzitic sandstone of the Table Mountain Group (TMG). The bedding planes dip approximately 50° downstream and slightly towards the left flank (See Figure 15). Between this competent rock there are inter-bedded layers of weaker, consolidated phyllite which generally vary in thickness, up to a maximum of approximately 0.3m (Hobbs et. al., 1967: 257). This phyllite material deteriorates rapidly when saturated and exposed to air. Hobbs (1967: 257) also noted that boreholes drilled in the outlet tunnel showed that the quality of the foundation improved considerably with depth.

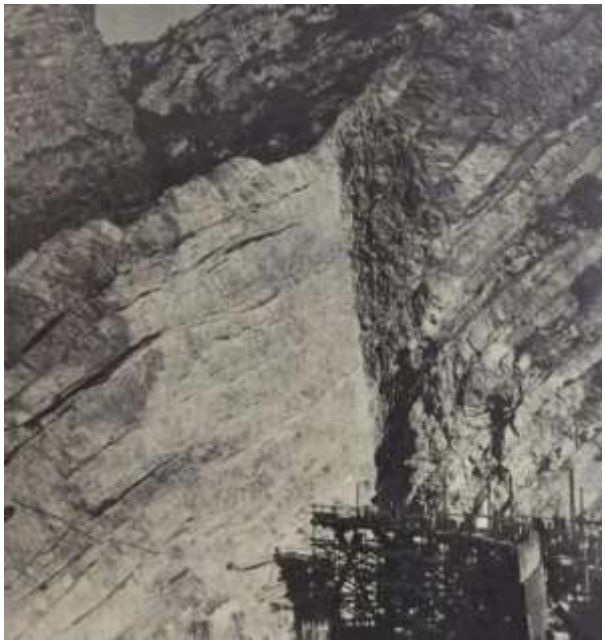

Figure 15: Close-up of right flank abutment (Hobbs et. al., 1967: 255)

3.2.5 Right flank foundation conditions

General

Forbes Dick (1989) concludes that the left and central foundations of Kouga are stable due to the favourable orientation of the strata with relation to the arch thrusts. The arch forces on the left flank act almost perpendicular to the strike of the bedding planes and this keys the arch into the abutment.

The right flank of the arch abuts into a spur on the mountain (See Figure 16). Upstream of the spur is a gully and on the downstream is a deep embayment. The embayment results in less support against the arch thrust. During excavation of the right flank foundation phyllite seams were encountered which rapidly deteriorated. This raised further concerns regarding the integrity of the foundations.

Figure 16: Right flank prior to completion and stress pad remedial measures (Hobbs et. al., 1967: 654)

Remedial measures

Unfavourable conditions were identified on the right flank foundation during construction, and as a result remedial measures were undertaken to improve the foundation conditions and to ensure the stability of the right flank. These remedial measures were also undertaken in light of the Malpasset Dam failure noted in Section 2.3.3. Hobbs (1967: 660-665) notes the following remedial measures undertaken at the dam;

i. Treatment of phyllite seams
ii. Provision of extensive concrete apron
iii. Foundation grouting
iv. Increasing the radii of the arch rings
v. Reinforced concrete thrust pad
vi. Capping beam with slab on surface of right flank
vii. Drainage and grout curtains

The primary function of the capping beam (See Figure 17) is to act as a thrust block and to redistribute the resultant forces from the upper arch into the right abutment as parallel to the strike of the strata as possible. This allows more bedding planes to contribute in resisting the thrust. Foliation or lifting of the strata is reduced the more parallel the thrust is relative to the strata. This lowers the force perpendicular to the bedding planes.

The stressing slab is anchored into the right abutment with 62 high tensile steel cables. These cables are anchored to a depth of 40m and post-tensioned to 245 tonnes. The anchoring confines the layers of strata together into a monolith and as a result deepens the load carrying rock mass. This further reduces the tendency of buckling failure of the strata under the arch thrust load.

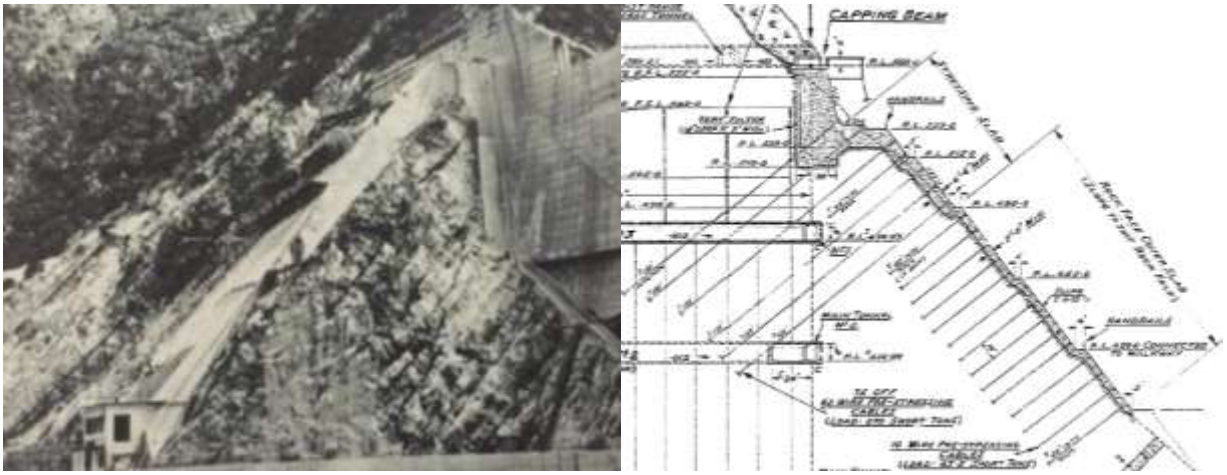

Figure 17: Capping beam and stressing slab on right flank (Hobbs et. al., 1967: 664,650)

3.2.6 Loading on right flank foundation

Potential failure mode

Figure 18 shows the stratification of the foundation and arch thrusts of the structure. Forbes Dick (1989: 13) notes that the most probable potential failure mode in the direction of thrusting on the right flank is shear across the bedding planes in combination with tensile foliation of the phyllite layers. The bedding layers act as cantilever slabs that are stacked on each other, with the fixed end within the abutment and the free end closest to the dam. Movements within the foundation on the right flank may be initiated by deteriorating phyllite layers and produce near perpendicular forces relative to the bedding planes, acting in a downstream direction. This would result in excessive bending moments on the bedding layers, cause the layers to buckle under the load, and initiate a shear failure downstream.

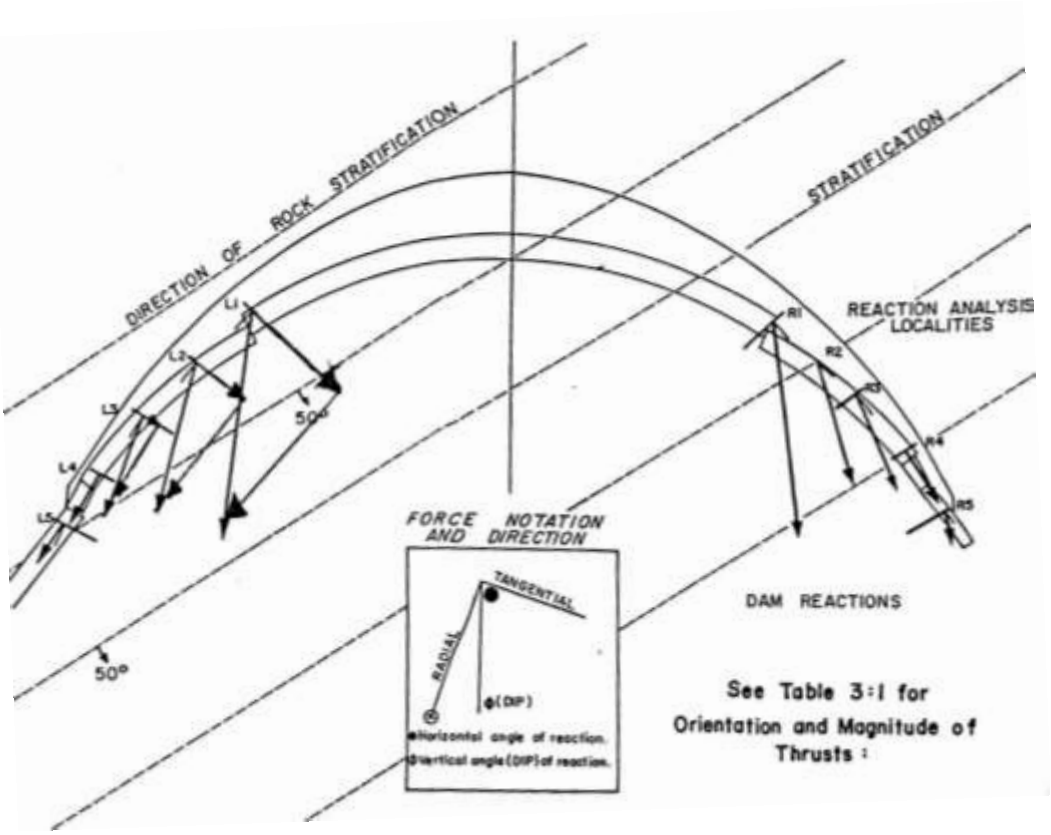

Figure 18: Arch and cantilever reactions on the rock foundation in relation to the stratification dip and strike directions (Forbes Dick, 1989: 14)

Arch thrusts

Due to the valley shape and arch design the structure transfers the imposed loading to a larger extent via cantilever action to the central and lower flank foundations (The transfer of forces to the foundation is discussed in Section 4.4). The magnitude and dip of the resultant forces decrease from the centre of the arch to the abutments (See Figure 19) with the orientation tending towards the right abutments.

The forces which could initiate shear failure occur adjacent to the spillway due to its large resultant and downstream components. The thrust has a similar dip to the bedding planes and is directed towards the right abutment well below the power station. The thrusts closer to the abutment are less favourable in terms of the orientation as the resultant forces are near horizontal. The resultant and downward components are significantly lower compared to that closer to the spillway. The upper arch thrusts on the capping beam and assists in redirecting the forces along the strata below the stress pad.

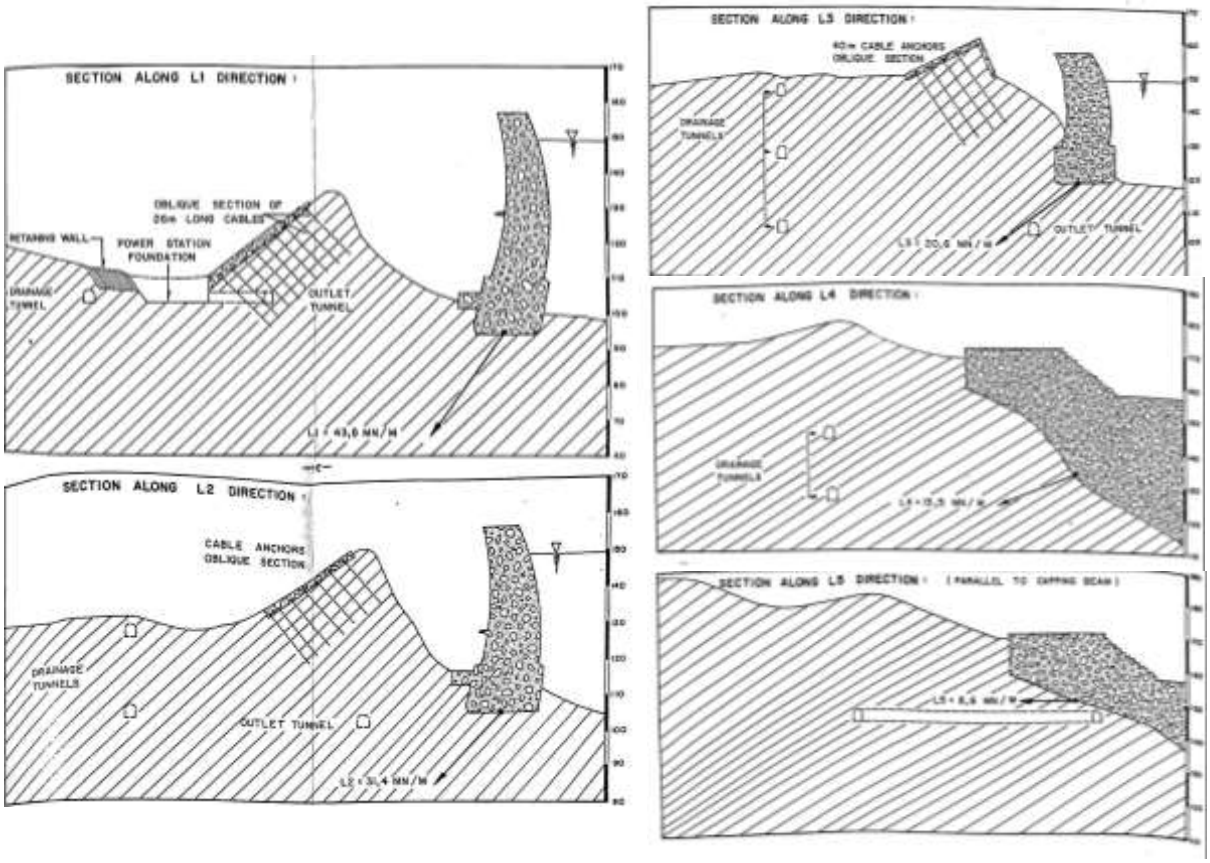

Figure 19: Resultant forces on the right foundation (Forbes Dick, 1989: 16)

The arch thrusts on the right flank and adjacent to the spillway seem favourable due to the strata which keys in the arch. Closer to the abutment the capping beam and anchored stress slab reduce the risk of sliding failure due the redirection of the thrusts to displace a much larger rock mass in order to induce failure. At present the embayment is not a concern with regards to a lack of abutting mass, due to the direction of the resultant forces of the wall being well into the foundation in a mostly downward direction. The effect of ASR on the re-orientation of arch thrusts may be a cause for concern and should be investigated in order to assess the safety of the right foundation.

3.3 Monitoring System

3.3.1 Overview

The previous dam safety evaluations at Kouga dam have raised concerns regarding the potential instability of the right abutment and the aforementioned ASR. As a result the monitoring and surveillance of the dam has intensified. The following parameters were investigated and are summarized in Table 8.

Table 8: Investigated parameters

Type	Parameters	Description	Instrumentation
Load	Hydraulic	Water level	Gauge plates
	Temperature	Ambient, water, concrete	Thermometers
	Dynamic	AVM	Accelerometers
Response	Displacements	Dam wall face and crest	Geodetic surveys
			Global Navigation Satellite System (GNSS)/Global Positioning System (GPS)
			Crack width gauges
		Dam wall and foundation	Trivec systems
Integrity	Dynamic response	Natural frequencies and mode shapes	Processing of AV data

3.3.2 Water Levels

A gauge plate installed at the dam is used to record the water level on a daily basis. The gauge plate level refers to the height at which the water surface is above the lowest inlet level. This gauge reading can be converted to the corresponding reduced level above mean sea level and volume of water within the dam.

3.3.3 Temperature

A total of four thermometers have been installed on the upstream face of the dam wall. Two closer to the left flank and two closer to the right flank. Figure 20 shows the approximate locations (red dots) of the thermometers. The thermometers are estimated to have been installed at the gallery level. Temperature readings are recorded 4 times per day (6-hourly).

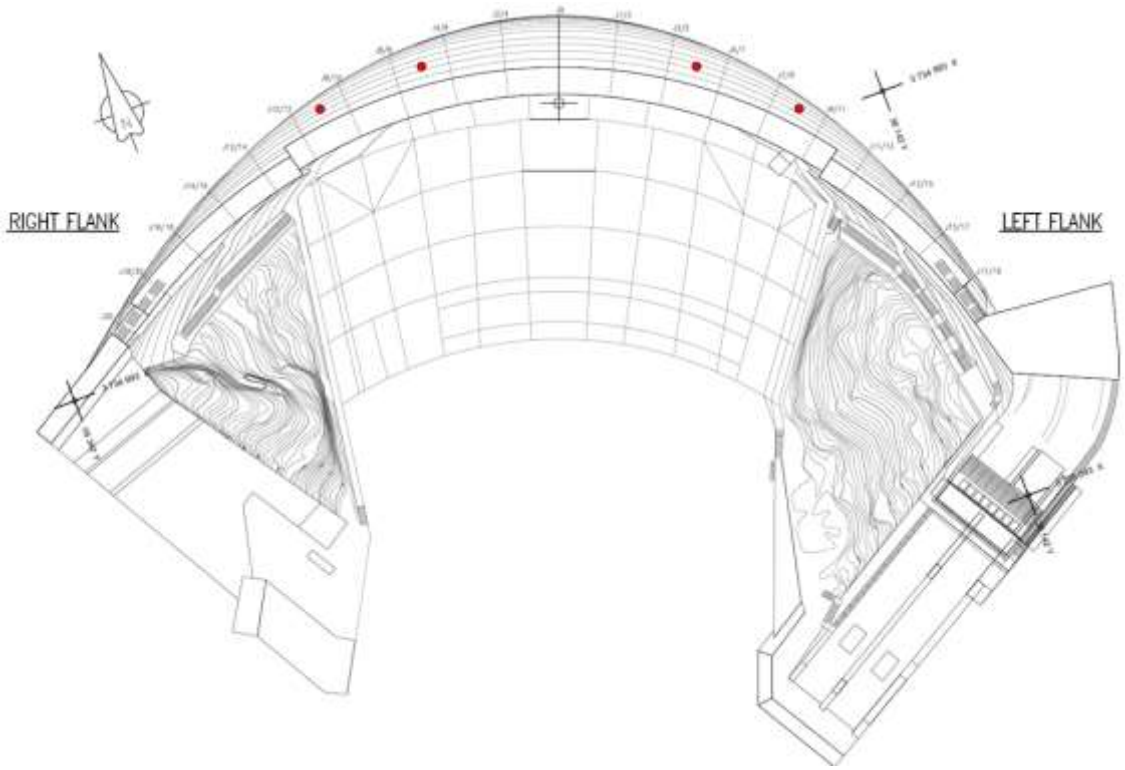

Figure 20: Top view showing locations of thermometers on upstream face

3.3.4 Displacements

Geodetic Network

The geodetic system uses a triangulation network of beacons and targets on the downstream face of the dam wall and is complimented by precise traverse measurements within the gallery. The final results are three dimensional displacements of the monitoring points. The accuracy in the x and y directions are approximately 0.3-0.5mm while the z (vertical) measurements are 0.1-0.2mm (Pretorius et. al., 2001: 210).

Figure 21 shows the location of measurement targets for geodetic surveys. The geodetic surveys are carried out twice a year, once during summer (March) and again during winter (September). The points investigated are all positioned at RL144.780m (gallery level) and measure displacements in three directions.

Three positions were investigated in detail and these are located at two quarter points and the mid-point of the dam wall. The right flank quarter point is represented by traverse station 111, the midpoint stations are 116 and 117, and the left flank quarter points are 122 and 123. The recorded displacements are referenced to a baseline date (15/12/1972) for comparison purposes.

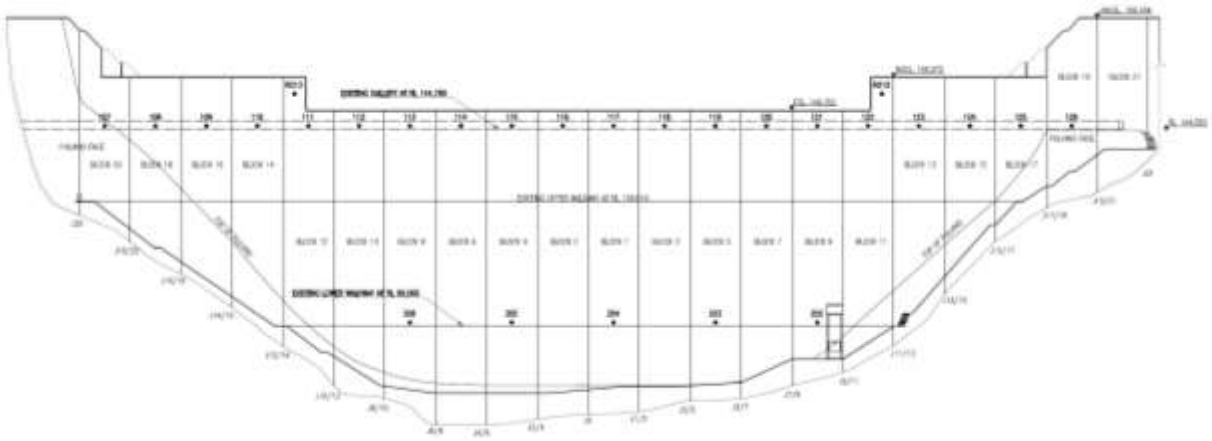

Figure 21: Downstream general elevation of monitoring points

GNSS/GPS

The GNSS/GPS is an automatic monitoring system that operates continuously to provide deformation information in the x, y, and z directions. It records displacements at a logging rate of 1 hour and allows the behaviour of the structure to be observed in much more detail compared to the geodetic survey data which only allows for data points every six months.

The installation layout includes two primary base sensors in the surrounding area of the dam structure. These include two secondary sensors on the dam structure and a server located in the outlet house. The base stations are used as reference stations for the relative positioning during post-processing. The two secondary sensors are positioned adjacent to the overspill section on the dam wall. The layout is shown graphically in Figure 22.

Figure 22: Kouga Dam GNSS/GPS Network (Pretorius & du Toit, 2014: 8)

The four Trimble Net R5 receivers and Trimble Zephyr Geodetic antennae are used to make the observations (See Figure 23). The features of the GNSS/GPS system are summarised below;

- Period of Observation: 24 hours
- Sampling rate: 10 seconds
- Tracking Interval: 1 Hz
- Continuous Logging Rate: 1 hour
- Minimum Number of Satellites: 5
- Satellite Elevation Mask: 5° (Ibid.: 6)

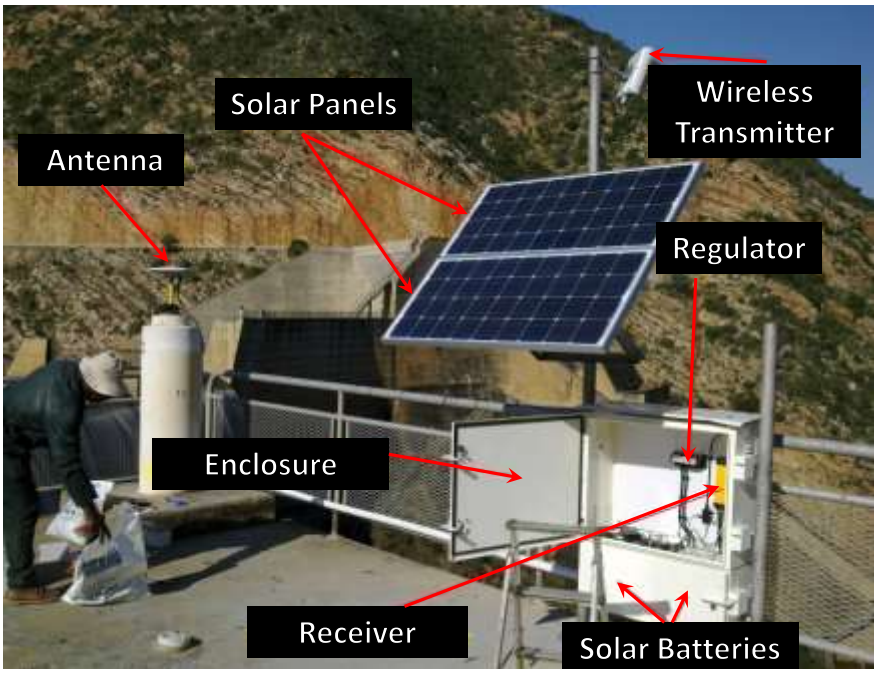

Figure 23: GNSS/GPS System at Kouga Dam (Ibid.: 4)

Crack width gauges

The then Department of Water affairs and Forestry (DWAF) developed in-house crack width measuring devices in the 1990's which were implemented throughout the country (Oosthuizen et.al, 2003: 600). The three dimensional crack width gauges are still used at Kouga and many other dams in South Africa despite a national upgrade to automatic crack width gauge systems. The device allows the crack widths (translations) and relative rotations (tilt) to be measured across cracks or joints. *Sinco* 3-D crack gauges from the USA have been installed within the gallery of Kouga dam, while the DWAF94 gauges are used to record the crack and joint displacements throughout the rest of the dam. The readings are manually recorded on a monthly basis with electronic digital indicator gauges. The accuracy of both crack width gauge types in the x (across the crack or tangential direction), y (vertical), and z (radial) directions is 0.02mm for all translations

For the purpose of this study the three dimensional crack width gauges located on the downstream face construction joints and gallery of the dam wall were investigated.

Trivec

The Trivec system measures the relative displacements in three directions (x, y, and z) at 1m intervals along a vertical borehole. Unplasticized polyvinyl chloride (uPVC) tubes which are connected with stainless steel measuring couplings are installed within the borehole and grouted into position. A measuring probe is lowered into the casings and records the displacements in all three directions at the various measuring points. The first set of readings acts as the baseline data set to which the future readings are compared. The measurements are done bi-annually, once during summer and another during winter. The equipment used for the system is shown in Figure 24.

Figure 24: Trivec system components (Naude, 2002: 4)

At first four probes were first installed at the dam (Kogr1-4) with the baseline readings taken between 2001 and 2002. In 2013 two more probes were installed. The majority of the Trivec systems are located on the right flank due to the concerns about the foundation stability. The locations of the Trivec systems are shown in Figure 25.

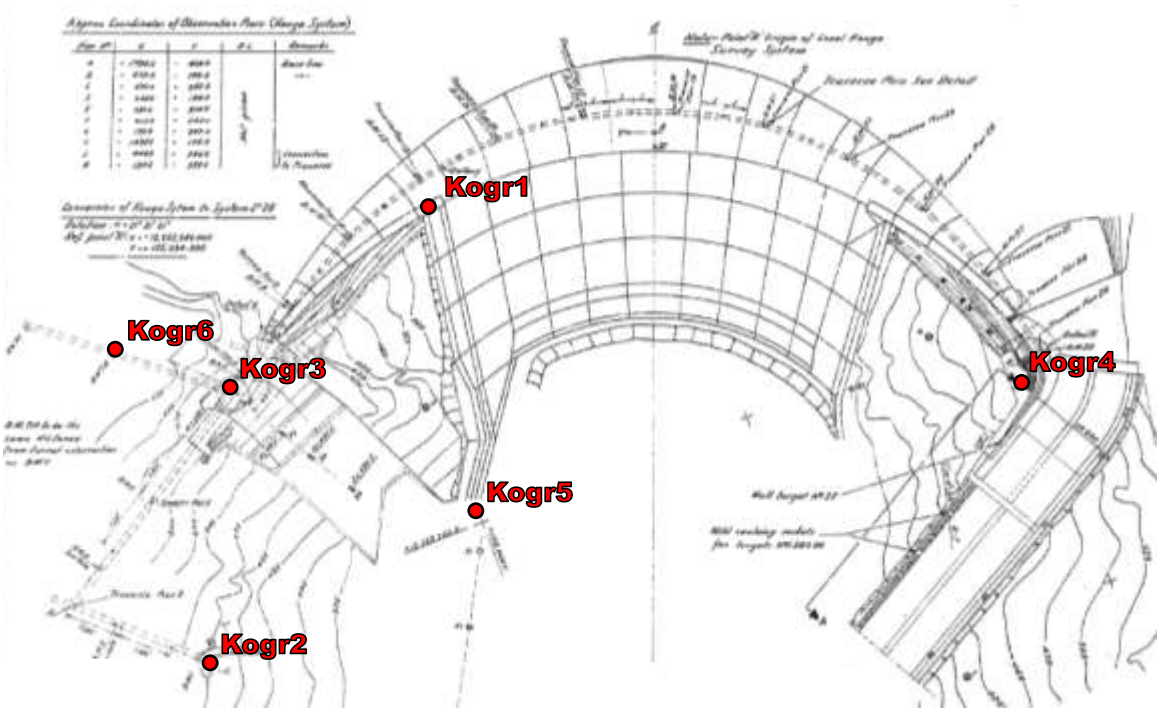

Figure 25: Locations of Trivec systems

Kogr1 is the only probe which has been installed through the dam wall and it extends approximately 25m into the foundation. Kogr2 and Kogr5 are located on the right flank and Kogr4 is on the left flank. Kogr3 and Kogr6 were installed in the lowest main inspection tunnel on the right flank. The installation level (highest measuring point on Trivec) and height of the boreholes are given in Table 9.

Table 9: Installation levels and height of Trivec systems

Trivec System	RL (m)	Height (m)
Kogr1	156.9	87.2
Kogr2	144.8	47.6
Kogr3	103.6	33.5
Kogr4	140.2	54.0
Kogr5	99.1	47.0
Kogr6	103.6	49.0

3.3.5 Ambient Vibration Measurements

Operational modal analysis (OMA) is used to extract the dynamic modal parameters during ambient conditions. The modal parameters include natural frequencies, mode shapes, and damping ratios. This method is often used on large civil structures because of the relatively low cost and the recorded measurements are comparable with that of forced vibration tests. The ambient loads that act on the dam during operation include, but are not limited to the following; wave action, wind, atmospheric pressure, and human activities.

Instrumentation

Kouga dam has an extensive AVM system in place to record the ambient vibrations. Accelerometers that are permanently positioned within the gallery measure the vibrations which are then recorded by a data acquisition system. Post-processing is done in order to extract the modal parameters from the recorded data. The equipment used at Kouga dam to record the ambient vibrations are listed below.

- Accelerometers

The permanent AVM system comprised of AC-2x tri-axial (Figure 26) accelerometer sensors manufactured by GeoSIG is used to measure the ambient vibrations acting on the structure. Some of the specifications associated with this accelerometer includes; bandwidth of 0.1-100Hz, dynamic range of >125 dB, and an accuracy of ±0.4 dB. The roving system used Q-Flex QA-700 accelerometers manufactured by Honeywell. Some of the specifications associated with this accelerometer includes; bandwidth of >300Hz, dynamic input range of approximately 30g, and resolution of <1µg (GeoSIG, 2010: 1, 2).

Figure 26: Tri-axial accelerometer sensor (GeoSIG, 2010: 1)

- Data Acquisition System

The CR-5P monitoring system (Figure 27) is also manufactured by GeoSIG and was used to monitor and record the accelerations of the structure. The dynamic seismic data logger digitized the data to a 24 bit resolution and at a sampling rate of up to 250 samples per second. The raw data is then downloaded to a computer (Figure 28) for processing and modal extraction.

Figure 27: Data Acquisition System

Figure 28: The computer used for data acquisition and processing

Test Layout and Procedure

The dynamic measurements were performed using two set-ups. One set-up was a permanent system which had a total of 21 tri-axial accelerometers with a fixed reference location. The other set-up used only six accelerometers and the travelling accelerometer method in order to cover all the blocks. The two systems were used in order to verify the recorded data. The accelerometers were placed at the centre of blocks 106 to 126 within the gallery of the dam (See Figure 29). The permanent accelerometers were housed inside survey brackets which were mounted on the

upstream side of the gallery wall while the roving accelerometers were placed on top of the brackets (See Figure 30).

Figure 29: Location of accelerometers within gallery

Figure 30: Roving and permanent accelerometers

The measurements were performed over three periods with the first in August 2011, the second in February 2014, and the third in March 2014. Trial measurements were done in order to test the system and to verify whether the data recorded was a realistic sample. For the roving set-up the data was recorded for periods which varied from 20-60 minutes. The permanent set-up recorded data continuously and only required the data to be downloaded from the data acquisition system in order to perform the data processing. A sampling frequency of 1000Hz was used for the measurements.

Data Processing

The dynamic modal parameters were extracted from the recorded acceleration data using ARTeMIS Extractor Pro 2010. The Enhanced Frequency Domain Decomposition (EFDD) method was used in order to determine the associated natural frequencies of the structure.

3.4 Chapter Summary

This chapter introduces Kouga dam as the case study of the thesis and provides a summary of the foundation conditions, loading on the structure, and ASR identified at the dam. In addition previous dam safety evaluations which have highlighted the instability of the right abutment as a potential failure mode are explored in greater detail.

The chapter outlines the monitoring system at Kouga dam and highlights how it has intensified over time as a result of the aspects identified in past dam safety evaluations. This chapter then discusses the layout of the instrumentation and measurement procedure associated with each instrument. The monitoring system records the imposed loading, structural response, and integrity of the structure. The parameters measured at Kouga dam and considered in this thesis include water level, temperature, displacement, and ambient vibrations.

CHAPTER 4

4 RESULTS AND DISCUSSION

4.1 Introduction

Monitoring systems are integral to dam safety surveillance. The chosen instrumentation is dependent on the type of dam, site specific conditions, and an understanding of which parameters are important for defining the structural behaviour and potential modes of failure. The specific parameters investigated at Kouga dam in order to deduce behavioural trends of the dam wall structure include; water levels, temperature, displacement data, and AVM.

This chapter presents the instrumentation results recorded at Kouga dam. A brief study is done with a dam of similar type and size to compare the natural frequencies and stiffness of the structures. Lastly an analysis is done to determine how Kouga transfers the forces on the structure to the foundations. The effects of the topographic conditions on the force transfer of the structure are discussed and a FEA is presented.

4.2 Instrumentation Data Results

4.2.1 Water Levels

The Eastern Cape experiences a cold and wet winter with minimum temperatures in August/September and a dry warm summer with maximum temperatures in February/March. There is cyclic behaviour with regards to the temperatures, rainfall, and corresponding water levels within the dam. However there are dry periods which occur for extended periods of time and these continual low water levels have had an effect on the behaviour of the dam. Figure 31 shows the water record for Kouga dam from 1972-2015.

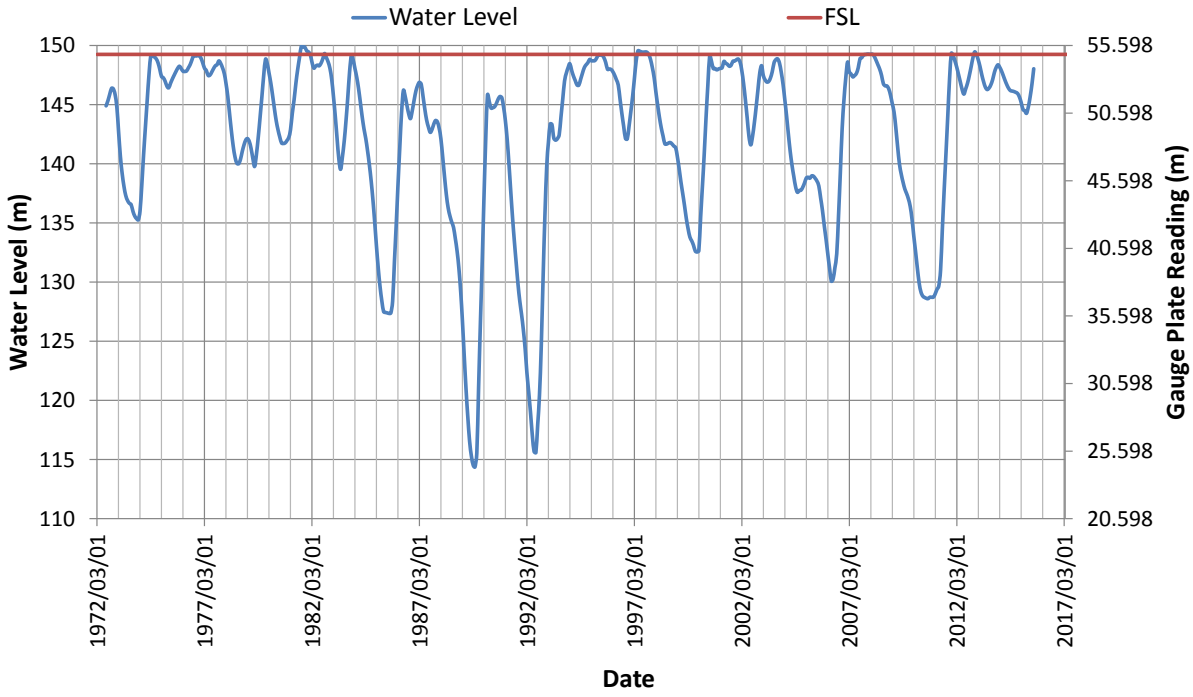

Figure 31: Water level record

4.2.2 Temperature

The dam spans approximately from East to West between a narrow valley along the Kouga River. The upstream side of the dam wall is North-facing and as a result the un-wetted portion of the upstream wall is exposed to constant and direct sunlight during the day. Conversely the downstream side of the wall is in constant shade. Figure 32 shows the position of the dam wall within the valley and the trajectory of the Sun.

Figure 32: Trajectory of the Sun across the dam wall

The recorded data of the thermometers on the left and right flanks were averaged in order to make the data more manageable. Figure 33 shows the recorded temperature data.

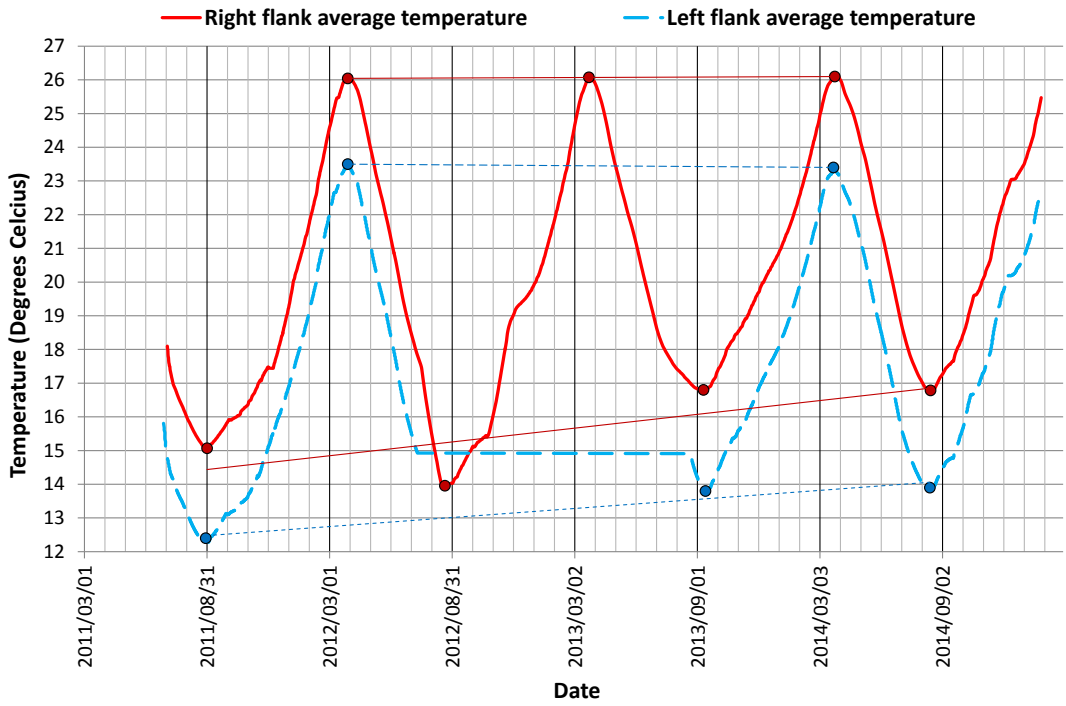

Figure 33: Average temperature for the left and right flanks

From this figure it is shown that the temperature of the upstream face is cyclic and changes seasonally. The recorded temperatures reach a maximum during summer (February/March) and are at its lowest during the winter (August/September) months. It is also evident that the right flank experiences slightly higher temperatures compared to the left flank and the average temperature difference is approximately 2.75°C. This could be attributed to the trajectory of the sun and the possibility of a morning shadow cast on the left flank due to the mountain.

The trends demonstrate that the maximum temperatures have remained constant (26°C and 23.5°C for the right and left flanks respectively) while the minimum temperatures have increased over the 3.5 year period. The minimum temperatures for both data sets have increased by approximately 1.5°C.

4.2.3 Geodetic Data

The relative displacements in the x, y and z directions are shown in Figure 34. The recorded data is presented with the water record (six monthly moving average) and sign convention used.

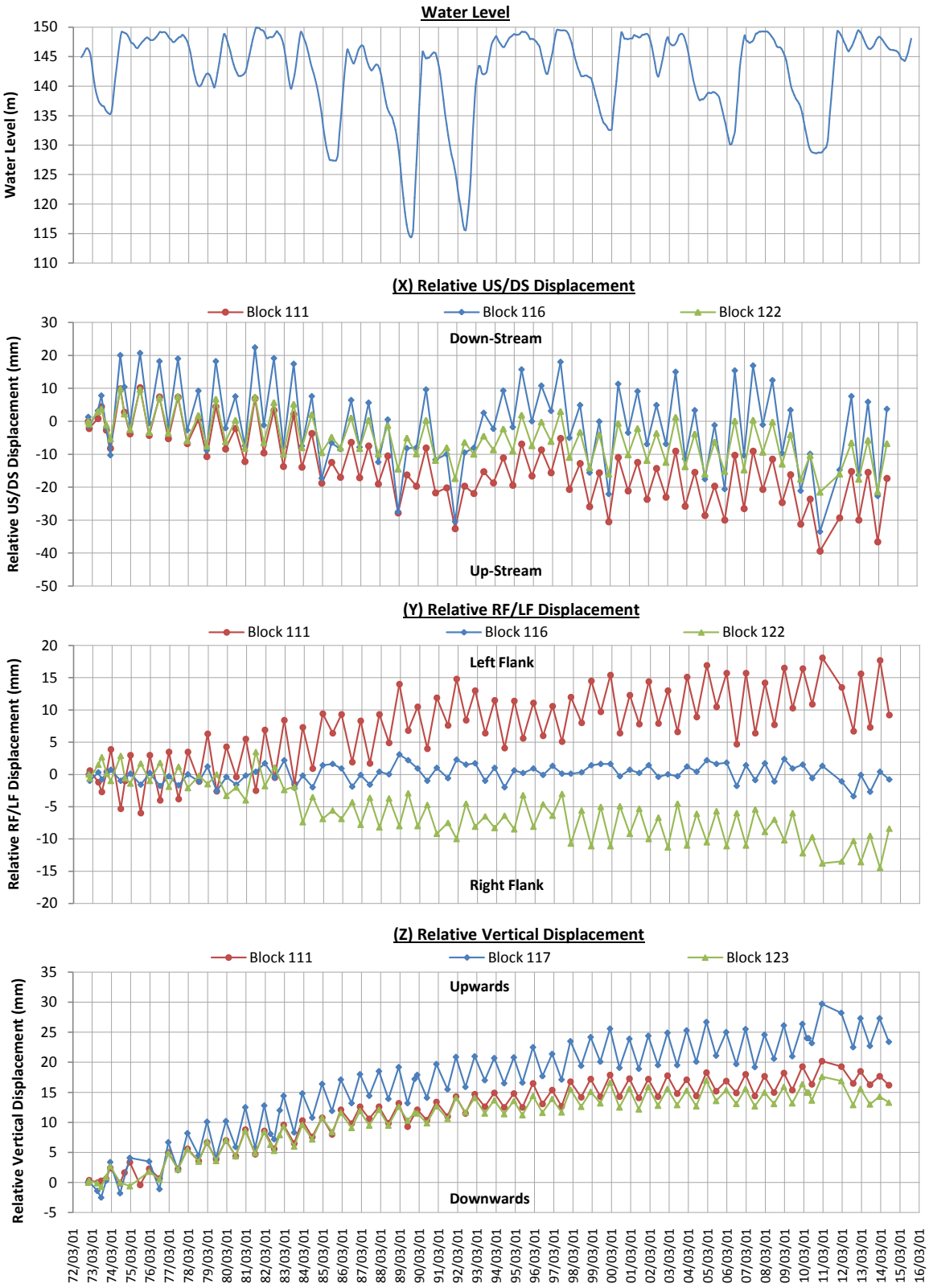

Figure 34: Water record and geodetic data

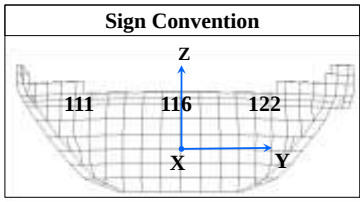

At the end of 1989 a severe drought occurred and reduced the volume of water within the dam to 10% of full capacity (13 million m^3). The following sections compare displacement trends before and after this drought.

Relative upstream/downstream Displacement (X): Centre point

As expected the upstream and downstream displacements are dependent on the water level. The severe droughts can be identified in the displacement graphs as the low extremities and this indicates upstream displacement (negative direction). The displacement for both quarter and centre points follow a similar signature. However since 1985 the right flank exhibits 10mm larger seasonal displacement fluctuations compared to the left flank. The upstream and downstream displacements for the centre of the dam are shown in Figure 35. In the figure the red line indicates the drought that occurred in 1989.

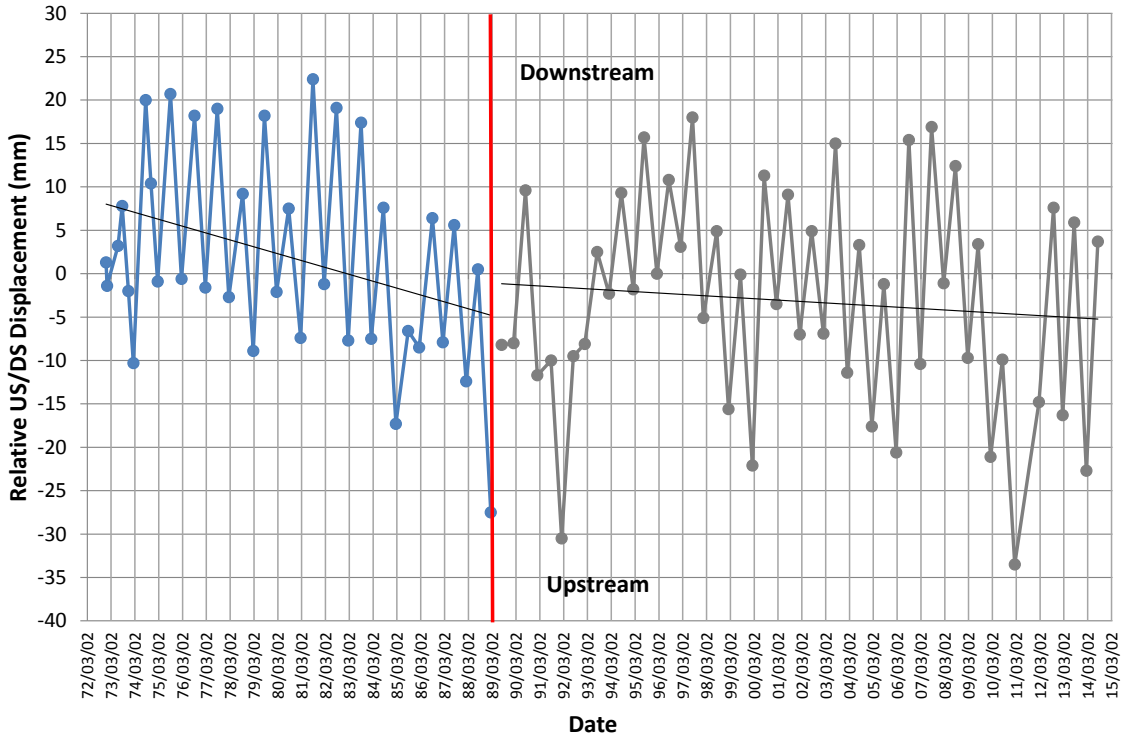

Figure 35: Relative upstream/downstream displacement (116)

The general radial displacement trend has been steadily moving towards the upstream. This rate has decreased following the drought of 1989.

Relative right flank/left flank Displacement (Y): <u>Right</u> flank quarter point

The right flank and left flank displacement of the centre of the dam wall fluctuates around 0mm, whereas the right and left quarter points diverge towards its opposite flank. The tangential displacement of the right flank quarter point is shown in Figure 36.

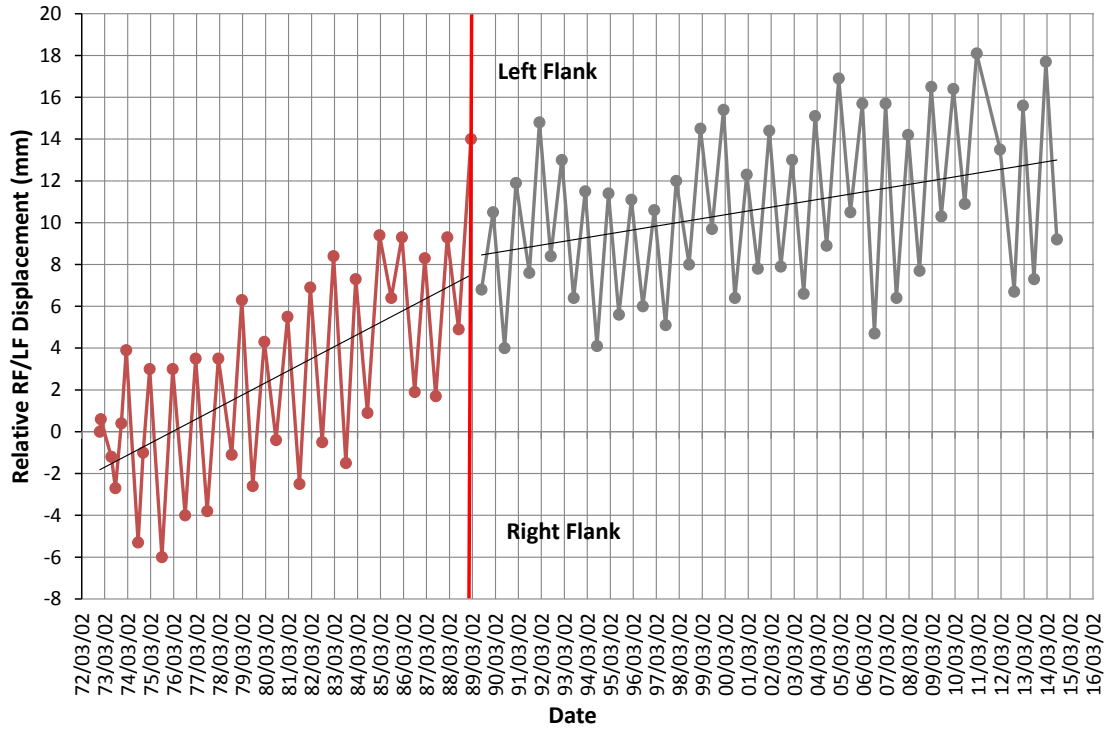

Figure 36: Relative right flank/left flank displacement of right flank quarter point (111)

Block 111 on the right flank tends to displace towards the left flank. This rate has decreased following the drought of 1989.

Relative right flank/left flank Displacement (Y): Left flank quarter point

The tangential displacement of the left flank quarter point is shown in Figure 37.

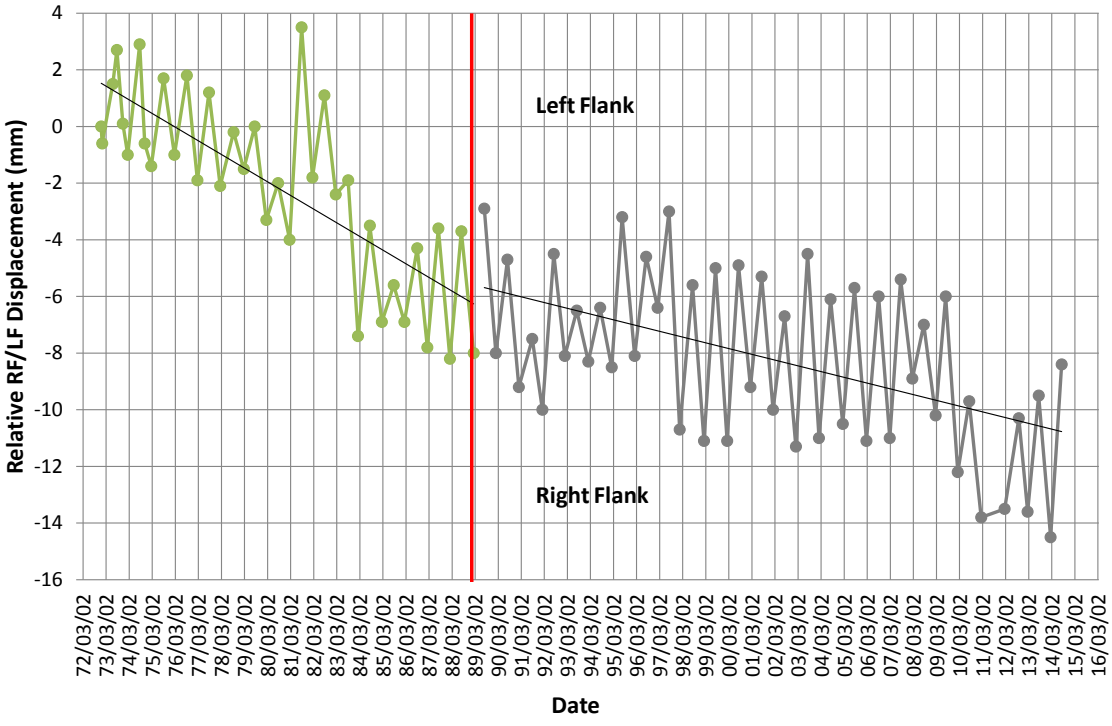

Figure 37: Relative right flank/left flank displacement of left flank quarter point (122)

Block 122 on the left flank tends to displace towards the right flank. This rate has decreased following the drought of 1989.

The strain rate for the entire period (1973-2014) is larger on the right flank compared to the left flank (See Table 10). The right flank also exhibits larger seasonal fluctuations of 6-9mm compared to 4-6mm on the left flank. In part this may be attributed to the higher average temperature and longer length of the right flank section of the wall.

Relative Vertical Displacement (Z): Centre point

The displacement for both quarter and centre points follow a similar signature. The centre of the dam wall exhibits the greatest relative vertical displacement and has a larger strain rate compared to the flanks. The vertical displacements for the centre of the dam are shown in Figure 38.

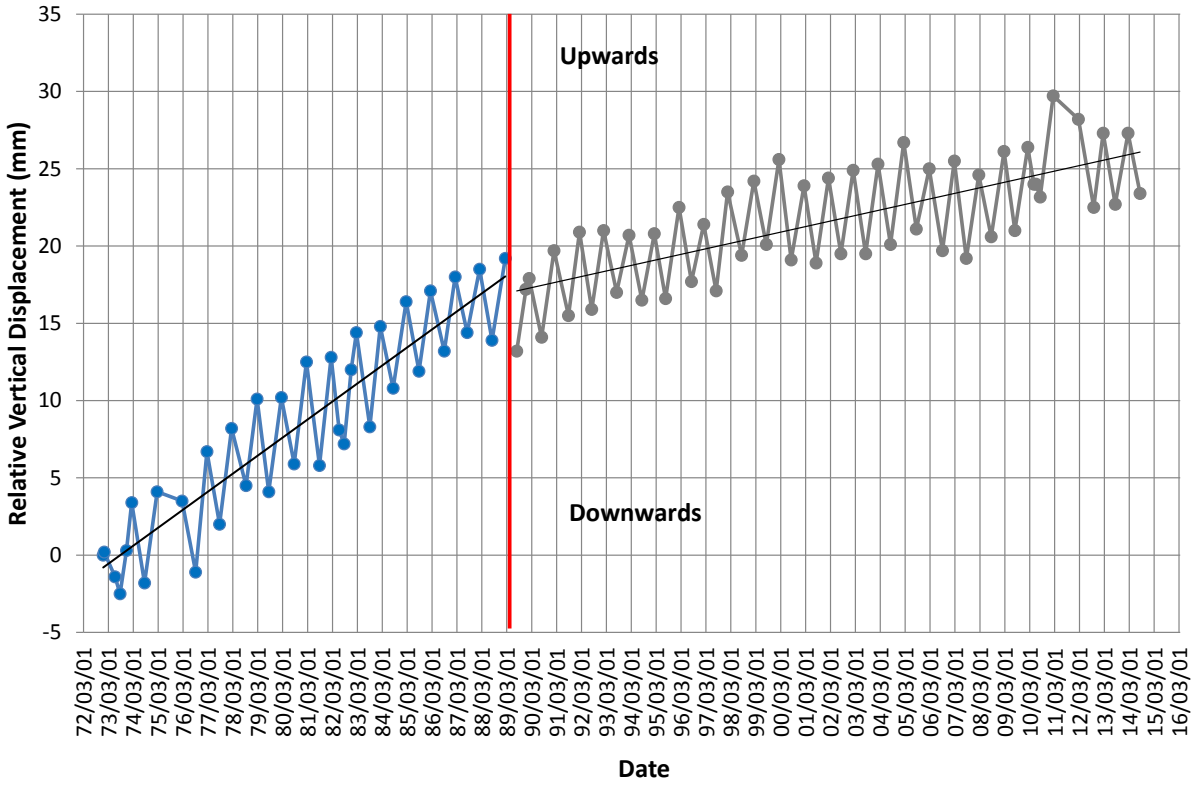

Figure 38: Relative vertical displacement at centre (117)

The seasonal fluctuations have remained constant at approximately 5mm. The dam tends to displace upwards. The general trend shows that the rate of vertical displacement has decreased over time. The strain rates in the vertical direction are considerably larger than that in the tangential direction (See Table 10).

Summary

The geodetic targets at the gallery level indicate that the dam is displacing in upward and upstream directions and the quarter points tending towards opposite flanks. Table 10 summarizes the results.

Table 10: Summary of displacement and strain rates

Period	Displacement Rate (mm/annum)	Strain Rate (με/annum)		
	US/DS (Centre)	RF/LF (RF quarter point)	RF/LF (LF quarter point)	Vertical (Centre)
1973-1988	-0.8	2.5	-2.2	17.2
1989-2014	-0.2	0.7	-0.9	5.0
1973-2014	-0.3	1.6	-1.3	8.6
Reduction in rate since 1989 (%)	75	72	59	71

Curtis (2000) notes that the response of ASR-affected arch dams are vertical and upstream displacements over. Kouga is swelling to a lesser extent in the constrained direction towards the flanks and considerably more along the unrestrained boundaries in the upward and upstream directions. The average permanent displacements (in the x-y plane) exhibited by the dam are shown in the schematic below (Figure 39).

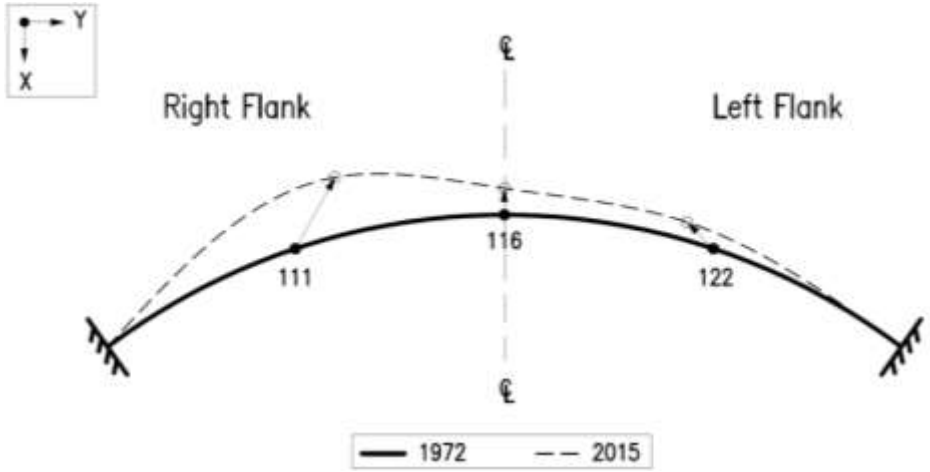

Figure 39: Schematic of permanent x-y displacement of dam wall

The whole structure has moved upstream with the right flank undergoing significantly larger relative displacement. The additional stiffness on the left flank could be attributed to the favourable orientation of the foundation bedding planes, parking area, and spillway chute. It appears that due to the increased axial load associated with the swelling the structure may be buckling in an attempt to relieve the swelling stresses. This is due to the foundations being more rigid than the "softer" dam wall structure and this provides a fixed restraint against the swelling load that occurs

within the concrete. The dam wall is not symmetrical and the buckling is occurring at the slightly longer section on the right portion of the wall.

Previously it has been assumed that until 1976 the swelling may have closed up the vertical contraction joints of the dam (Elges et. al., 1995: 3), therefore during this early period (1972-1977) the dam does not show any clear swelling evidence in the vertical direction. The strain rates in all directions have steadily decreased over the years and are expected to plateau in the near future. This indicates that the ASR has appeared to stabilize. The fact that this decrease in strain rate occurred after the major drought indicates that the dam may have permanently displaced into a position which manages the stresses in a more effective manner.

The geodetic data provides evidence of general seasonal variations and long term trends. However, the small temperature sample does not provide enough data to make confident conclusions on its effect on the structure's response.

4.2.4 GNSS/GPS Data

The GNSS/GPS has a higher resolution when compared to the geodetic data and this enables the behaviour of the structure to be observed in more detail. As the GPS monitoring points were only installed in 2011/08/09 the data sample is much smaller compared to the geodetic sample space. Over this small period both flanks exhibit similar behaviour in terms of seasonal fluctuations and amplitudes. See Figures 40 and 41.

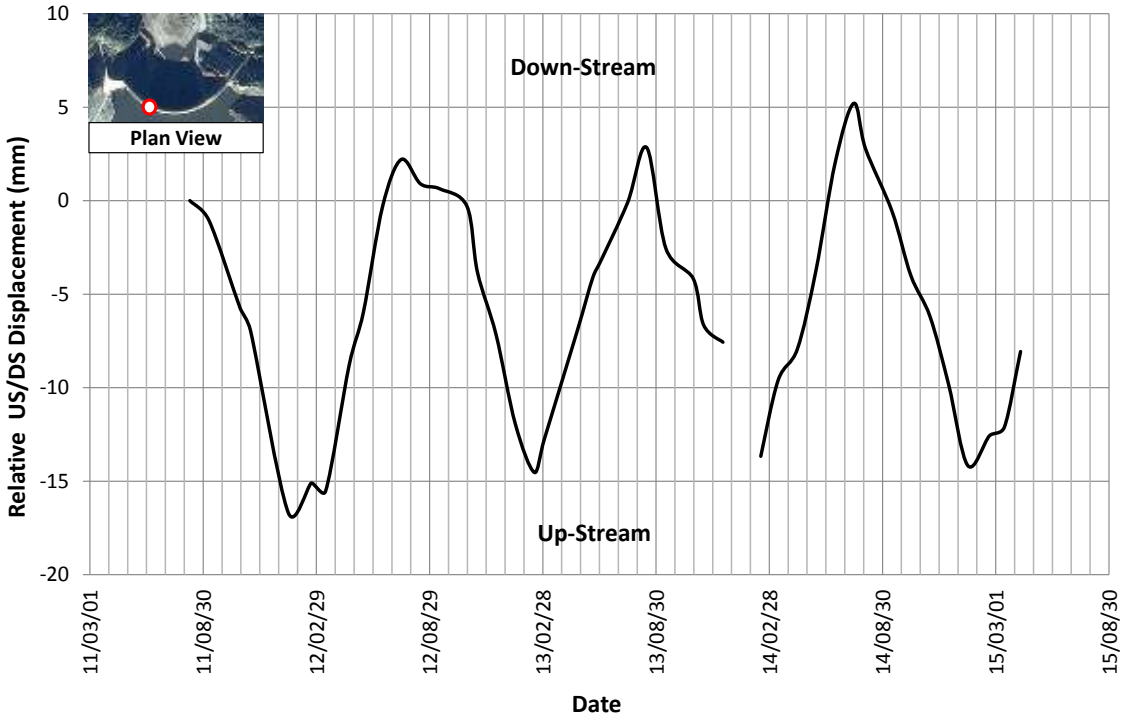

Figure 40: Displacement data for left flank (KG12)

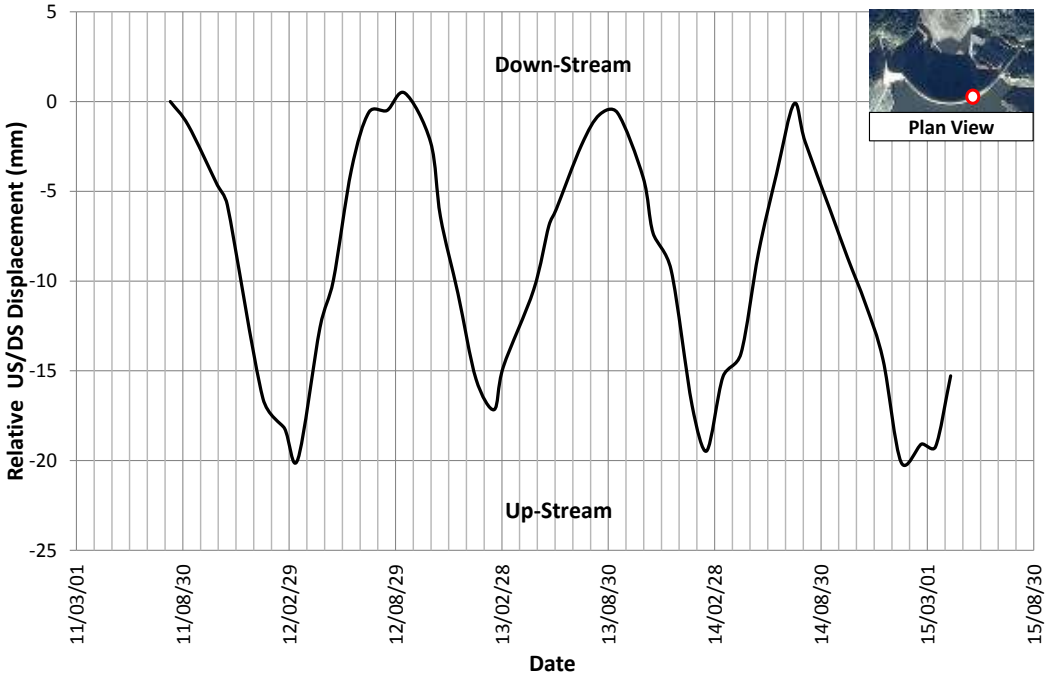

Figure 41: Displacement data for right flank (KG13)

4.2.5 GNSS/GPS and Water Level

Both the displacements and water levels follow cyclic patterns. Intuition would suggest that the larger the hydraulic loading the greater the downstream deflection. However it is clear from Figure 42 and 43 that the structure's response is not initiated by changes in the reservoir level.

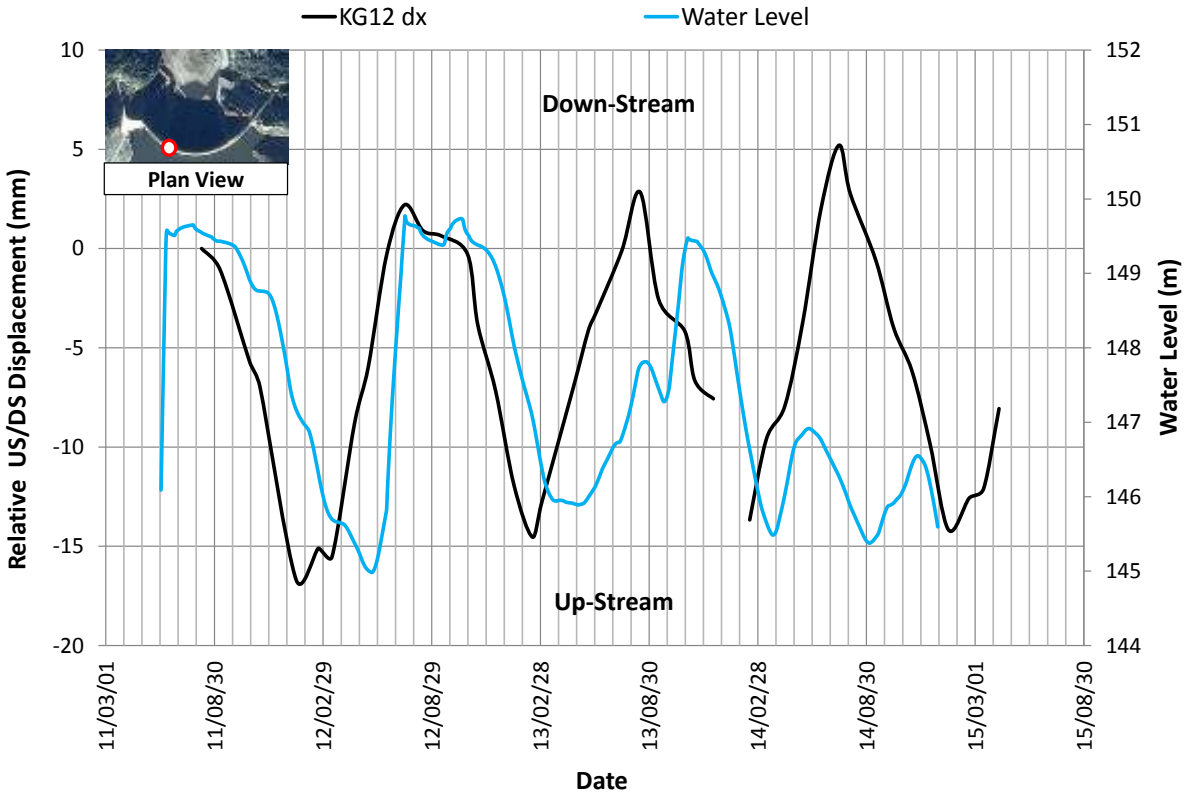

Figure 42: Displacement and WL data for left flank

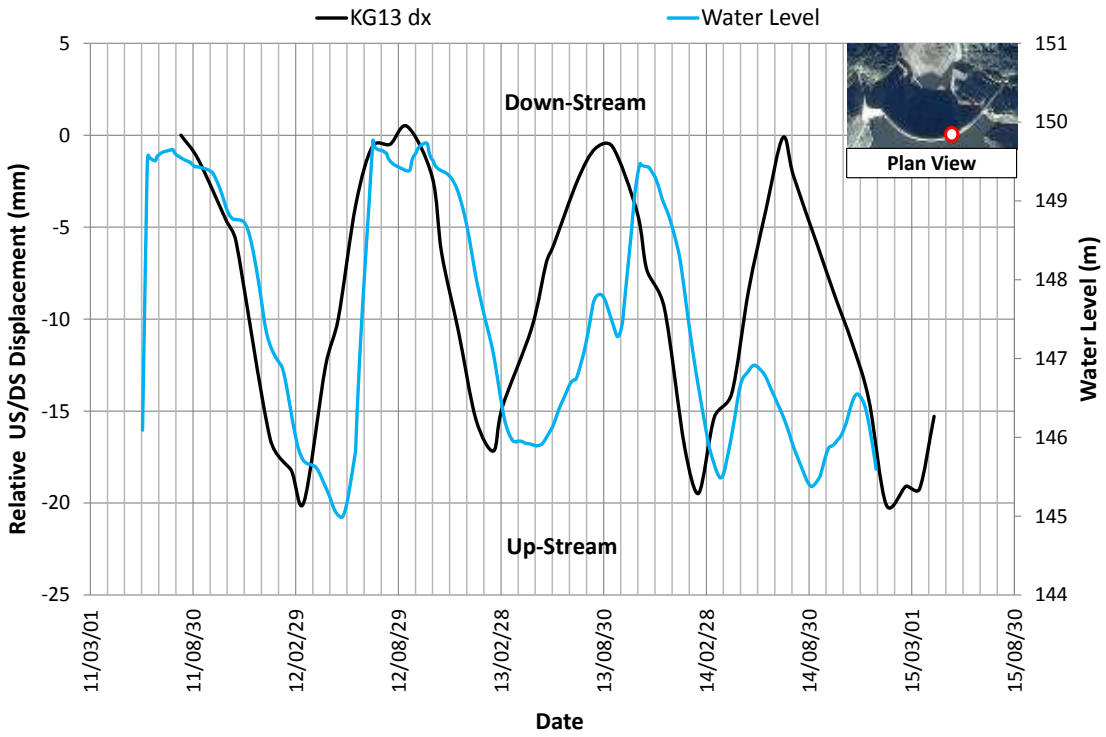

Figure 43: Displacement and WL data for right flank

The graphs show that the structure changes the direction of displacement before the water level changes. The dam moves downstream between one to three months before the water level rises and vice versa. This phase lag may be due to another loading which has a more immediate effect on the dam's behaviour.

Figure 44 shows the relationship between displacement and water level. The relationship between the two variables is complex and no clear or obvious correlation is evident.

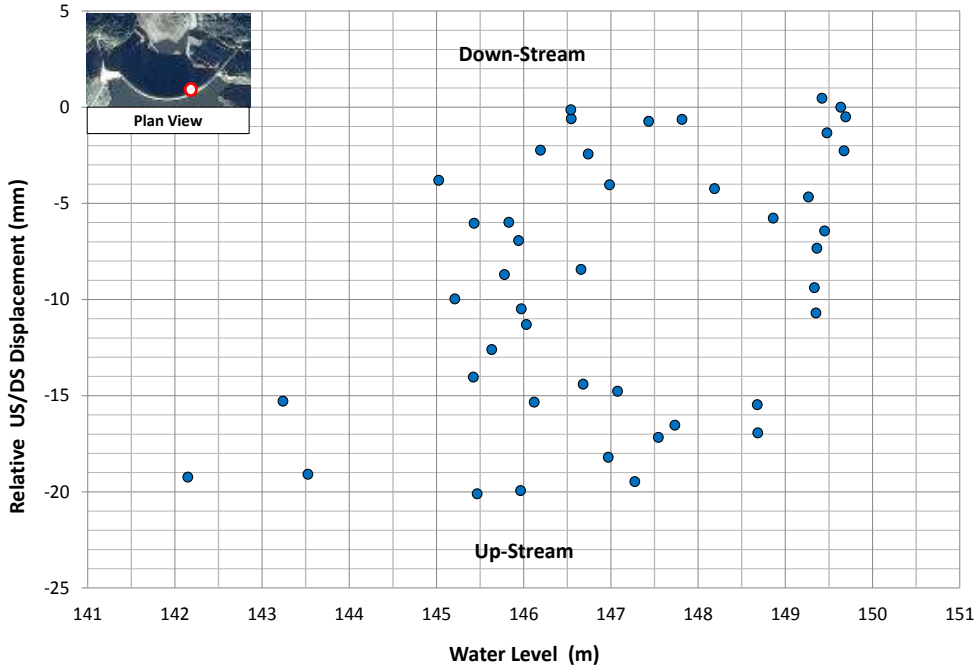

Figure 44: Displacement VS Water Level

4.2.6 GNSS/GPS and Temperature

The displacements of the structure are approximately 180 degrees out of sync with the temperature at any given point in time. See Figures 45 and 46 below.

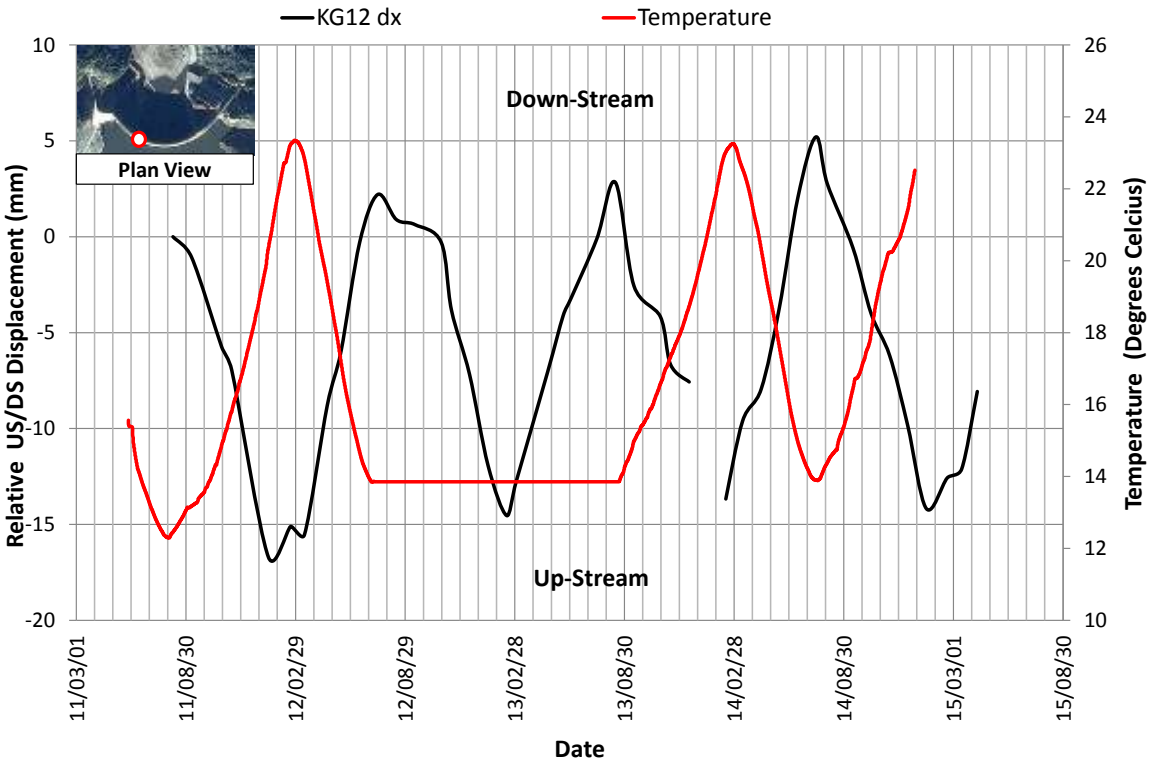

Figure 45: Displacement and Temperature data for left flank

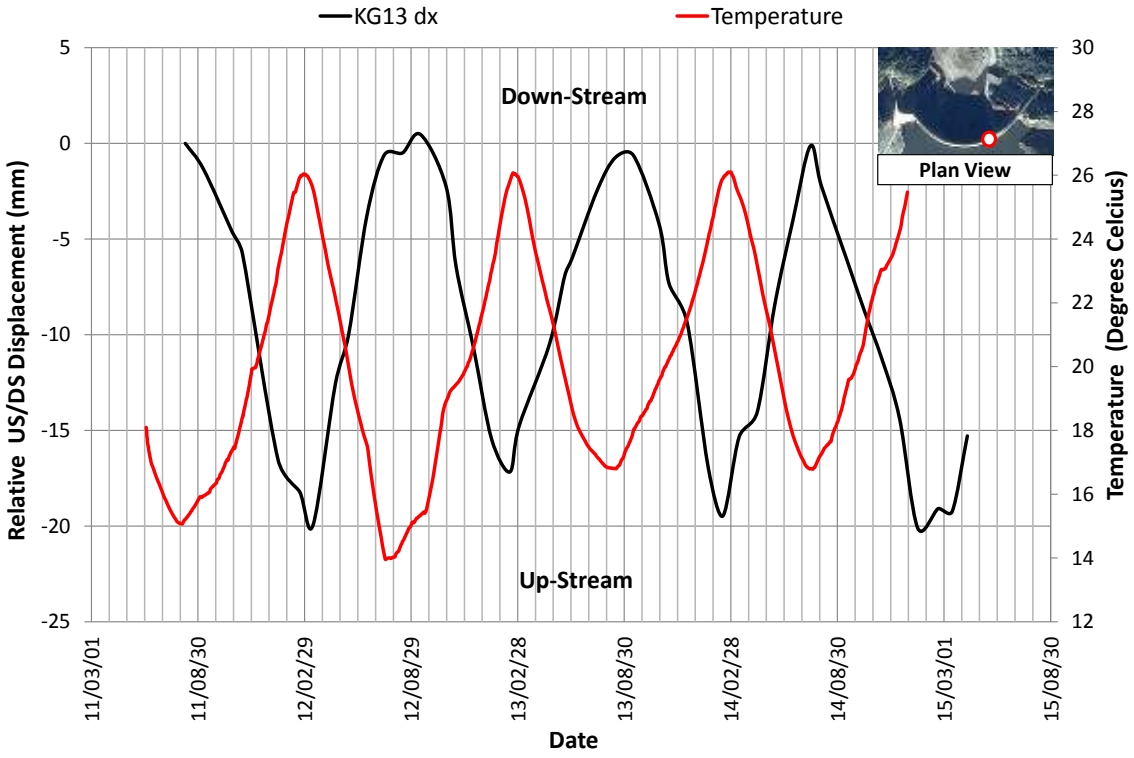

Figure 46: Displacement and Temperature data for right flank

Figure 47 shows the relationship between displacement and temperature. The relationship is linear with an increase in temperature resulting in an upstream displacement and vice versa.

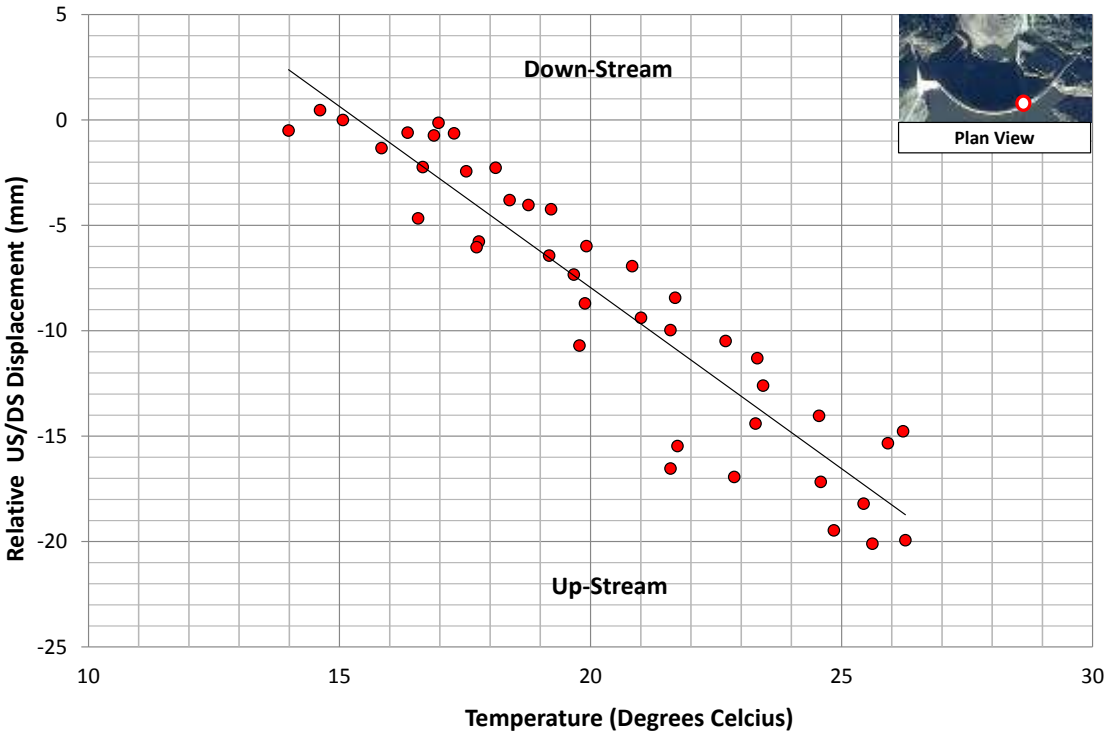

Figure 47: Displacement VS Temperature

4.2.6 Trivec System

For the Trivec analysis the recorded data during high water levels were compared to that of low water levels. Figure 48 shows Kogr1 during high water levels. The warmer colours represent the data that was recorded during summer while the cooler colours represent the data that was recorded during winter.

The full set of displacement graphs are shown in Appendix A. A summary of the results for each Trivec is given in Table 11.

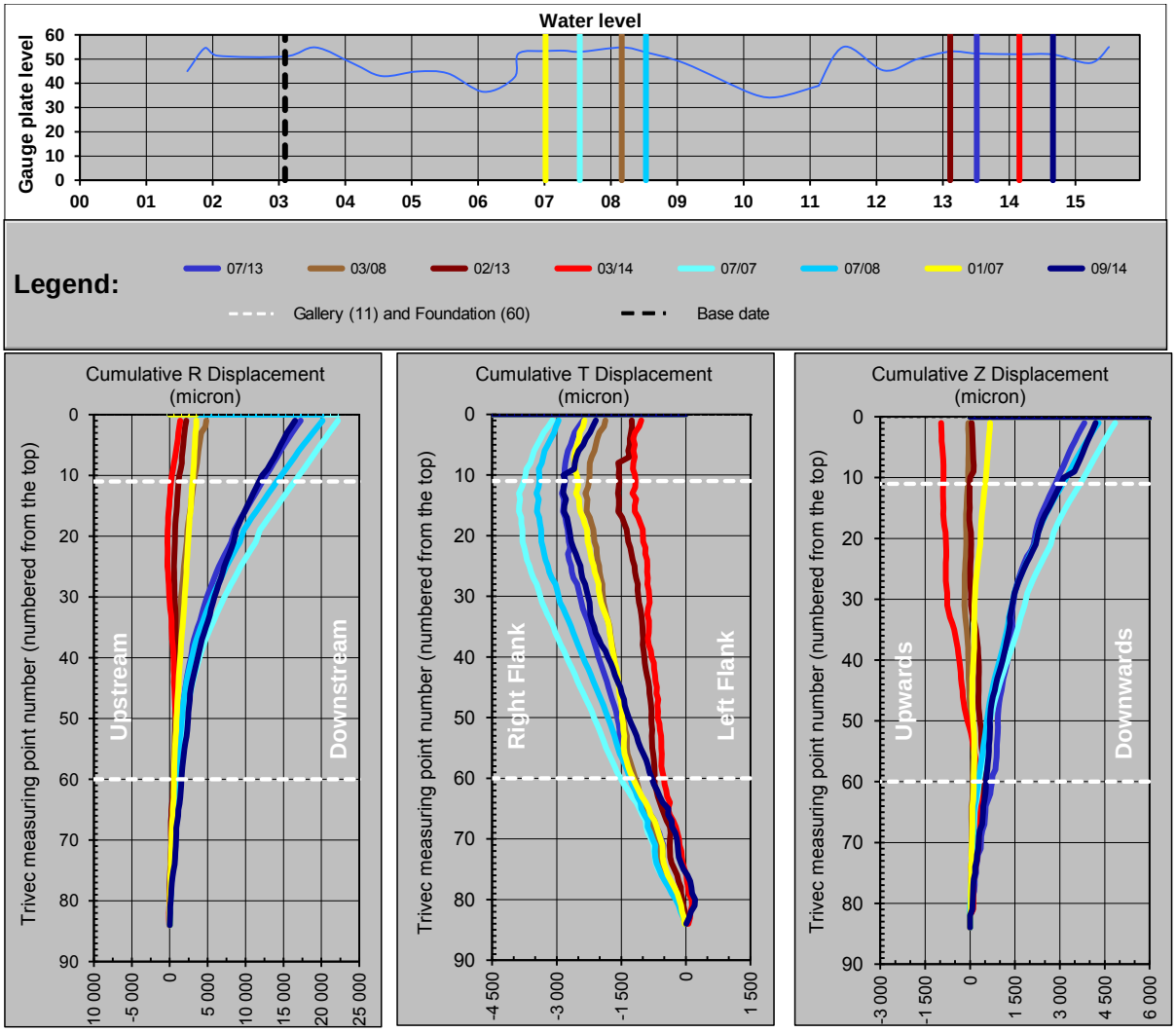

Figure 48: Trivec Kogr1 during high water levels

Summary

The displacement trend of Kogr1 for the top third of the dam is consistent with the geodetic measurements. The quarter points of the dam wall at the gallery level and above tends towards the opposite flank. However below this level the Trivec measurements of Kogr1 show that the lower two thirds of the wall is displacing towards the same flank, namely the right flank. This may be because the dam is stiffer below the FSL compared to the section between FSL and NOC. The missing concrete section across the spillway and NOC levels result in the observed behaviour of the top third of the dam wall tending to the opposite direction compared to the lower stiffer sections.

The displacements throughout the foundations (right and left) fluctuate within a bandwidth of approximately 0.2mm. The largest tangential displacement towards the right flank occurs in winter during the high water levels. This increases the forces on the foundation and can be seen to have an effect on Kogr2 and Kogr5 which are positioned in the right flank foundation downstream of the dam. The displacements

may be an indication of weaker phyllite material inter-bedded between the highly folded and compressed sandstone and quartzites.

Table 11: Trivec data summary

Trivec System	High Water Level	Low Water Level	Common trend
Kogr1	• Largest downstream and downward displacement during winter. • Below 2/3 of height, dam tends towards the right flank. Above, tends slightly towards left flank (Observed in geodetics). Exaggerated during winter.	• Largest upstream and upward displacement during summer. • Below 1/2 of height, dam tends towards the left flank. Above, tends slightly towards right flank. Only observed for summer readings.	• Below foundation level the movements are stable (<0.2mm) in all directions. • Clear temperature effect on behaviour of dam wall
Kogr2	• Clear displacement trends changing in direction from left to right flanks throughout the height of the borehole.	• No clear displacement trends	• Generally stable with movements <0.2mm throughout height. • Erratic movements in top 5m. • No clear temperature effect on behaviour
Kogr3	• Similar behaviour regardless of water level or season. • Greatest radial and tangential displacement range in lower half of borehole.		
Kogr4	• Similar behaviour regardless of water level or season. • Generally stable with movements <0.2mm throughout height. • Erratic movements in top 10m. • Slight tendency within the top 5m to displace downstream and upwards during summer, and vice versa during winter.		
Kogr5	• Spike in displacements for all directions (including vertical) 10m into borehole (<0.3mm.)	• No clear displacement trends	• Generally stable with movements <0.2mm throughout height.
Kogr6	• Generally stable with movements <0.2mm throughout height.		

4.2.7 AVM and Water Level

Clear changes occur in the recorded natural frequency as a result of changes in water level. The natural frequencies (ω_n) for the first four modes of vibration (φ_i), at varying water levels are shown in Figure 49.

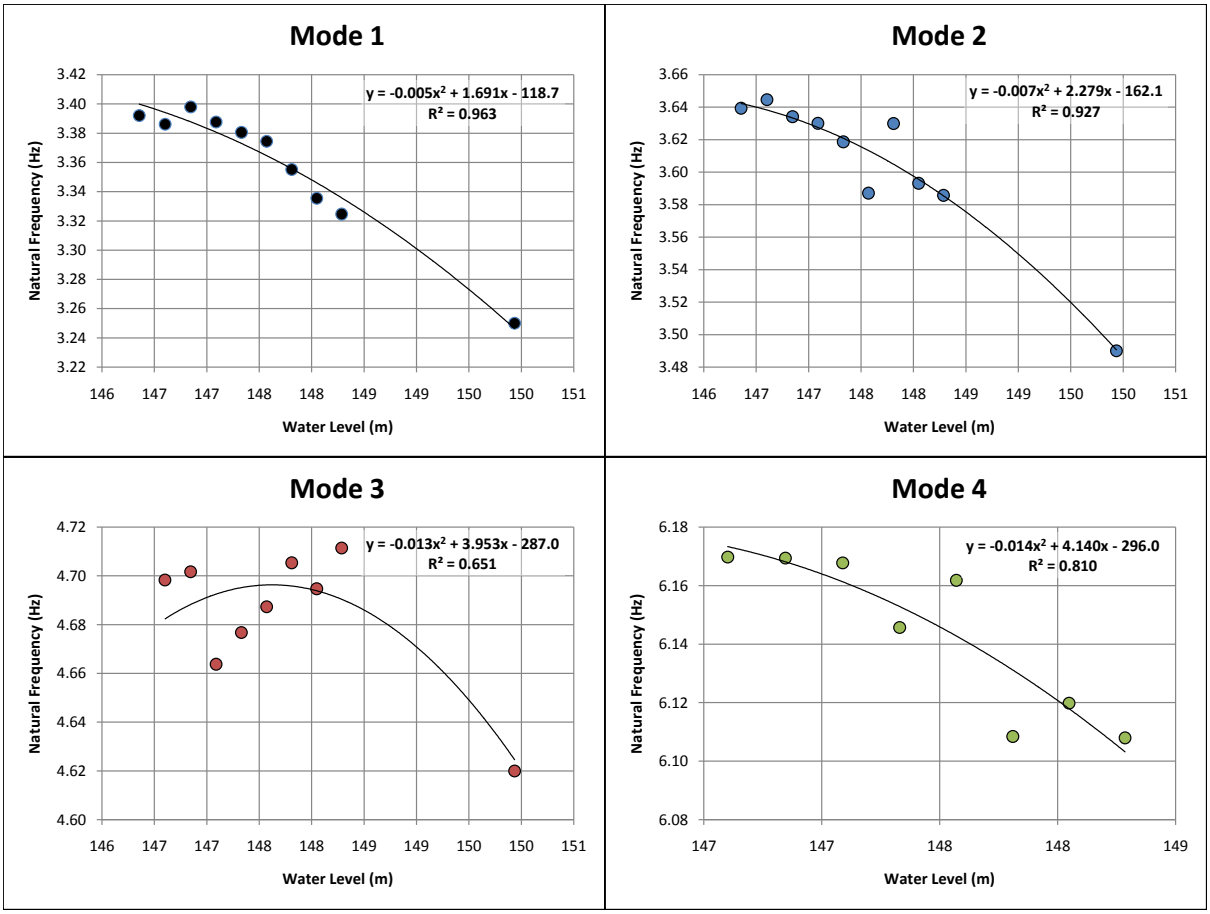

Figure 49: Natural frequencies of the first four modes of vibration at varying water levels

As the water level increases the impounded water has an added mass effect on the dam wall structure. The relationship between ω_n, stiffness (k), and mass (m) has previously been discussed (See Equation 2.4 in section 2.3.2), and is repeated here for convenience.

$$\omega_n = \sqrt{\frac{k}{m}}$$

As the water level rises (and added mass increases) the ω_n decreases. The first, second, and fourth modes strongly fit a second order polynomial regression line. These strong modes are easily identifiable during the data processing of the AVM. Mode three is often referred to as a weak mode and displays a low coefficient of determination for a similar regression model.

The natural frequencies for the higher modes increase sequentially given that the water level is constant. This is shown in Figure 50.

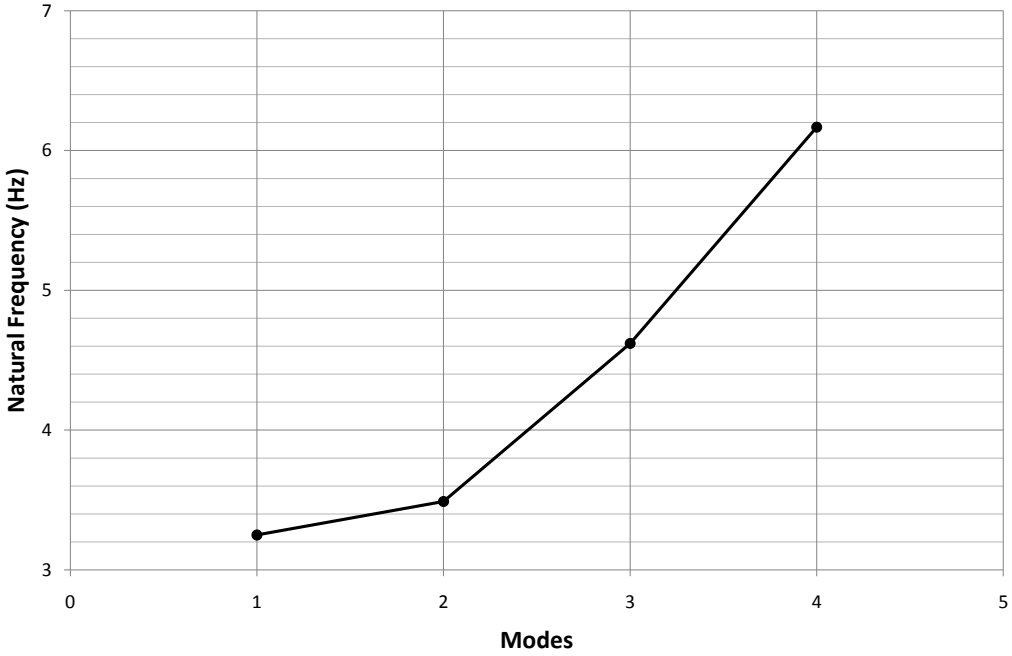

Figure 50: Natural frequencies for varying modes of vibration at FSL

The AVM signature (ω_n) for a structure will change if either the mass or stiffness changes. Therefore if the signature of the structure at a certain water level (constant mass) is compared at various time periods the changes may be attributed to the structural stiffness. A downward shift of the ω_n's for the respective modes would thus indicate a decrease in the stiffness of the structure. This demonstrates the importance of AVM's over long periods of time in order to identify possible structural deterioration.

4.2.8 Crack widths

The three dimensional crack width gauges were installed at five levels of the downstream face of the dam wall (See Figures 51 and 52). Two gauges on each of the joints on the Ultimate Non Overspill Crest (UNOC), NOC, and gallery levels. Only single gauges were installed at the upper and lower walkways.

Two periods were investigated in order to observe the impacts of rising and falling water level on the vertical construction joints of the structure. The periods are summarized in Table 12. The first date acts as the baseline reading for the specific period.

Table 12: Crack width measurement periods

Period	Date	Water Level (m)	Volume (million m^3)
A: Falling Water Level	2009/01/27	RL 144.03	99
	2010/12/20	RL 127.51	39
B: Rising Water Level	2010/12/20	RL 127.51	39
	2011/07/28	RL 149.97	130

Figures 51 and 52 show the crack width gauge results for the displacement across the joints (tangential). A positive value indicates an opening (green) of the joint while a negative value indicates a closure (red/orange) of the joint. The yellow values indicate little change in joint movement.

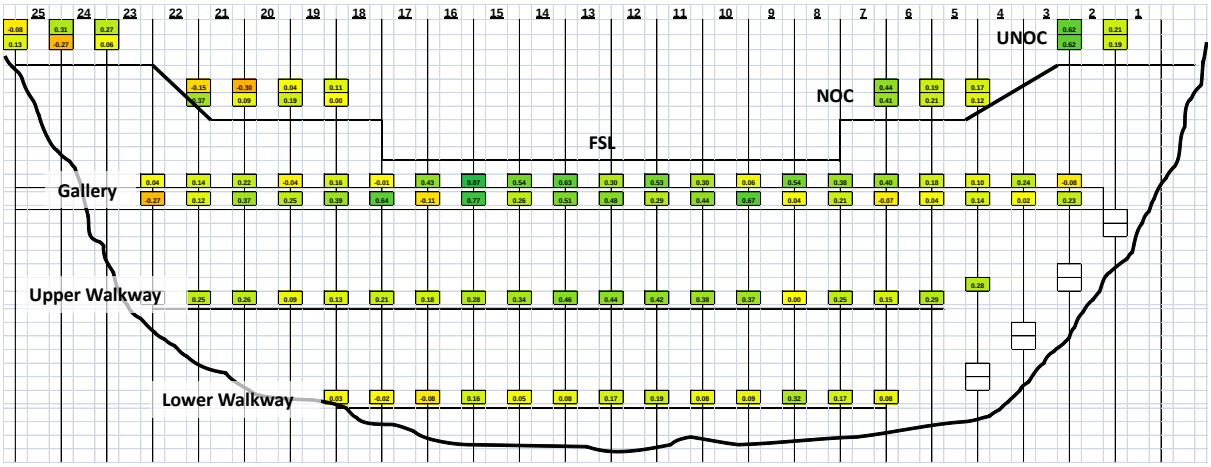

Figure 51: Period A - Falling water level

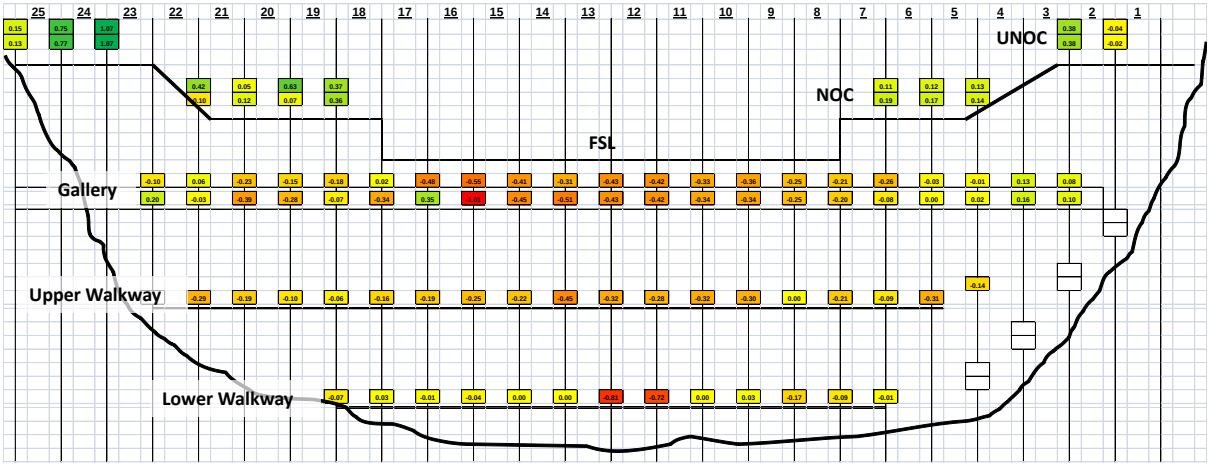

Figure 52: Period B - Rising water level

For period A the water level falls from just below the FSL to approximately the upper walkway. The joints open up with the maximum being approximately 1mm.

For period B the water level increases from the upper walkway to above the FSL. The joints are more closed compared to period A and have a maximum closure of approximately 1mm. The closure of the joints seems to only occur below the level of the water surface (FSL). It is also evident that the largest joint movements for both periods occur in the middle of the structure.

The data indicates that the joints of the structure are more open during low water levels. Thus the hydrostatic loading is not transferred to the foundations predominantly via hoop stresses because the dam wall does not act completely as a monolith. When the water level is high the joints are more closed and the dam wall is

in a more compressed state. The joints above the water level are however still open despite the high water level. This may also indicate that the swelling effects associated with ASR may be predominantly located in the lower sections of the dam wall.

4.3 Comparative Study

Roode Elsberg Dam is a thin, double curvature, arch dam located in the Western Cape Province of South Africa. Kouga and Roode Elseberg dams are similar in terms of dam type and size, and a comparison was done on the respective recorded modal parameters and stiffness of the dams. The fact that Kouga has been exposed to ASR may allude to the dam having a high stiffness as a result of the added restraint caused by the swelling of the concrete. Table 13 compares statistics of Kouga to Roode Elsberg dam.

Table 13: Comparative dam statistics

Parameter	Roode Elsberg Dam	Kouga Dam
Height (m)	72	69
Crest Width (m)	2.6	6.3 (10m at pulvino)
Crest Length (m)	274	317
Spillway Length (m)	76	127

Although the dams exhibit similar heights Kouga spans a greater length and is much thicker in comparison. As a result Kouga has a greater mass and presumably lower natural frequencies for the various modes at a given water level. Figure 53 compares the natural frequencies of both dams.

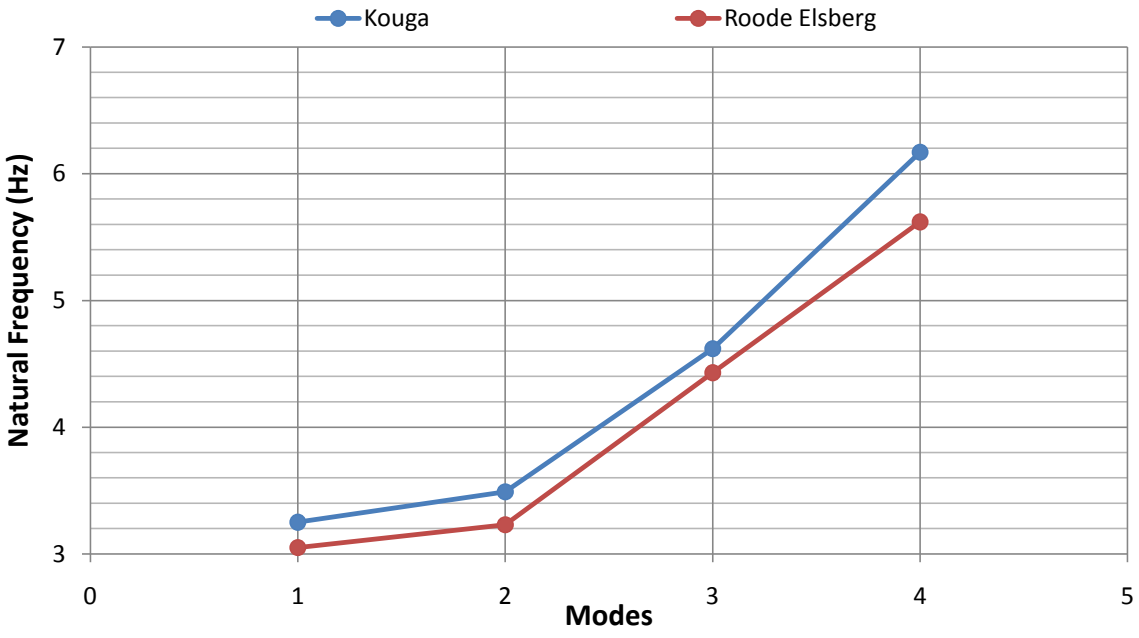

Figure 53: Natural frequencies for Kouga and Roode Elsberg Dams

Figure 53 indicates that Kouga exhibits greater natural frequencies for the respective modes of vibration, despite it having the greater mass. This confirms that Kouga dam is a stiff structure for its size.

4.4 Dam Forces on Foundation

The valley in which Kouga dam was constructed exhibits a canyon shape factor (k) of approximately 5.3 (See section 2.1.2), and this relates to a wide U-shaped valley. With a base width and height ratio of approximately 0.15 Kouga may be described as a thin arch dam. Due to the combination of topography and design it can be argued that the dam wall would naturally tend to transfer the imposed loading via dominant cantilever action to the central foundations. Carvalho et. al. (2014: VI17) observed that the upper construction joints of the dam opened during the low water levels. This observation corresponds with the crack width results (See section 4.2.8). The structure therefore does not act as a monolith during low water levels and the forces are transferred to the foundation predominantly via cantilever action.

The simplified finite element model of Kouga dam with a hydrostatic load at full supply level is shown below in Figure 54. This model illustrates how the structure transfers stresses to the foundations.

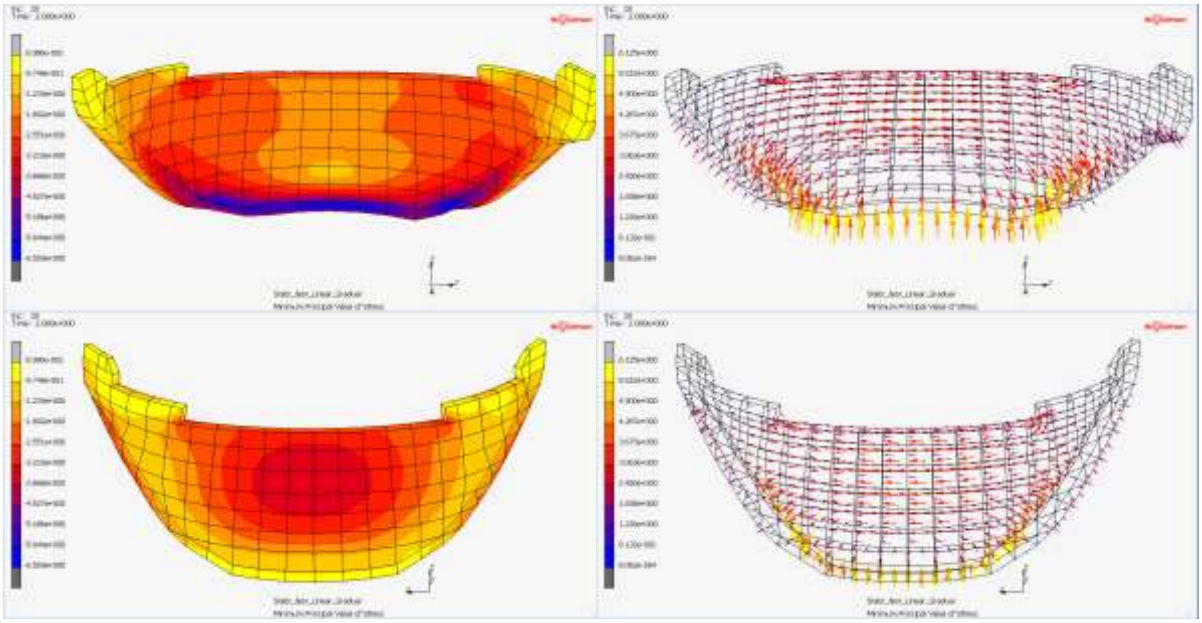

Figure 54: Force transfer through arch during FSL hydrostatic loading

The upstream face displays significant arch action with maximum compressive stress occurring at approximately two thirds of the height of the dam. The thrusts then drop rapidly on the downstream face and result in the largest compressive stresses which are located at the wide river bed. It is evident that the structure transfers the imposed loading predominantly via cantilever action to the central foundation. This results in relatively large tensile stresses at the heel of the dam. In light of the aforementioned ASR identified at the dam, which would most likely be

located on the wetted upstream face, the reduction in tensile capacity associated with the deterioration together with the high tensile stresses increases the possibility of tensile cracking at the heel.

4.5 Chapter Summary

This chapter presents the results of the instrumentation data recorded by the monitoring system at Kouga Dam. An analysis of the individual data sets is discussed and some of the results are overlaid in order to deduce the relationship between certain measured parameters. In addition this chapter presents a comparative study between Kouga and Roode Elsberg Dam. These two dams are similar in terms of dam type and size, and a comparison was done on the respective recorded modal parameters and stiffness of the dams. In conclusion the chapter describes how a simplified finite element model was used to determine the magnitude and nature of the forces within the concrete arch structure during operation.

CHAPTER 5

5 CONCLUSION AND RECOMMENDATIONS

5.1 Summary

The NWA mandates that dams with a safety risk be routinely evaluated on their safety. Monitoring systems installed at the dams assist the engineers with this task and gives insights into the structure's operational behaviour. Following the data analysis instrumentation results identify the structural response to changes in loading, and long term trends may indicate deterioration of the structure over time. Once the behaviour is understood a more informed argument can be made for the potential failure modes of the structure and the likelihood thereof.

The purpose of this research is to analyse the instrumentation data recorded at a double curvature arch dam in order to identify trends and better understand the operational behaviour of the structure. The case study of this thesis is Kouga Dam in the Eastern Cape Province of South Africa. Kouga was completed in 1969, and after the catastrophic failure of Malpasset Dam in 1959, a decision was made to stabilise the right abutment due to suspected instability. In 1981 ASR was positively identified in the dam wall. Due to the aforementioned aspects and catastrophic consequences associated with a dam failure an extensive monitoring system has been installed at Kouga Dam.

In the sections below the conclusions of the analysis of the monitoring system and recommendations for future work relating to this thesis are presented.

5.2 Conclusion

The individual instrumentation results from the comprehensive monitoring system have created a more complete picture of the structure's behaviour. The data analysis has assisted in identifying trends and has provided significant insights into the operational behaviour of the structure. The way in which the data was organised and displayed proved most telling when identifying how the structure responds to specific loads and long term tendencies.

The following conclusions were drawn from the results and discussion of this thesis:

i. A linear relationship exists between temperature loading and displacement response of the dam wall. Temperature initiates the response of the structure almost instantaneously. An increase in temperature results in an upstream displacement and vice versa. The most extreme upstream displacement occurs during low water levels and high temperature. The former allowing a larger portion of un-wetted concrete (upstream face) exposed to direct sunlight.

ii. A phase lag of approximately one to three months is evident between hydrostatic loading and the displacement response of the structure. The relationship between these two variables is complex. Hydrostatic loading however exhibits a more significant effect on natural frequencies, with the relationship for most of the lower modes of vibration fitting a second order polynomial regression line. An increase in water level results in a decrease in natural frequency for the respective modes and vice versa. The recorded natural frequencies, and in light of the ASR, has also indicated that Kouga dam is a relatively stiff structure when compared to a dam of similar type and size.

iii. Since construction the dam wall has tended towards the upstream (y), upwards (z), and quarter points of the structure tending towards opposite flanks (gallery level). The displacement and strain rates in the y and z directions are 0.3mm/annum and 8.6με/annum respectively. However, since 1989 there has been a reduction in the average displacement and strain rates in all directions by approximately 70%. This may suggest that the ASR has stabilized.

iv. The vertical construction joints, especially the central and upper joints, are relatively open during low water levels. Therefore the dam wall does not act completely as a monolith, and transfers the imposed loading mainly to the central foundation via dominant cantilever action. The reaction forces on the upper foundations have been found to be relatively low when compared to the central foundation, lowering the risk of potential shear failure of the right foundation.

v. Small foundation movements of less than 0.3mm have been observed within the foundation downstream of the dam wall on the right flank. These movements which are between 10 and 40m within the foundations are most notable during winter at high water levels. This is the period when the dam is in its most downstream position.

5.3 Recommendations

The following recommendations are given for future work relating to this thesis:

i. The extent and activity of the ASR should be determined. This information would assist in the development of a calibrated finite element model.

ii. A finite element model should be developed and should incorporate the swelling effects associated with ASR, temperature, and hydraulic loading. This model should be calibrated using the data obtained from the monitoring system.

REFERENCES

Addis, B. 1998. *Fundamentals of Concrete.* G. Owens, Ed. Midrand, South Africa: Cement and Concrete Institute.

Ballim, Y., Alexander, M., Beushausen, H. 2009. *Chapter 9: Durability of Concrete*. In *Fulton's Concrete Technology*. Owens, G. Ed. 9th ed. Midrand, South Africa: Cement & Concrete Institute. 155-188.

Bathe, K. J. 1996. *Finite Element Procedures.* Upper Saddle River, New Jersey: Prentice Hall.

Brandt, M. 2011. *Seismic Hazard in South Africa.* (Report Number: 2011-0061). Pretoria, South Africa. Council for Geoscience.

Carvalho, E., Valentim, N. & Oosthuizen, C., 2014. *On-line dynamic monitoring of Cahora Bassa Dam.... the next level*. Proceedings of the International Symposium on Dams in a Global Environmental Challenges. 1-6 June 2014. Bali, Indonesia. VI-11 to VI-20.

Chang. P. C., Flatau, A., Liu, S. C. 2003*. Review Paper: Health Monitoring of Civil Infrastructure.* Sage. 257-267.

Concrete Microscope Library. 2016. *Alkali-Silica Reaction.* Available: http://publish.illinois.edu/concretemicroscopylibrary/alkali-silica-reaction/ [2016, November, 26].

da Silva, V. D. & Júlio, E. N. B. S. 1995. *Design and Analysis of Arch Dams by the Membrane Method.* Proceedings of the International Conference on Education, Practice and Promotion of Computational Methods in Engineering Using Small Computers. 1-4 August 1995. Macau, China. 533-538.

Dam Safety Office. 2011. *Registration Details of a Dam Registered in terms of Dam Safety Legislation of Chapter 12 of the National Water Act (Act No. 36 of 1998)*. Pretoria, South Africa: Directorate: Dam Safety Office, Department of Water and Sanitation.

Elges, H., Geertsema, A., Lecocq, P., Oosthuizen, C. 1995. *Detection, monitoring and modelling of alkali-aggregate reaction in Kouga Dam (South Africa)*. (Report CONF-9510182--TRN: 95:008180-0012). Denver, CO, United States. Committee on Large Dams.

Engineering Profession Act, No. 46 of 2000. 2000. *Government Gazette*. 426(1821). 1 December. Government notice no. 1304. Cape Town: Government printer.

Federal Energy Regulatory Commission, 1999. *Chapter 11 - Arch Dams*. Engineering Guidelines for the Evaluation of Hydropower Projects. Washington, DC.

Federal Energy Regulatory Commission, 2014. *Chapter R5 - Concrete Dam Analysis: Arch, Gravity Buttress Dams.* Engineering Guidelines Risk-Informed Decision Making. Washington, DC.

Forbes Dick. 1989. *Engineering Geological Report on the Safety of Paul Sauer Dam*. (Report Number: GSO/1/89/5). Forbes Dick and Associates (Consulting Engineering Geologists). Claremont.

GeoSIG. 2010. AC-23/AC-22/AC-21 Accelerometer [Leaflet].

Ghanaat Y. 2004. *Failure Modes Approach to Safety Evaluation of Dams*. Proceedings of the 13th World Conference on Earthquake Engineering. 1-6 August 2004. Vancouver, Canada. Paper no. 1115.

Gillian, C., Lund, G., Weldon, J. 2011. *Three Predominate Failure Modes of Thin Arch Dams.* Proceedings of the 31st Annual USSD Conference: 21st Century Dam Design - Advances and Adaptations. 11-15 April 2011. San Diego, California. 173-187.

Google Earth 7.1.2.2041. 2013. *Baviaanskloof Nature Reserve, Eastern Cape, South Africa* [Map, July 10]. 33° 44' 26.00"S, 24° 35' 16.00"E. Borders and labels; places layers. NOAA, US Department of State Geographer 2016. [2016, November 27].

Hobbs, L.D., du Plessis, J.G., Kriel, J.P. 1967. *Stabilising highly stratified rock in the right abutment of Tweerivieren Dam.* Proceedings of the Commission Internationale Des Grands Barrages. Istanbul, Turkey. 647-667.

Shaw, Q.H.W. 2015. *The Structural Function of Different Arch Dam Types*. Proceedings of the SANCOLD Annual Conference 2015. 1-3 September 2015. Cape Town, South Africa. 320-332.

Kuo, J. S. 1982. *Fluid-structure Interactions: Added Mass Computations for Incompressible Fluid.* National Science Foundation.

Lombardi, G. & Fanelli, M. 1992. *Practice and Theory of Arch Dams*. Proceedings of the International Symposium on Arch Dams. 17-20 October 1992. Nanjing, China. 1-4.

Moyo, P. 2013. Dynamics: Definitions and concepts. [CIV5113Z PowerPoint presentation]. Department of Civil Engineering, University of Cape Town.

Moyo, P. 2014. Operational Modal Analysis - Ambient Vibration Testing. [CIV5119Z PowerPoint presentation]. Department of Civil Engineering, University of Cape Town.

National Water Act, No. 36 of 1998. 1998. *Government Gazette*. 398(19182). 26 August. Government notice no. 1091. Pretoria: Government printer.

National Water Act, No. 36 of 1998. Regulation. 2012. *Government Gazette*. 560(35062). 24 February. Government notice no. R139. Pretoria: Government Printer.

Naude, P. 2002. *Kouga Dam: Dam Safety Installation Report on Trivec System.* (Report Number: L820/01/DX02). Pretoria, South Africa. Directorate: Civil Design, Sub-Directorate: Dam Safety, Department of Water Affairs and Forestry.

Oberholster, B. 2009. *Chapter 10: Alkali-Silica Reaction.* In *Fulton's Concrete Technology*. Owens, G. Ed. 9th ed. Midrand, South Africa: Cement & Concrete Institute. 189-218.

Okuma, N., Etou, Y., Kanazawa, K., Hirata, K. 2008. *Dynamic properties of a large arch dam after forty-four years of completion.* Proceedings of the 14th World Conference on Earthquake Engineering 2008. 12-17 October 2008. Beijing, China.

Oosthuizen, C., 2014. Safety of Special Structures. [CIV5118Z: Guest lecture] Department of Civil Engineering, University of Cape Town.

Oosthuizen, C., Naude, P.A., Dorfling, C.J. 2003. *A simple 3-Dimensional crack-width-tilt gauge out of Africa.* (ISBN 90 5809 602 5). Field Measurements in Geomechanics. Proceedings of the 6th International Symposium. 23-26 September 2003. Oslo, Norway. 599-604.

Poraver. 2016. *Influence of expanded glass granulate on the alkali-silica-reaction in cementitious systems.* Available: http://www.poraver.com/us/influence-expanded-glass-granulate-alkali-silica-reaction-cementitious-systems-2/ [2016, November, 26]

Pretorius, C.J. & du Toit, I. 2014. The Department of Water Affairs in South Africa expands Dam monitoring to GPS/GNSS Deformation Monitoring [Paper]. Pretoria, South Africa. Directorate: Strategic Asset Management, Sub-Directorate: Dam Safety Surveillance, Department of Water and Sanitation. (Unpublished)

Pretorius, C.J., Schmidt, W.F., van Staden, C.S., Egger, K. 2001. *The Extensive Geodetic System used for the Monitoring of a 185 metre High Arch Dam in Southern Africa*. Proceedings of the 10th International Symposium on Deformation Measurements. 19-22 March 2001. California, United States of America. 203-213.

Shaw, Q.H.W. 2015. *The Structural Function of Different Arch Dam Types*. Proceedings of the SANCOLD Annual Conference 2015. 1-3 September 2015. Cape Town, South Africa. 320-332.

South African National Committee on Large Dams. 1991. *Guidelines on Safety in Relation to Floods.* (Report no. 4). Pretoria, South Africa: Safety evaluation of dams, SANCOLD.

United States Army Corps of Engineers. 1993. *Theoretical Manual for Analysis of Arch Dams.* (Technical Report no. ITL-93-1). Washington, DC.

United States Army Corps of Engineers. 1994. *Arch Dam Design.* (Engineering Manual no. 1110-2-2201). Washington, DC.

United States Bureau of Reclamation. 1977a. *Design of Arch Dams: Design Manual for Concrete Arch Dams.* Denver, Colorado: A Water Resources Technical Publication.

United States Bureau of Reclamation. 1977b. *Guide for Preliminary Design of Arch Dams.* Denver, Colorado: A Water Resources Technical Publication.

United States Bureau of Reclamation. 2016. *Flaming Gorge Unit.* Available: http://www.usbr.gov/uc/rm/crsp/fg/ [2016, November 25]

Westergaard, H. M. 1933. *Water Pressures on Dams During Earthquakes.* Transactions. American Society of Civil Engineers. Volume 92. 418-433.

World Bank. 2016. *Average precipitation in depth (mm per year).* Available: http://data.worldbank.org/indicator/AG.LND.PRCP.MM?end=2014&locations=1W&start=2012&view=map [2016, November, 22].

APPENDICES

A. TRIVEC RESULTS

Position 1: High water Level

Version 2016/08/29 3:33 PM

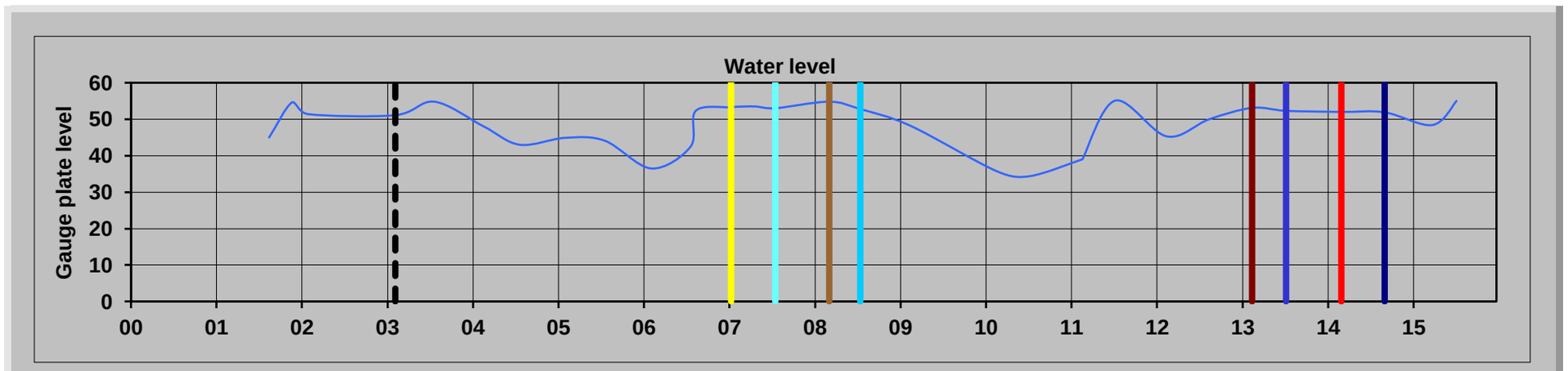

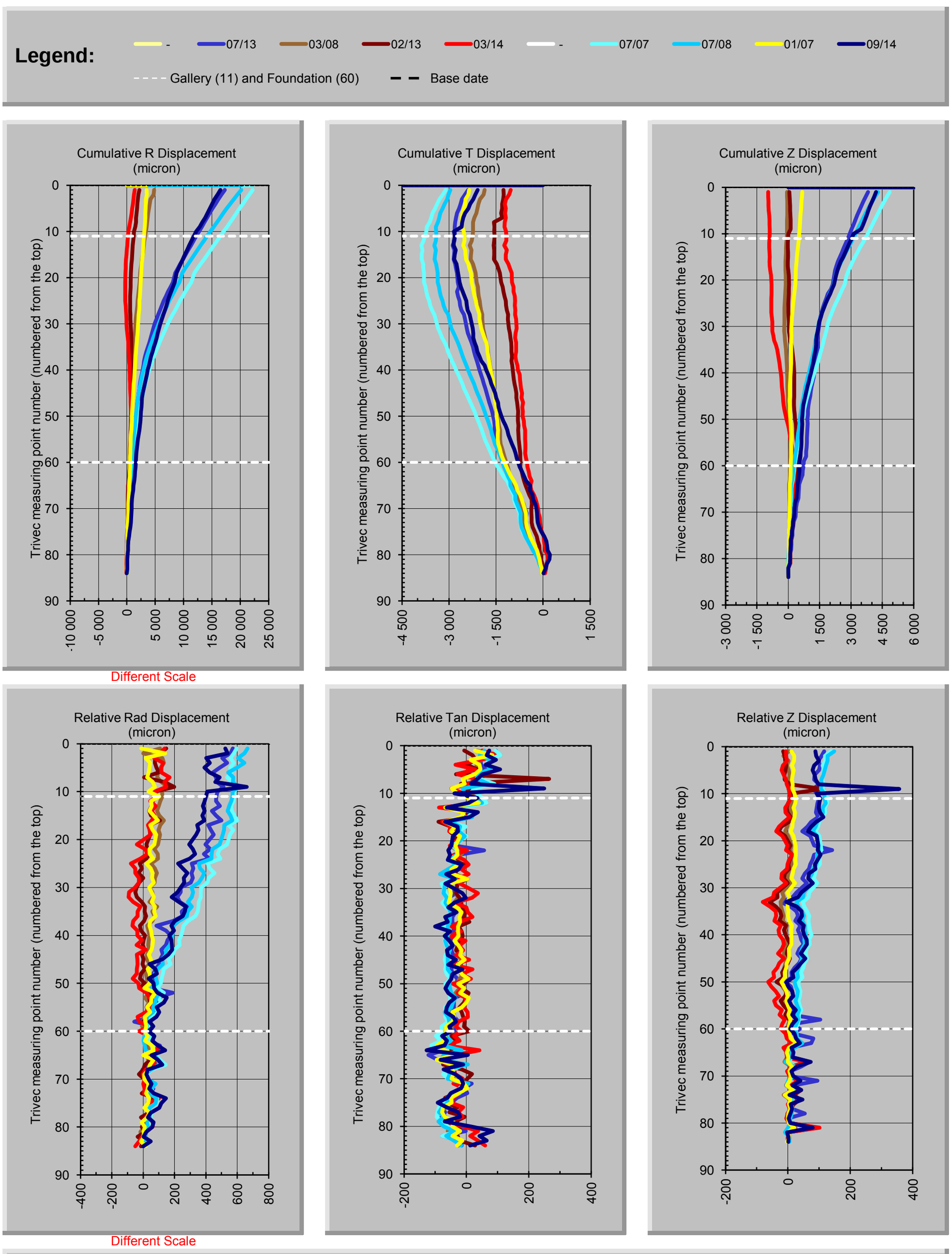

Figure 1 Kouga Dam: Kogr1 Displacements obtained with the TRIVEC at position 1.

Position 1: Low water Level

Version 2016/08/29 3:35 PM

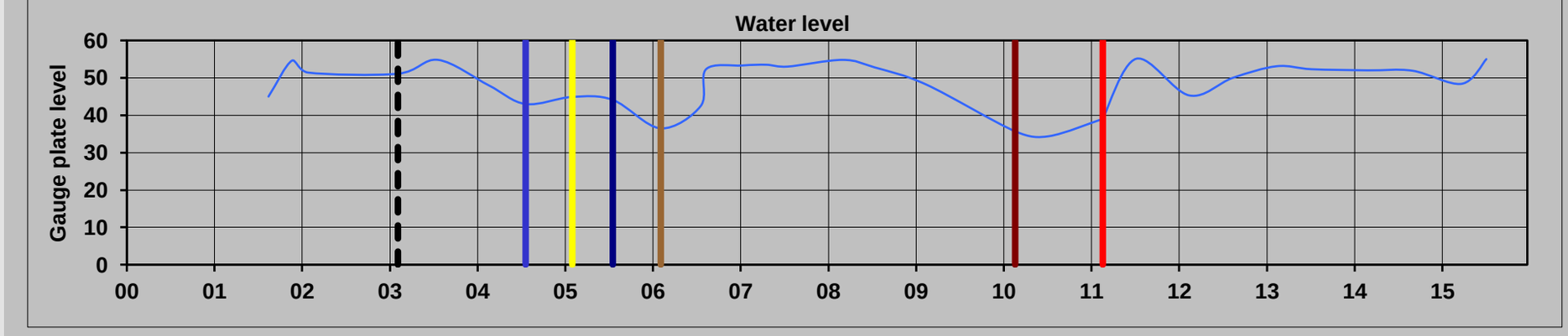

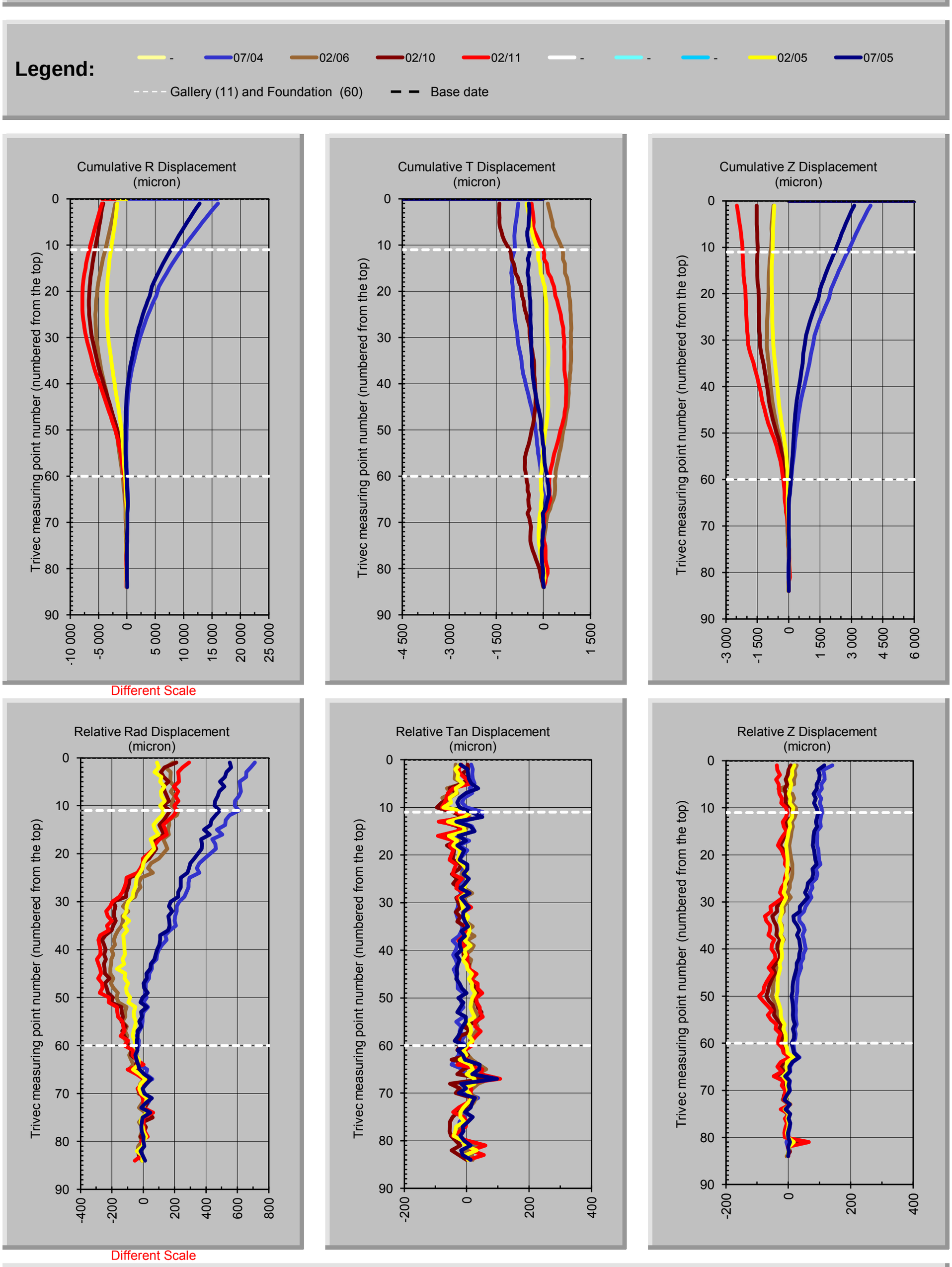

Figure 1 Kouga Dam: Kogr1 Displacements obtained with the TRIVEC at position 1.

Position 2: High water Level

Version 2016/08/25 12:44 AM

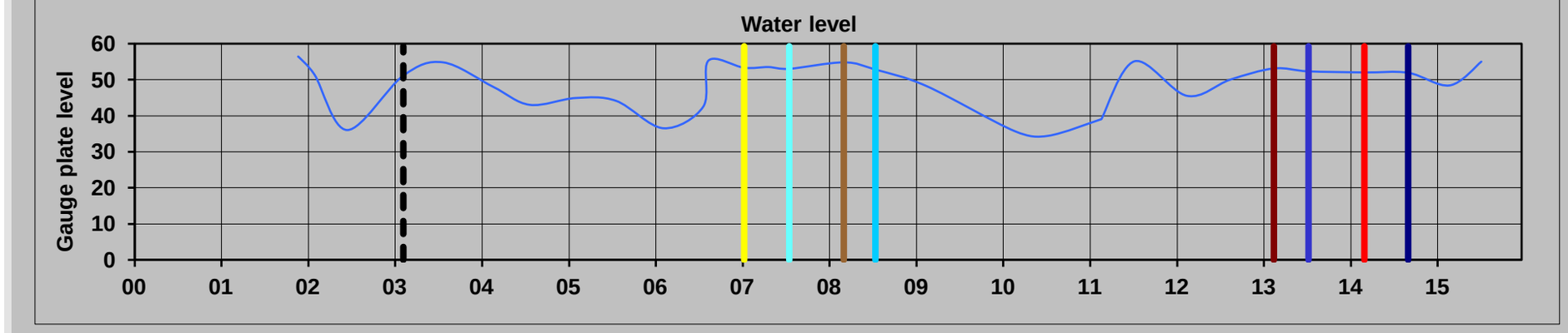

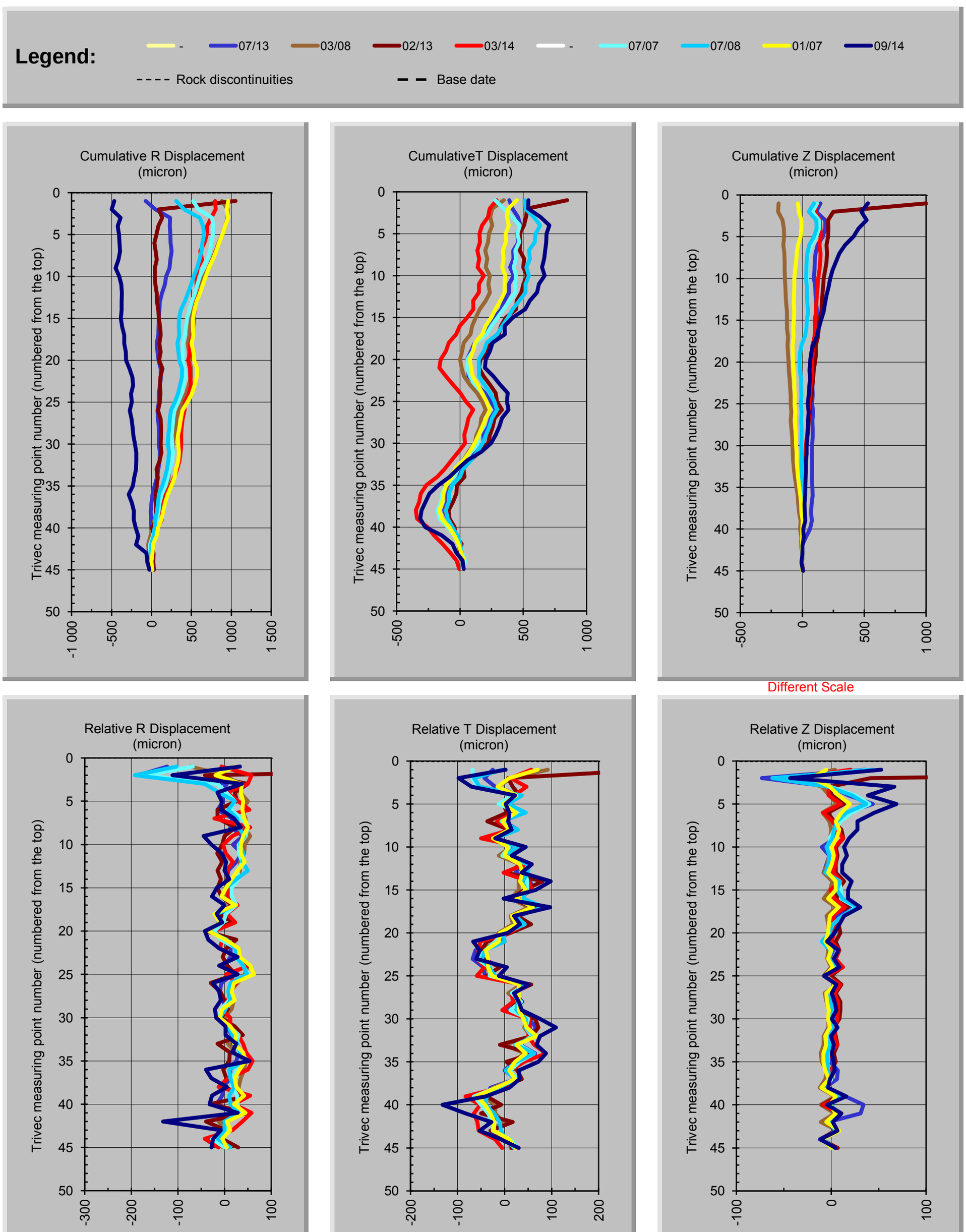

Figure 2 Kouga Dam: Kogr2 Displacements obtained with the TRIVEC at position 2.

Position 2: Low water Level

Version 2016/08/25 12:33 AM

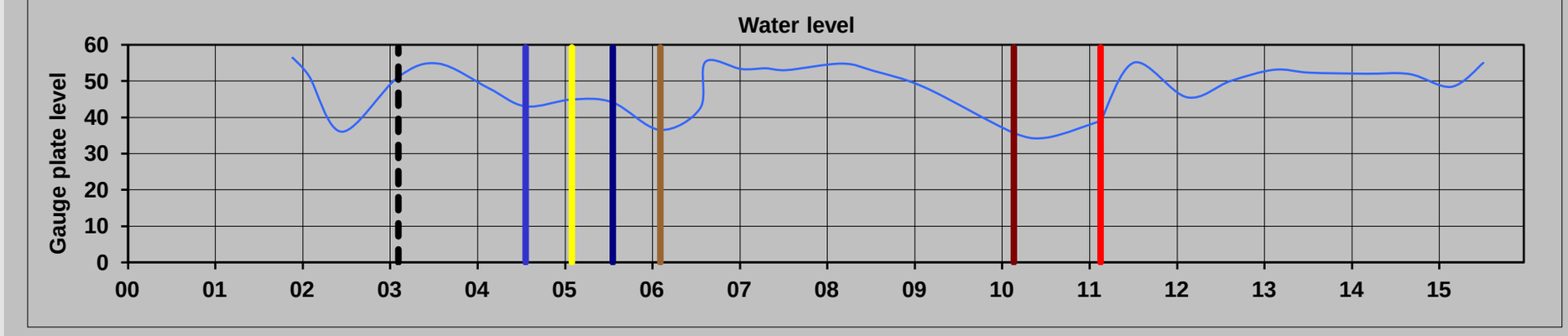

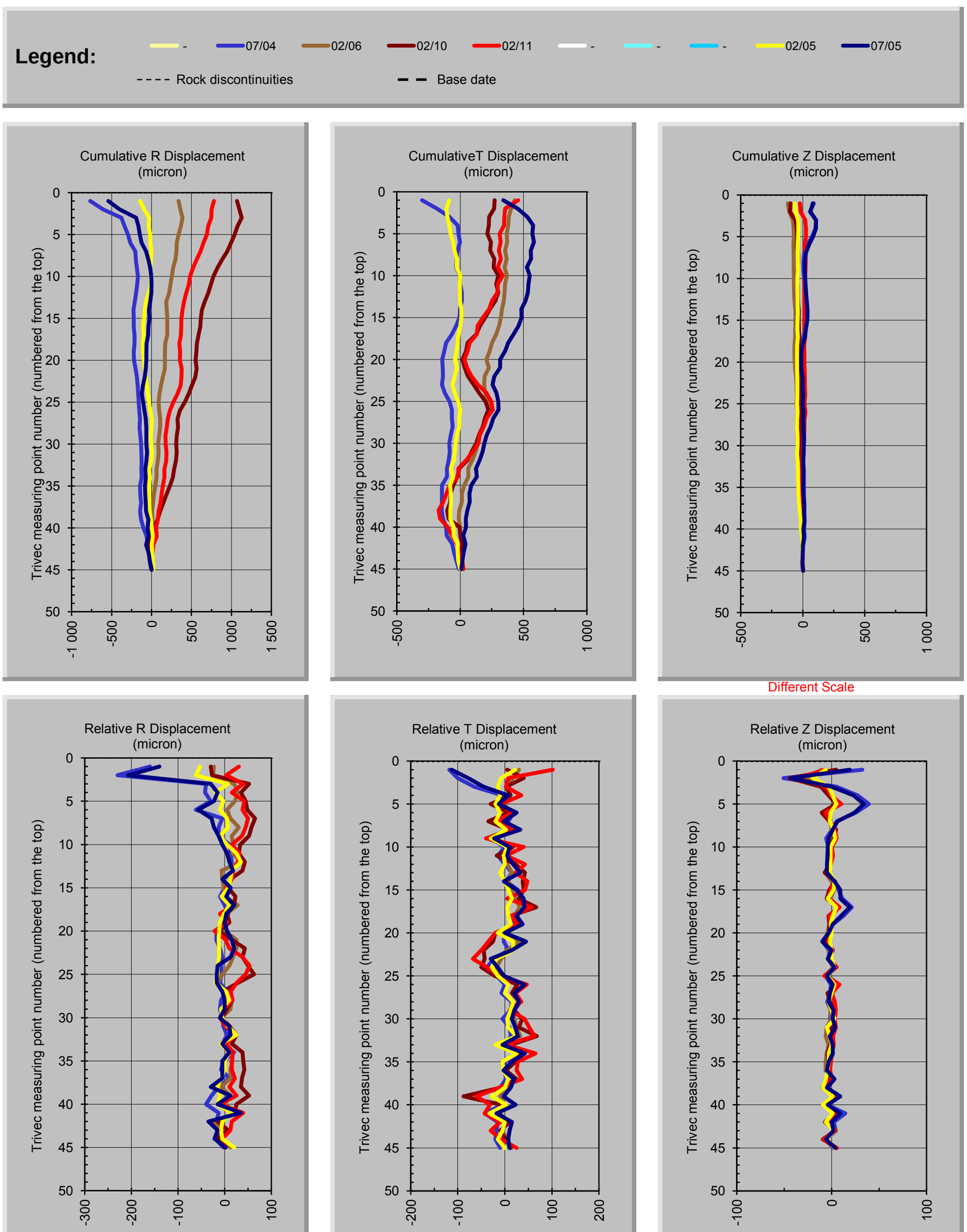

Figure 2 Kouga Dam: Kogr2 Displacements obtained with the TRIVEC at position 2.

Position 3: High water Level

Version 2016/08/25 1:42 AM

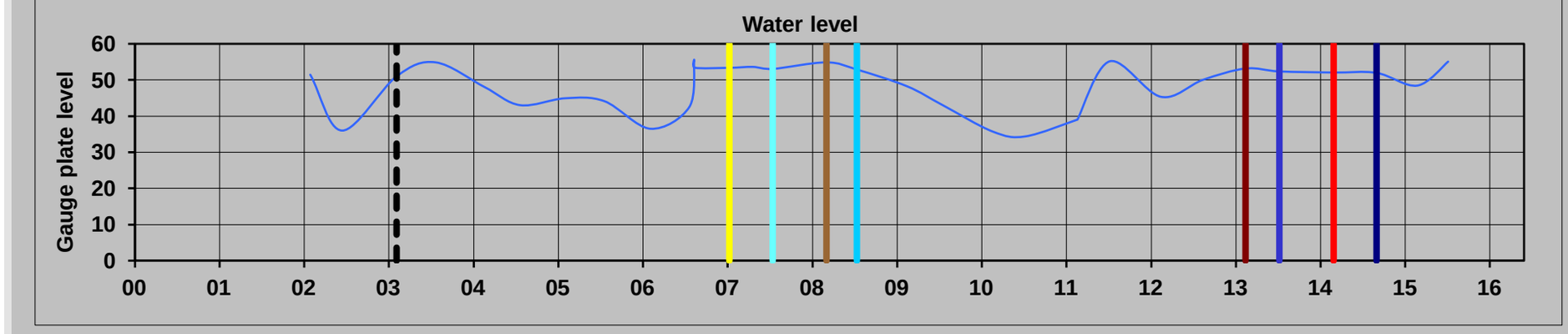

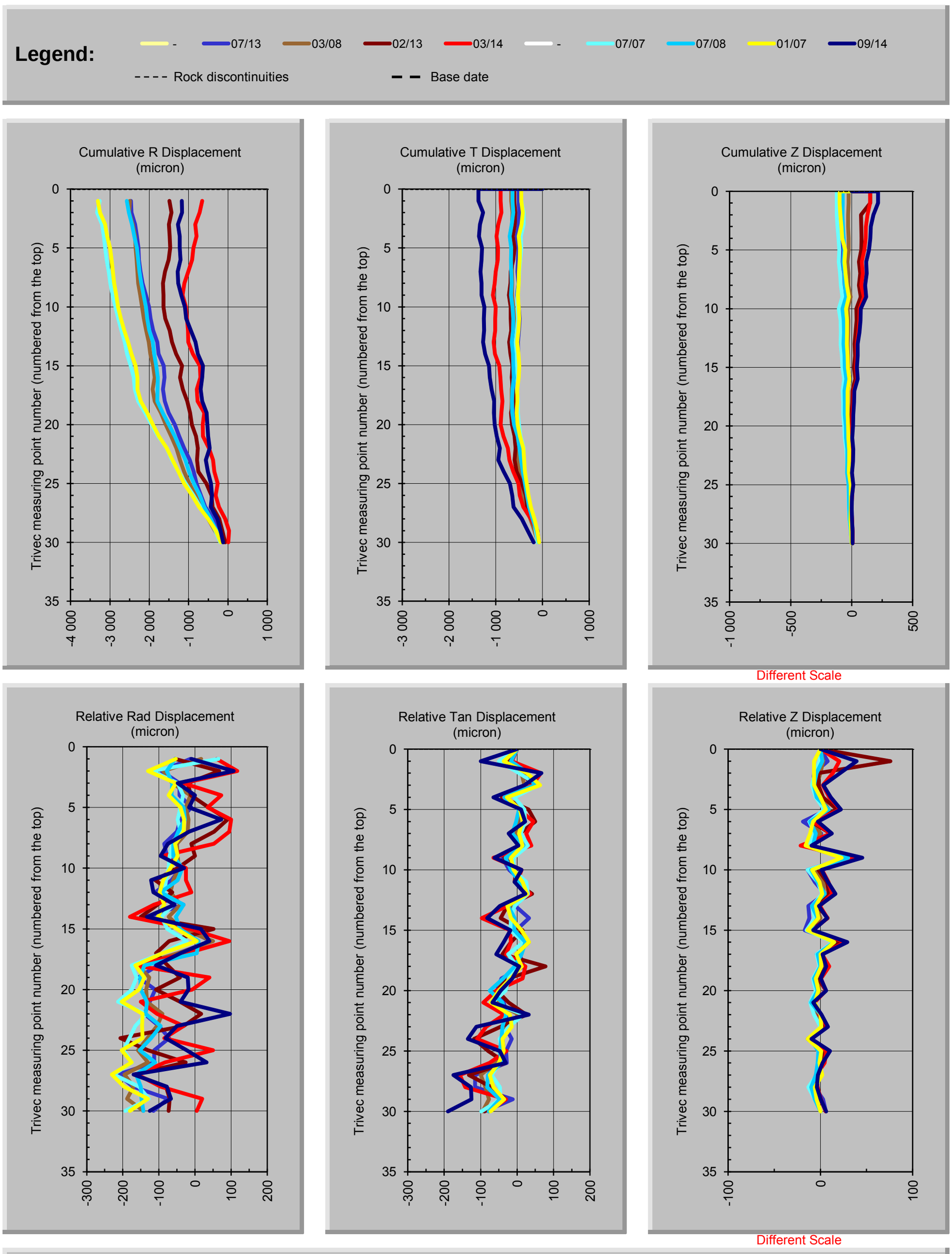

Figure 3 Kouga Dam: Kog3 Adjusted displacements obtained with the TRIVEC at position 3.

Position 3: Low water Level

Version 2016/08/25 1:43 AM

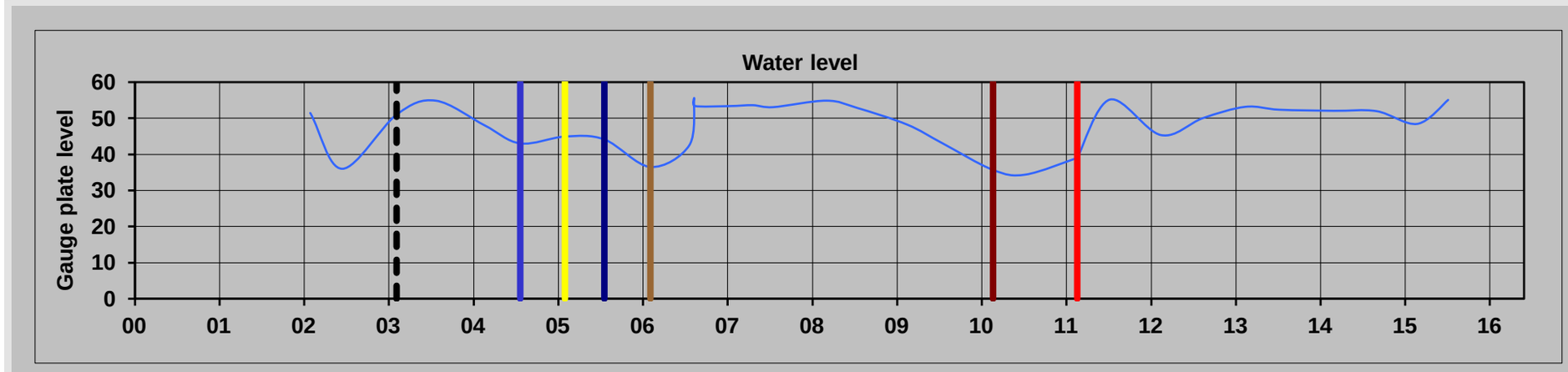

Legend: - 07/04 02/06 02/10 02/11 - - - 02/05 07/05

---- Rock discontinuities — — Base date

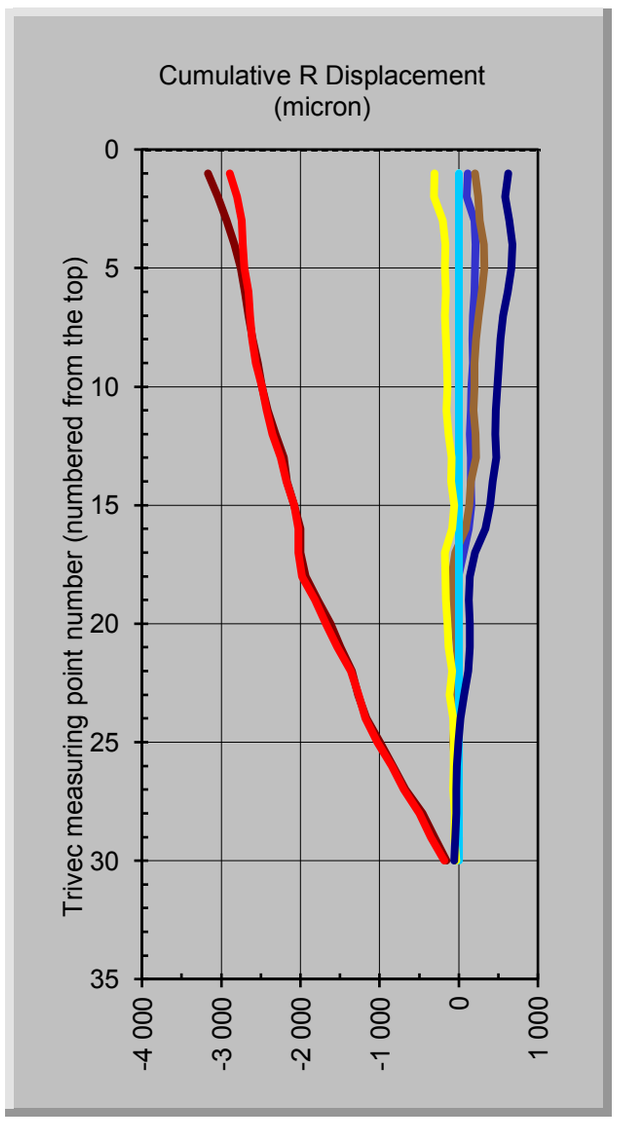

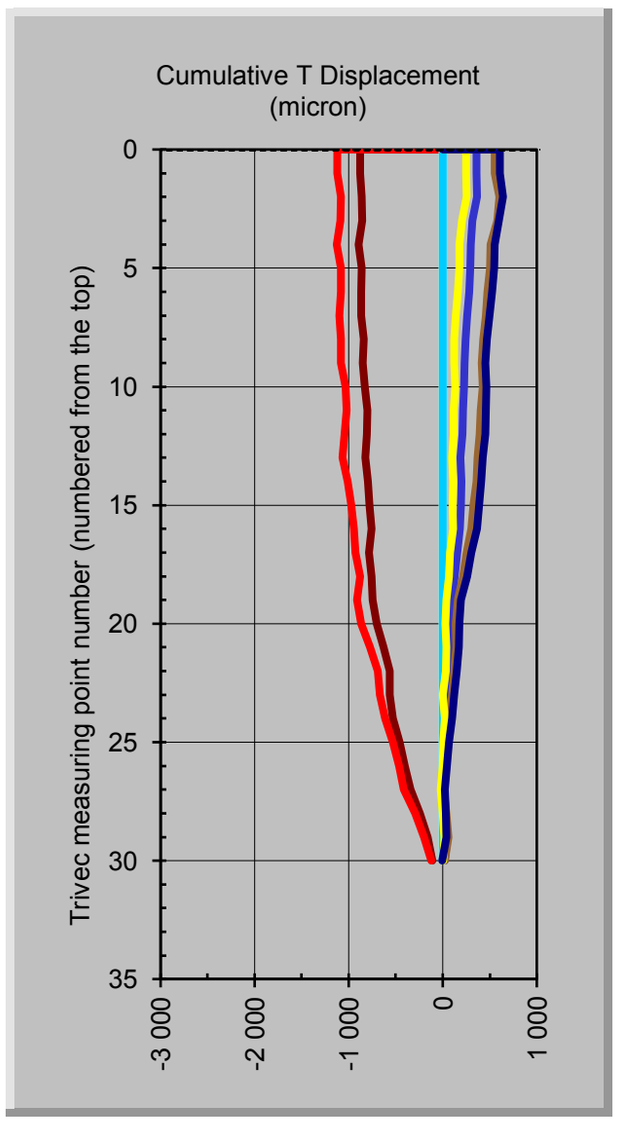

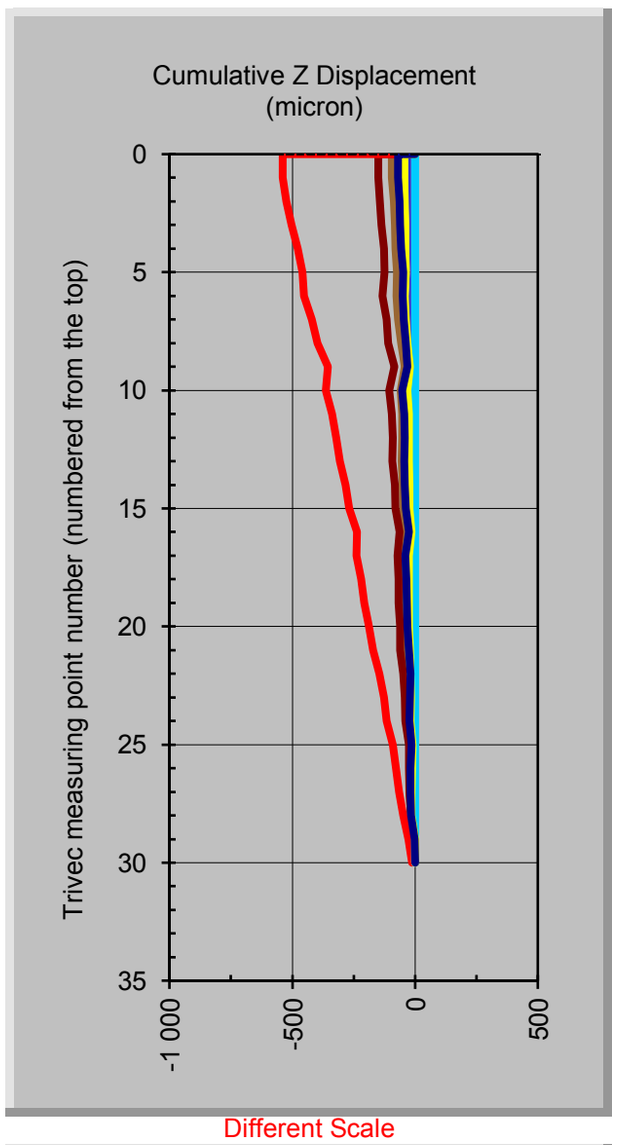

Different Scale

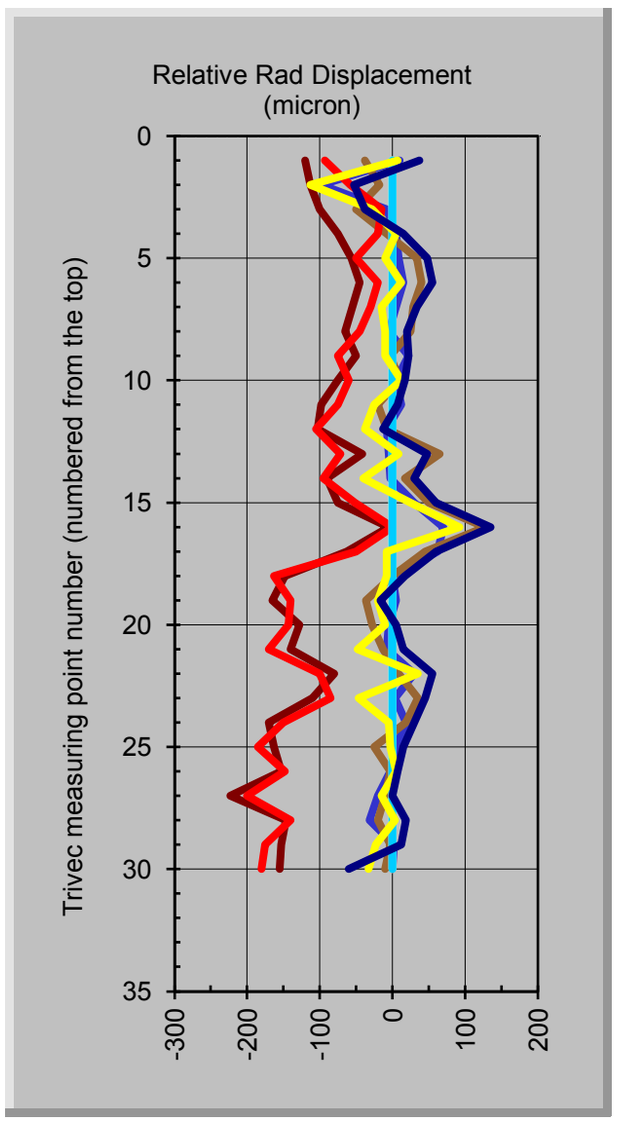

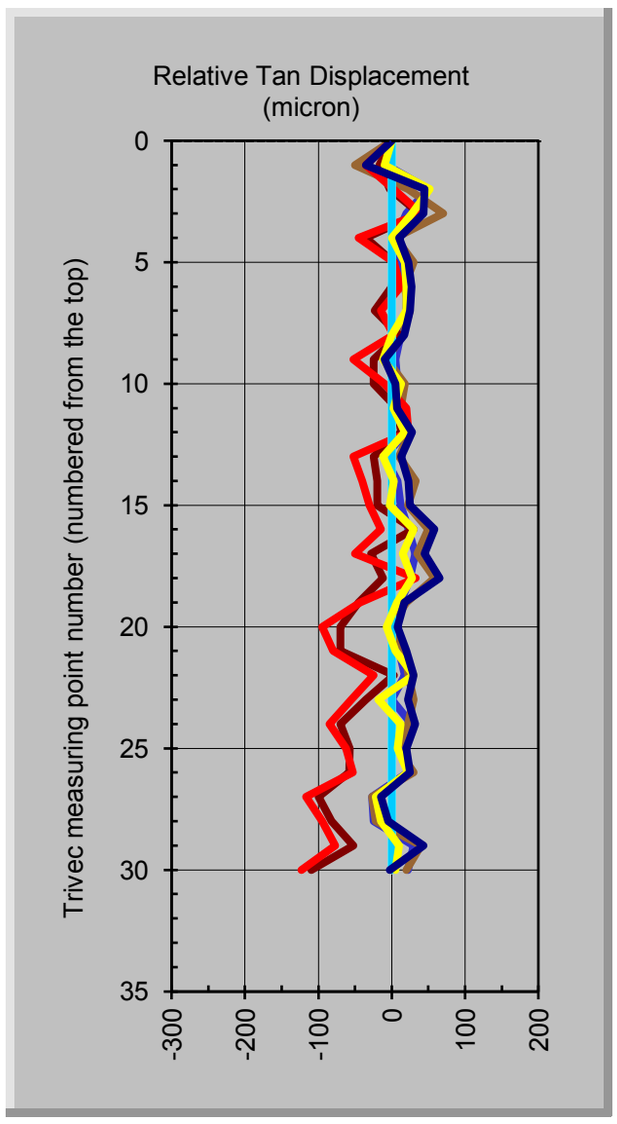

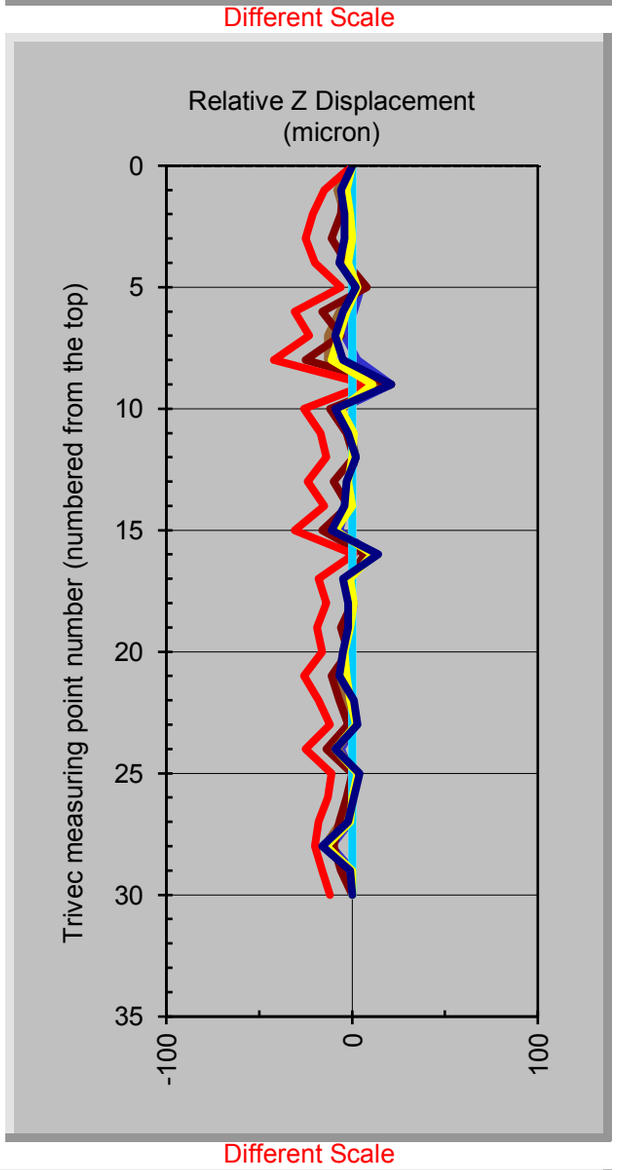

Different Scale

Positive directions: R=Downstream, T= Left Flank and Z= Vertical Downwards

Figure 3 Kouga Dam: Kog3 Adjusted displacements obtained with the TRIVEC at position 3.

Position 4: High water Level

Version 2016/08/25 2:43 AM

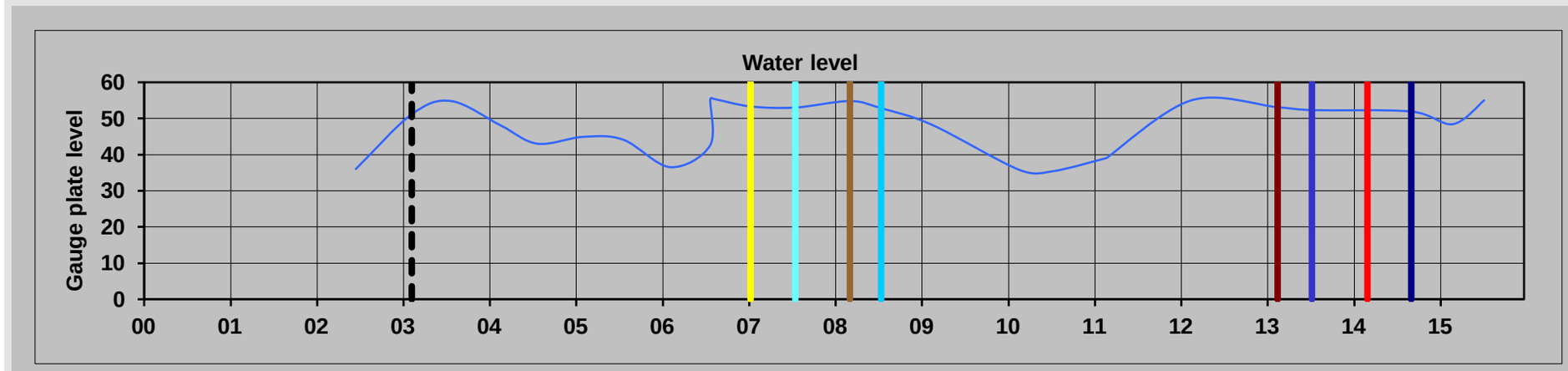

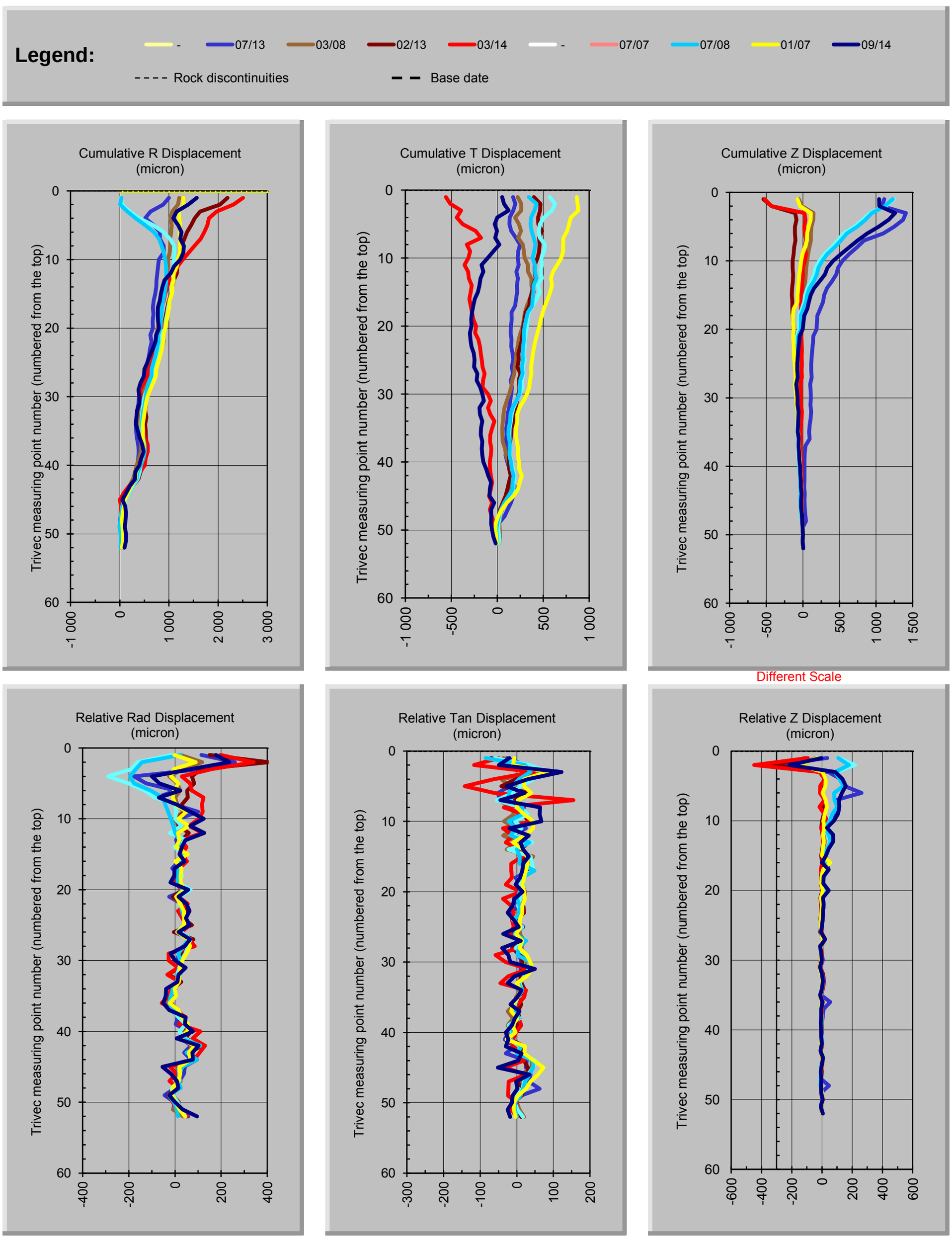

Figure 4 Kouga Dam: Kogr4

Adjusted displacements obtained with the TRIVEC at position 4.

Position 4: Low water Level

Version 2016/08/25 2:43 AM

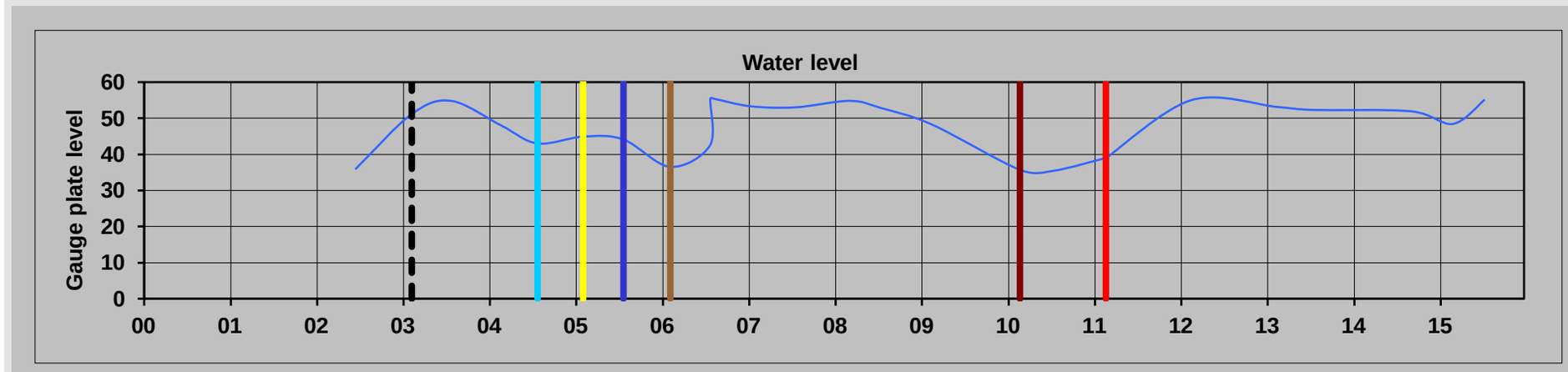

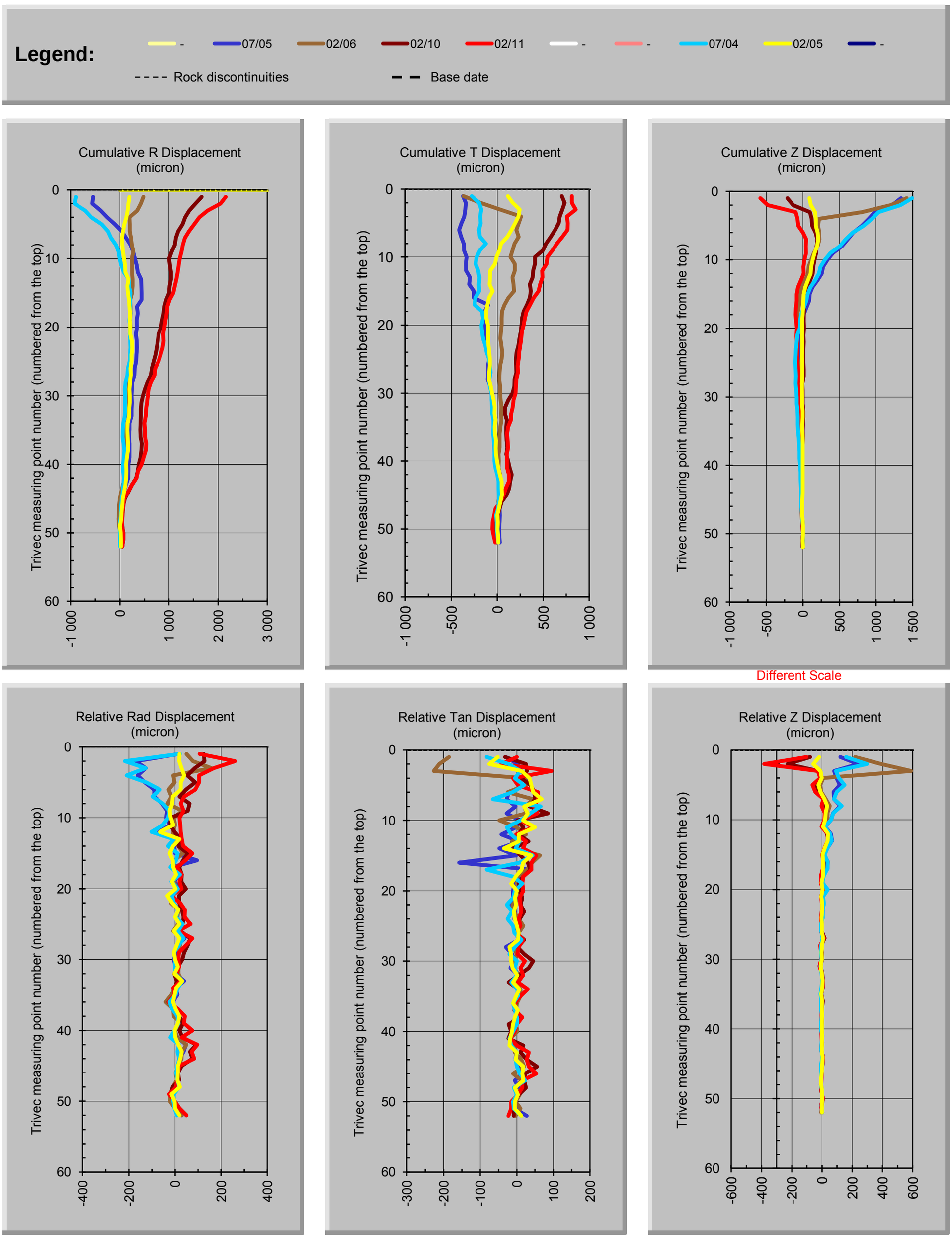

Positive directions: R=Downstream, T= Left Flank and Z= Vertical Downwards

Figure 4 Kouga Dam: Kogr4

Adjusted displacements obtained with the TRIVEC at position 4.

Position 5: Full Record

Version 2016/08/25 2:04 AM

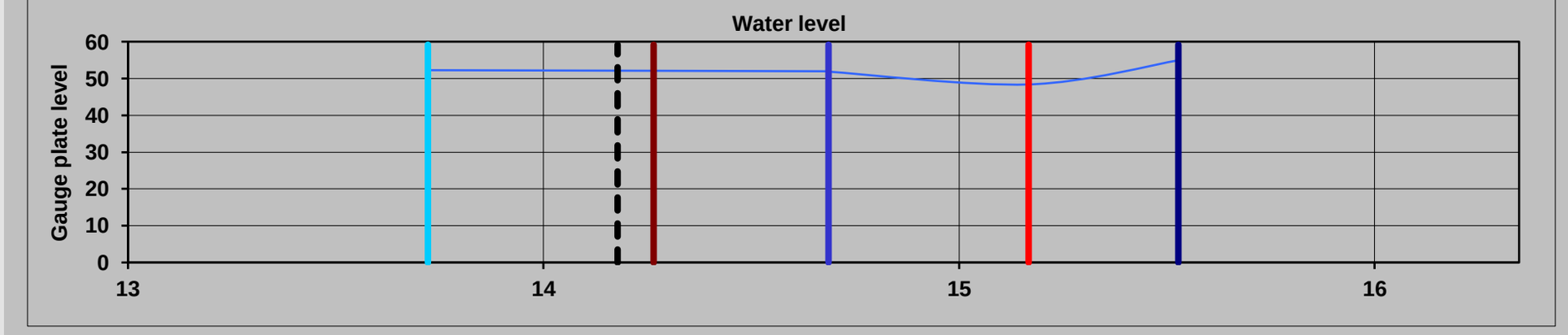

Legend:

- 09/14 - 04/14 03/15 - - 09/13 - 07/15

Rock discontinuities Base date

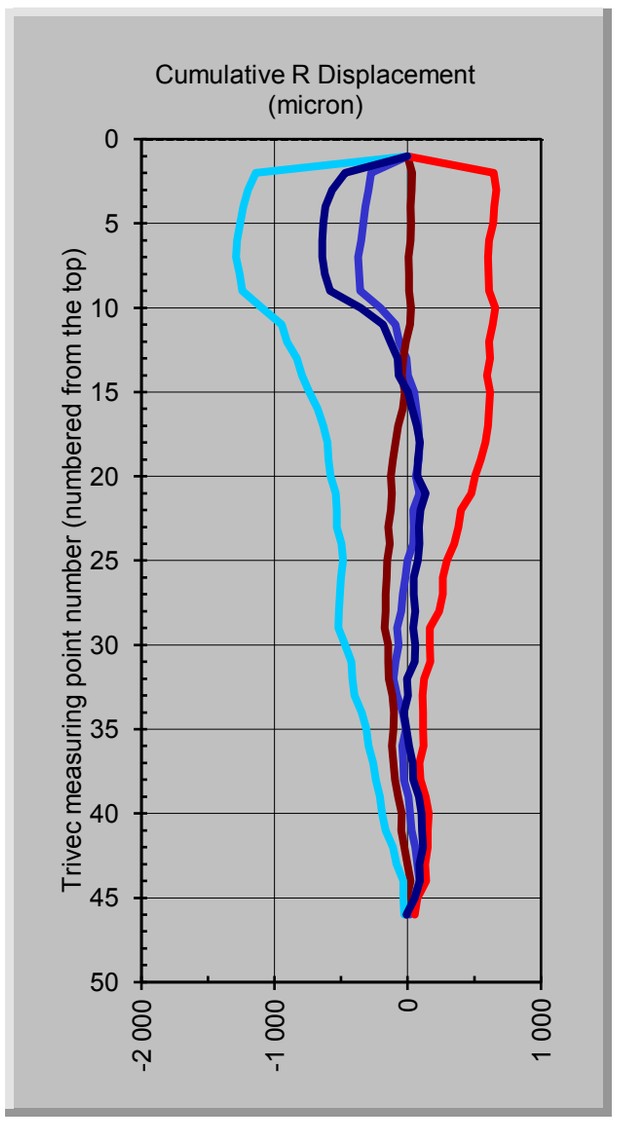

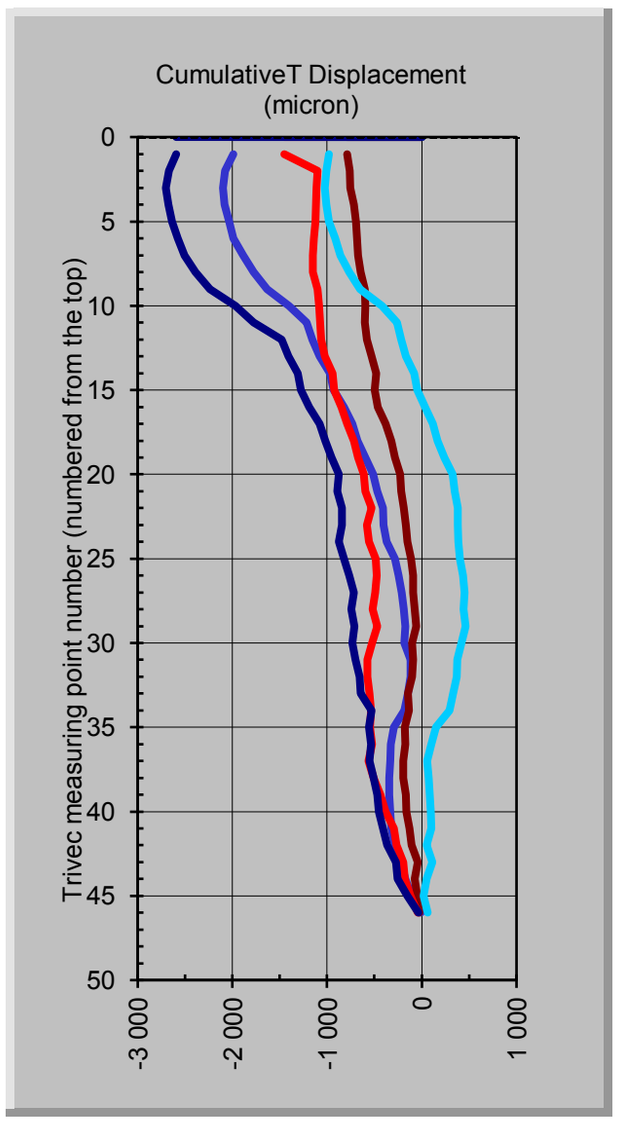

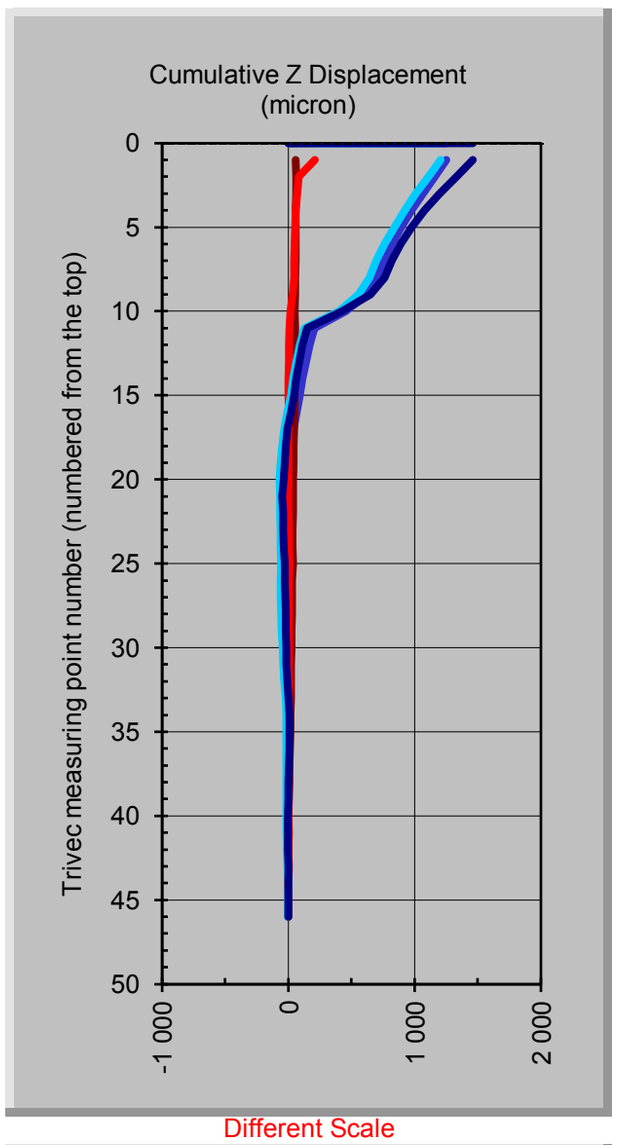

Different Scale

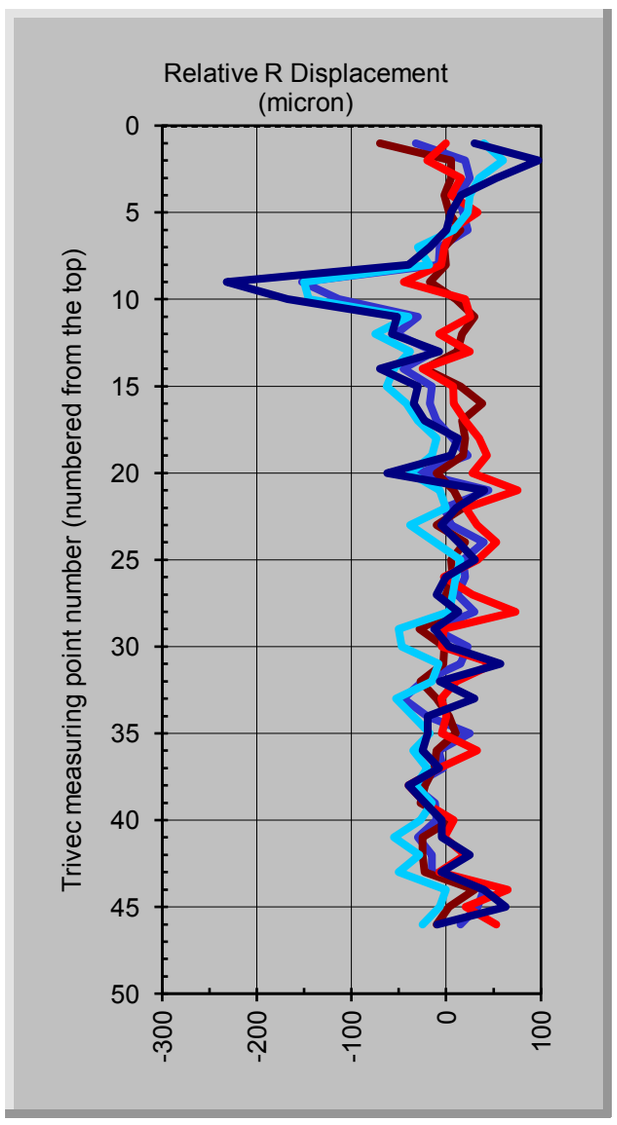

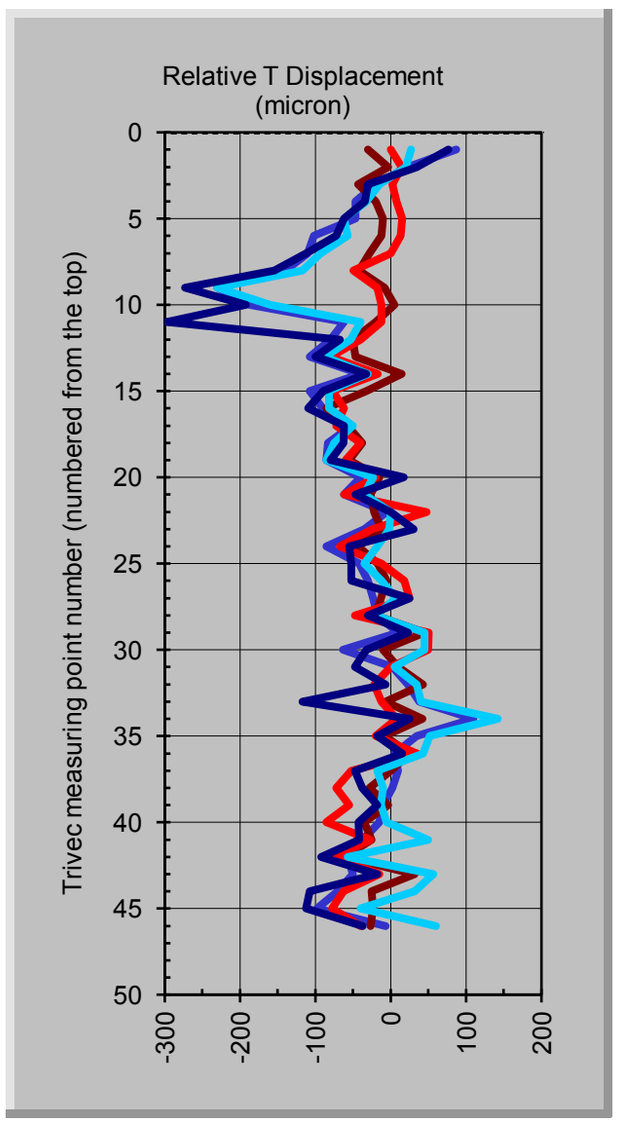

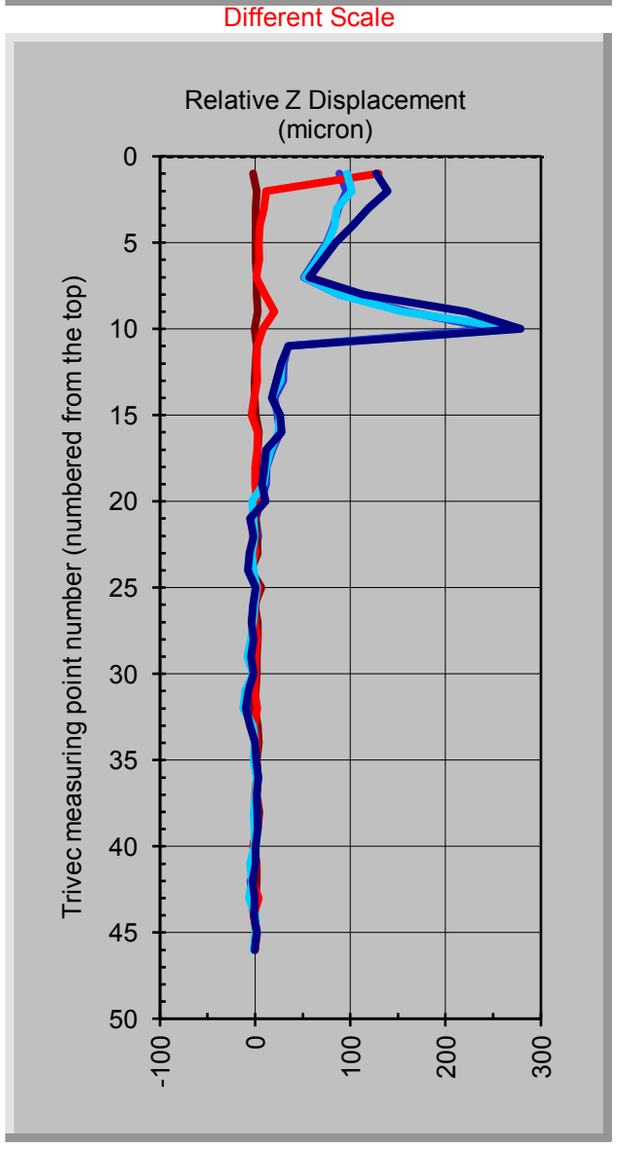

Positive directions: R =Downstream, T= Left Flank and Z= Vertical Downwards

Figure 5.1 Kouga Dam: Kogr5 Displacements obtained with the TRIVEC at position Kogr5.

Position 6: Full Record

Version 2016/08/25 2:17 AM

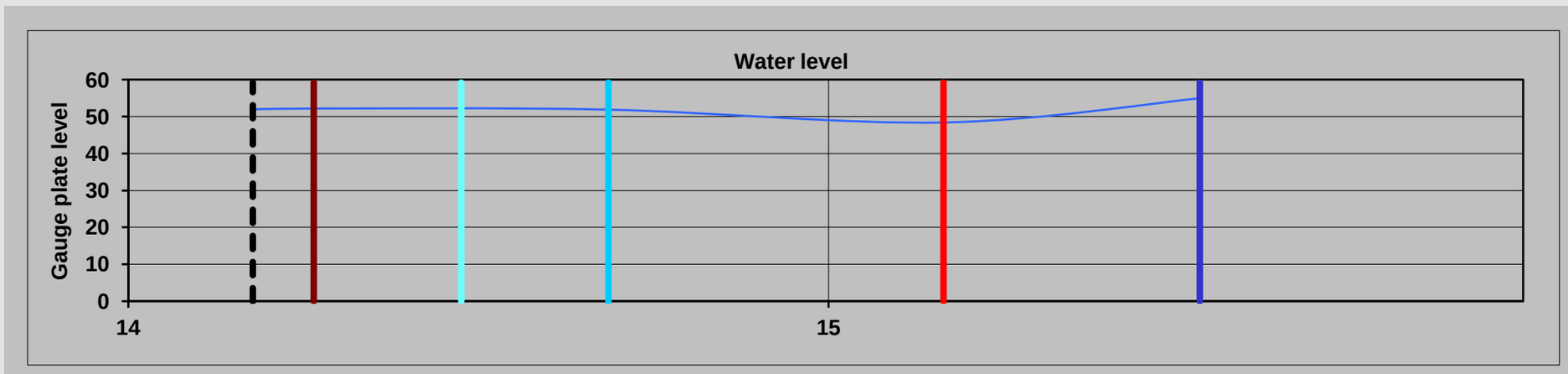

Legend: - 07/15 - 04/14 03/15 - 06/14 09/14 - -

---- Rock discontinuities — — Base date

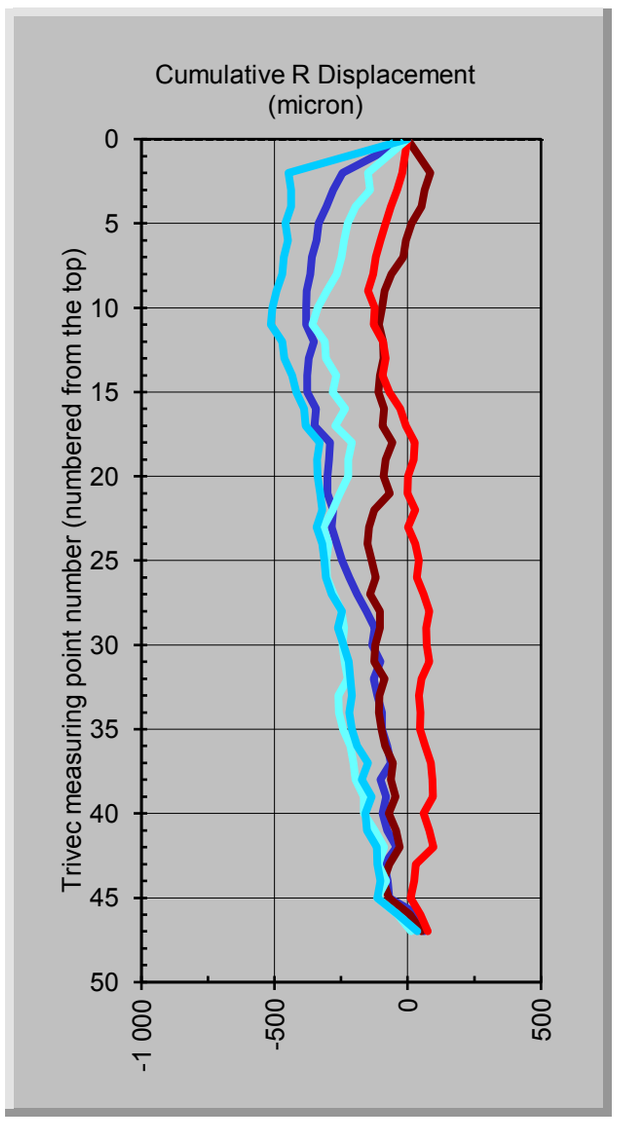

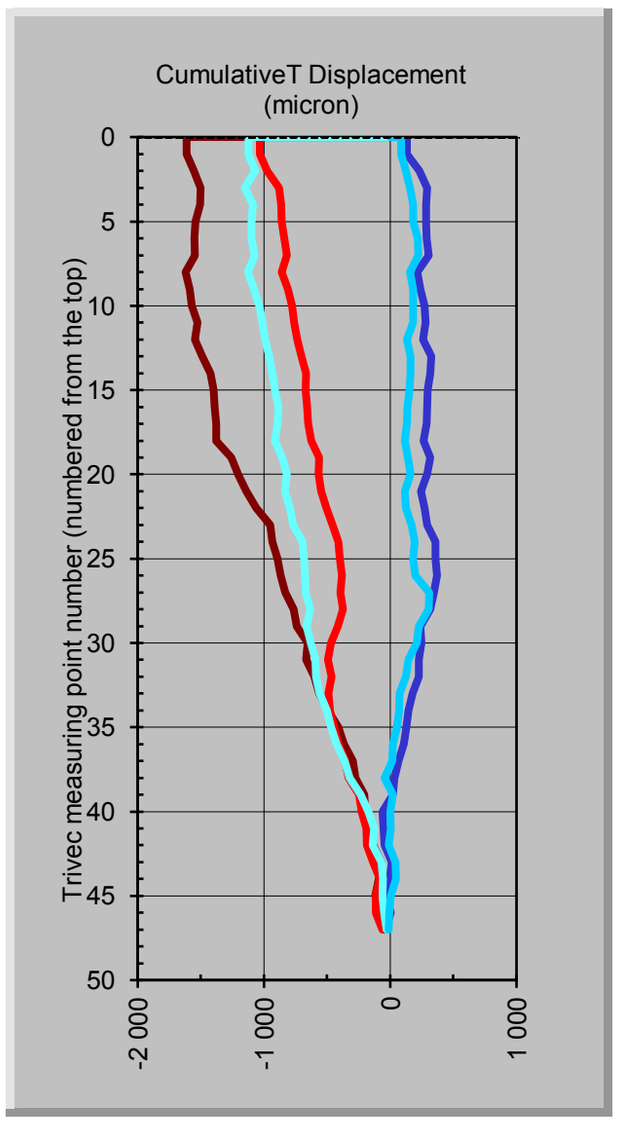

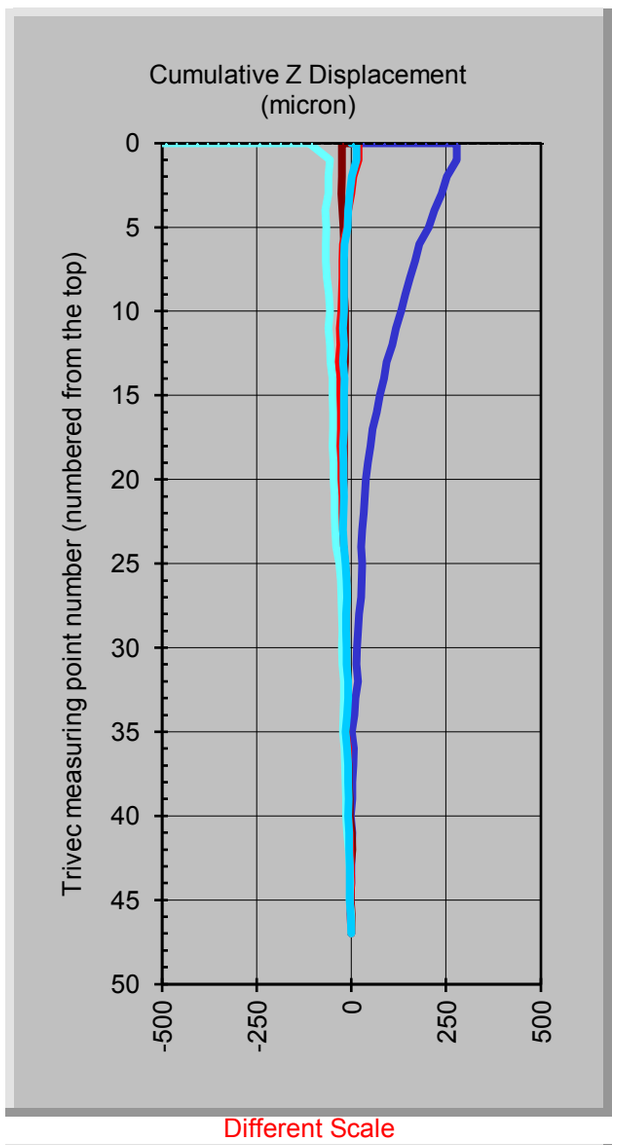

Different Scale

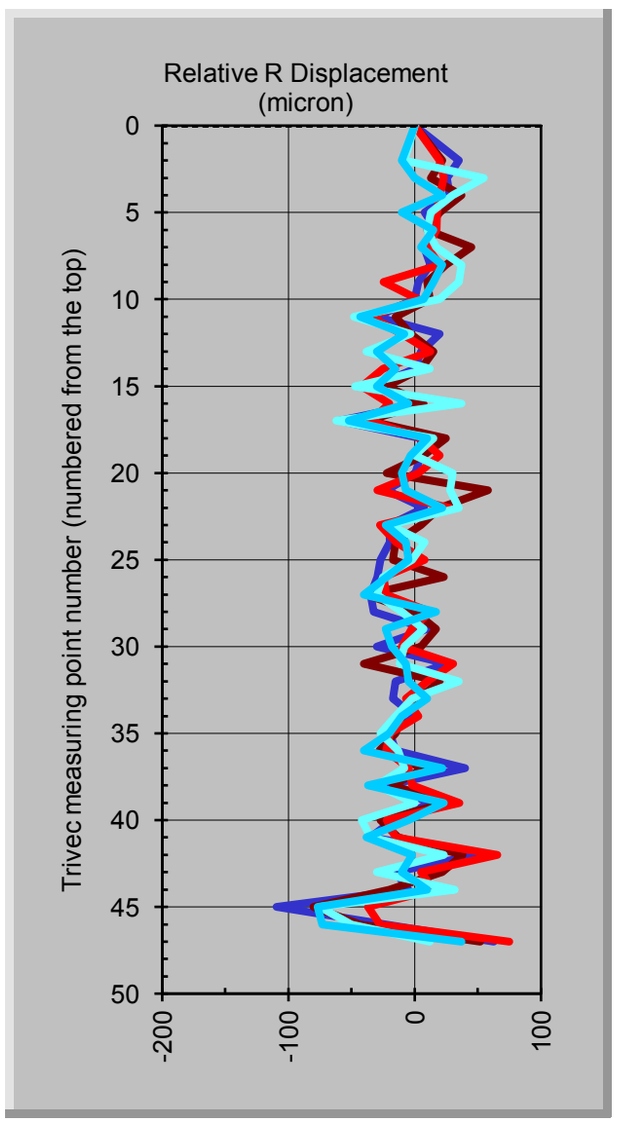

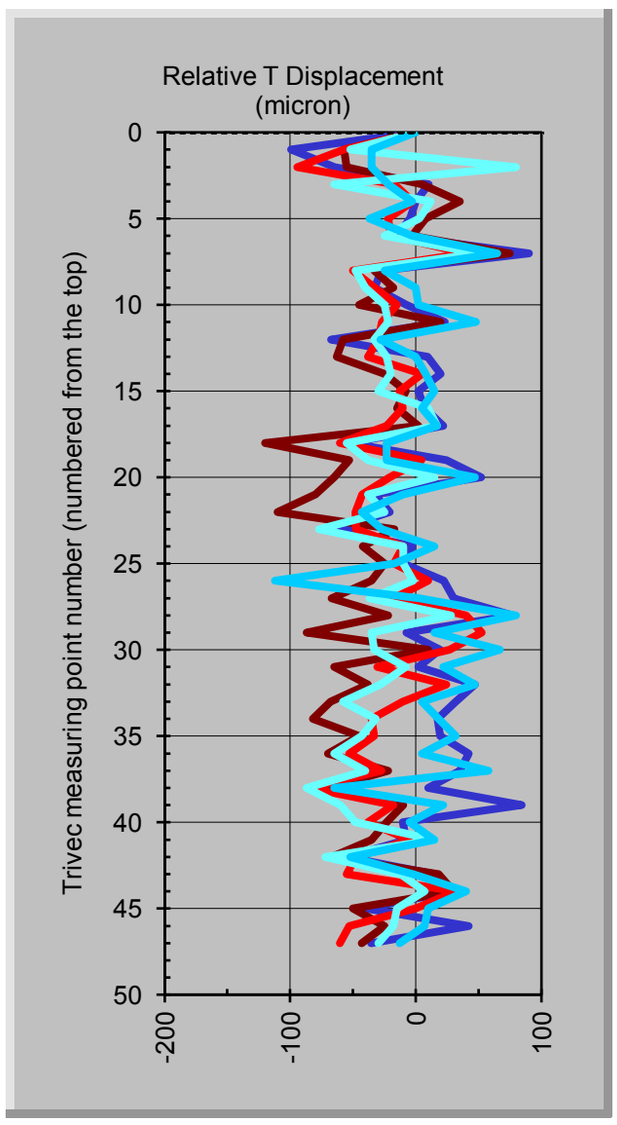

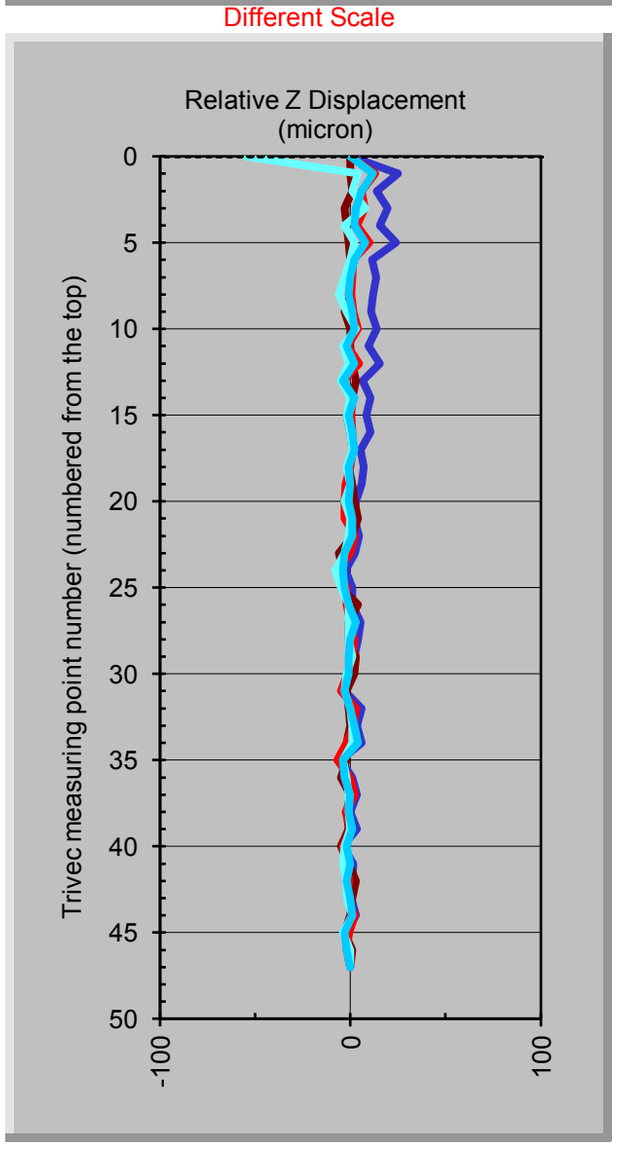

Positive directions: R =Downstream, T= Left Flank and Z= Vertical Downwards

Figure 6.1 Kouga Dam: Kogr6 Displacements obtained with the TRIVEC at position Kogr6.